EXAMINING THE RELATIONSHIP BETWEEN ANTECEDENT SOIL MOISTURE AND SUMMER PRECIPITATION IN THE U.S. GREAT PLAINS

A Dissertation

by

LEI MENG

Submitted to the Office of Graduate Studies of
Texas A&M University
in partial fulfillment of the requirements for the degree of

DOCTOR OF PHILOSOPHY

August 2009

Major Subject: Geography

EXAMINING THE RELATIONSHIP BETWEEN ANTECEDENT SOIL MOISTURE AND SUMMER PRECIPITATION IN THE U.S. GREAT PLAINS

A Dissertation

by

LEI MENG

Submitted to the Office of Graduate Studies of
Texas A&M University
in partial fulfillment of the requirements for the degree of

DOCTOR OF PHILOSOPHY

Approved by:

Co-Chairs of Committee,	Steven M. Quiring
	Daniel Z. Sui
Committee Members,	Hongxing Liu
	Cristine L.S. Morgan
Head of Department,	Douglas J. Sherman

August 2009

Major Subject: Geography

ABSTRACT

Examining the Relationship between Antecedent Soil Moisture and Summer Precipitation in the U.S. Great Plains. (August 2009)

Lei Meng, B.S., Nanjing University;

M.S., China Agricultural University;

M.S., University of Illinois

Co-Chairs of Advisory Committee: Dr. Steven M. Quiring
Dr. Daniel Z. Sui

This dissertation focuses on examining the relationship between antecedent soil moisture and summer precipitation in the U.S. Great Plains (GP). The influence of Niño sea surface temperatures (SSTs) on summer precipitation has also been investigated to compare their relative contributions to those from local moisture recycling. Both observational data and model simulations have been used to investigate how and why soil moisture can affect subsequent summer precipitation in the GP.

Observational analysis indicates that spring (May 1st) soil moisture is significantly correlated with summer precipitation only during periods when Niño SSTs are not strongly correlated with summer precipitation (e.g. 1925-1936). During periods when Niño SSTs are strongly correlated with summer precipitation (e.g. 1940-1970), spring soil moisture is not a good predictor of summer precipitation in the GP. The periods of strong correlation between Niño SSTs and summer precipitation are associated with strong SST persistence. This study suggests that both local soil moisture

and remote SST anomalies (deviation from SST climatology) influence summer precipitation in the GP. The soil moisture anomalies are of greatest importance during years when Niño SST persistence is low.

Model results have demonstrated that there are significant differences in precipitation response to soil moisture anomalies depending on their sign (+/-), timing and persistence. The influence of dry soil moisture anomalies on subsequent precipitation tends to last longer than wet soil moisture anomalies when initialized on May 1st. Dry soils can influence summer precipitation in the subsequent 2-3 months. However, the precipitation response to wet soil moisture anomalies is faster and greater in magnitude than the response to dry soil moisture anomalies. Persistent soil moisture anomalies that are sustained for an entire month produced larger precipitation changes than soil moisture anomalies only applied on the first day of the month. It appears that the length of soil moisture memory also depends on the sign of soil moisture anomaly. The results of this study may be model-dependent due to the significant inter-model variations in land surface parameterizations. This may restrict the potential for drawing general conclusions.

DEDICATION

To my grandma, my parents, and my wife

ACKNOWLEDGEMENTS

I would like to express my deepest appreciation to my primary advisor and committee co-chair, Dr. Steven M. Quiring. I could not have completed this dissertation without his inspirational instruction, guidance, and financial support. He has always provided proper and quick responses to the questions I have in my research. More importantly, I want to thank him for his friendship which makes my study and life at Texas A&M University joyful.

I am also deeply indebted to my committee co-chair Dr. Daniel Z. Sui for his vision, advice, and practical guidance. He encourages me to think about the big picture in research. This directional instruction guides me through my doctoral research.

I would also like to thank my committee members. Dr. Hongxing Liu taught me the technology skills needed to finish this research. Dr. Cristine Morgan provided valuable comments and suggestions which greatly improved my research.

I am also grateful to my fellow colleagues and faculty members in the department for their friendship and encouragements.

I want to thank my lovely wife, Xiaojing Sheng, for her love, understanding, and support. I also want to thank my family in China, parents, brothers, and the in-laws, for their continuous support and love.

TABLE OF CONTENTS

Page

ABSTRACT iii

DEDICATION v

ACKNOWLEDGEMENTS vi

TABLE OF CONTENTS vii

LIST OF FIGURES ix

LIST OF TABLES xiii

1 . INTRODUCTION 1

1.1 Research background 1
1.2 Objectives of the research 3

2 . LAND-ATMOSPHERE INTERACTIONS 5

2.1 Land surface processes 5
2.2 Strength of land-atmosphere coupling 6
2.3 Simulation of land-atmosphere interactions 8

3 . DATA AND METHODOLOGY 10

3.1 Study area 10
3.2 Data 11
3.3 Model descriptions 19
3.4 Methods 25

4 . VALIDATION OF SOIL MOISTURE MODELS 37

4.1 Introduction 37
4.2 VIC and DSSAT soil moisture simulations 37
4.3 CWB soil moisture simulations 43
4.4 Comparison of VIC, DSSAT, and CWB model performance 45
4.5 VIC and DSSAT evapotranspiration simulations 46
4.6 VIC and DSSAT drainage and runoff simulations 49

Page

4.7 VIC and DSSAT sensitivity analysis 52
4.8 Validation of VIC using Mesonet observations 60
4.9 Conclusions 63

5 . OBSERVATIONAL RELATIONSHIP BETWEEN SOIL MOISTURE AND SUMMER PRECIPITATION 67

5.1 Introduction 67
5.2 Spatial variations in the soil moisture-precipitation relationship 67
5.3 Temporal variations in the soil moisture-precipitation relationship 71
5.4 Persistence of spatial patterns in SM anomalies 74
5.5 Temporal variations in the relationship between GP summer precipitation and Niño SSTs 75
5.6 SST persistence versus SM persistence 83
5.7 Conclusions 84

6 . SIMULATION OF THE EFFECT OF SPRING SOIL MOISTURE ON SUMMER PRECIPITATION 86

6.1 Introduction 86
6.2 Influence of initial spring soil moisture anomalies on summer precipitation 86
6.3 Influence of persistent spring soil moisture anomalies on summer precipitation 95
6.4 Comparison between dry and wet soil moisture anomalies 100
6.5 Soil moisture response and recovery 104
6.6 Influence of the timing of soil moisture anomalies on summer precipitation 107
6.7 Conclusions 110

7 . SUMMARY AND CONCLUSIONS 113

7.1 Summary 113
7.2 Conclusions 114
7.3 Future research 118

REFERENCES 119

VITA 130

LIST OF FIGURES

Page

Figure 3.1 Great Plains study region and three zones based on annual precipitation. Zone 1 is the driest zone with mean annual precipitation of 419 mm; zone 2 is the moderate zone with mean annual precipitation of 668 mm; and zone 3 is the wettest with mean annual precipitation of 1010 mm. 11

Figure 3.2 Spatial distributions of SST anomalies in a high persistence (0.89) year from April (top) to JJA (bottom)..... 30

Figure 3.3 Histograms of SST anomalies in April and JJA (top) and the differences in SST anomalies between April and JJA (bottom) in Figure 3.2. 31

Figure 3.4 Spatial distributions of SST anomalies in a low persistence (-0.62) year from April (top) to JJA (bottom)..... 32

Figure 3.5 Histograms of SST anomalies in April and JJA (top) and the differences in SST anomalies between April and JJA (bottom) in Figure 3.4. 33

Figure 4.1 Measured (black) and modeled (DSSAT (blue) and VIC (red)) daily soil moisture (top) and soil moisture anomalies (bottom) at Bushland, TX in 2004 (left) and 2005 (right). 38

Figure 4.2 Measured (black) and modeled (DSSAT (blue) and VIC (red)) daily soil moisture (top) and soil moisture anomalies (bottom) at Powder Mill, MD in 2002 (left) and 2004 (right)..... 39

Figure 4.3 Measured (black) and CWB (red) monthly soil moisture from 1995-2005 at Bushland (top) and Prairie View (bottom), TX. 44

Figure 4.4 Scatter plot of measured and CWB monthly soil moisture..... 45

Figure 4.5 DSSAT and VIC simulated monthly evapotranspiration at Bushland, TX (left) and Powder Mill, MD (right)..... 48

Figure 4.6 DSSAT and VIC simulated monthly runoff at Bushland, TX (left) and Powder Mill, MD (right)..... 50

Page

Figure 4.7 DSSAT and VIC simulated monthly drainage at Bushland, TX (left) and Powder Mill, MD (right). 51

Figure 4.8 Measured (black) and VIC modeled (red) daily soil moisture (top) and soil moisture anomalies (bottom) at BUTL in 2006 (left) and 2007 (right). 61

Figure 4.9 Measured (black) and VIC modeled (red) daily soil moisture (top) and soil moisture anomalies (bottom) at KING in 2005 (left) and 2007 (right). 62

Figure 4.10 Measured (black) and VIC modeled (red) daily soil moisture (top) and soil moisture anomalies (bottom) at WIST in 2001 (left) and 2002 (right). 63

Figure 5.1 Spatial distribution of the correlation between spring soil anomalies in each grid and averaged JJA SPI in the GP. [Red grids indicate correlation significance at 90% confidence level]. 69

Figure 5.2 Temporal variations in the 15-year sliding correlation between fall (a) and spring soil moisture (b) and summer SPI in zone 1 (thick line), zone 2 (thin line) and zone 3 (dashed line). [Straight lines indicate correlation significance at 90% confidence level]. 72

Figure 5.3 Temporal variations in soil moisture persistence in zone 1, zone 2, and zone 3. A 15-yr smoothing was applied to remove the high frequency variations. [Three straight lines indicate the general trends in soil moisture persistence in zone 1, zone 2, and zone 3]. 75

Figure 5.4 15-year sliding correlations between SST anomalies in Niño 3 and Niño 4 regions and summer SPI in zone 1 (thick line), zone 2 (thin line), and zone 3 (dashed line). [Straight line indicates correlation significance at 90% confidence level]. 77

Figure 5.5 Persistence of SST anomalies from April to JJA over Niño 3 and Niño 4 regions. [Straight line indicates the long term mean (0.49)]. A 15-yr smoothing was used to remove the high frequency variations in the persistence variations of the SSTA. 78

Page

Figure 5.6 Distribution of the ranked SST persistence values (solid line) from lowest to highest and the corresponding ten-year sliding correlations (dashed line) between spring soil moisture and summer SPI. [Straight lines indicate 90% significance level]..... 81

Figure 5.7 Composite mean monthly SST anomalies during 12 negative persistence years (top), 12 low positive persistence years (middle), and 12 high positive persistence years (bottom). The mean persistence is -0.26, 0.18, and 0.86, respectively..... 82

Figure 5.8 Scatter plot of SM and SST persistence in zone 1 during the period of 1920-2007. The mean SM and SST persistence are 0.45 and 0.49, respectively. 84

Figure 6.1 Anomalies of precipitation (P, mm day^{-1}), surface temperature (TS, °C), sea level pressure (PSL, mb), 500 mb geopotential heights (m) and 500 mb wind (m/s) (Z500+Wind) in D01_May experiment as compared to Con_May experiment..... 88

Figure 6.2 Anomalies of soil moisture (SM, mm^3/mm^3) in the D01_May experiment relative to the Con_May experiment in May, June, July, and August. 89

Figure 6.3 Distribution of soil field capacity (mm^3/mm^3) at approximately 17 cm depth in the U.S..... 86

Figure 6.4 Bootstrap precipitation (mm day^{-1}) upper 10% (left), median 50% (middle), and lower 90% (right) confidence fields for May, June, July, and August (from top to bottom)in the D01_May relative to the Con_May experiment. 91

Figure 6.5 Same as in Figure 6.1, but for the W01_May experiment. 93

Figure 6.6 Same as in Figure 6.4, but for the W01_May experiment. 94

Figure 6.7 Same as in Figure 6.1, but for the D30_May experiment. 96

Figure 6.8 Same as in Figure 6.4, but for the D30_May experiment. 97

Figure 6.9 Same as in Figure 6.1, but for the W30_May experiment. 99

Page

Figure 6.10 Same as in Figure 6.4, but for the W30_May experiment. 100

Figure 6.11 Averaged precipitation change (mm day^{-1}) (relative to control ensembles) over the U.S. Great Plains in May, June, July, and August in the four experiments. 103

Figure 6.12 Ten-day running average of soil moisture anomalies for the entire GP in the top 6 soil layers in D01_May experiment as compared to the control experiment. The mean soil moisture anomaly in the 10 soil layers are approximately -0.1 mm^3/mm^3 106

Figure 6.13 Same as in Figure 6.12, but for the W01_May experiment. The mean soil moisture anomaly in the 10 soil layers is ~0.04 mm^3/mm^3.. 107

Figure 6.14 Averaged precipitation anomalies over the U.S. Great Plains in April through August in the D01_April and W01_April experiments. PRECC indicates convective precipitation rate and PRECL represents large-scale precipitation rate. 110

LIST OF TABLES

Page

Table 3.1 Measured versus calculated field capacity, wilting point, and available water holding capacity (AWC) at Bushland, TX and Powder Mill, MD..... 18

Table 3.2 Description of all of the CAM3 soil moisture experiments described in this study..... 35

Table 4.1 Model performance statistics for VIC, DSSAT, and CWB soil moisture models..... 40

Table 4.2 Annual drainage, runoff, and evapotranspiration (all in mm) simulated by DSSAT and VIC at Bushland, TX and Powder Mill, MD..... 48

Table 4.3 VIC factorial analysis for Bushland and Powder Mill sites. 53

Table 4.4 Design of the 2^4 half-fraction factorial sensitivity analysis for Bushland and Powder Mill sites for VIC-3L model..... 55

Table 4.5 DSSAT factorial analysis for Bushland and Powder Mill sites. 58

Table 4.6 Design of the 2^4 half-fraction factorial sensitivity analysis for Bushland and Powder Mill sites for DSSAT model..... 59

Table 4.7 Model performance statistics for VIC model using Oklahoma Mesonet observations. 61

Table 5.1 The SM-precipitation correlations in zone 1 during the defined four categories. 84

Table 6.1 Length of time (in days) needed for each soil layer to return to normal condition (for the period of May to October) based on the D01_May and W01_May experiments. 98

1. INTRODUCTION

1.1 Research background

Drought is a natural hazard that occurs somewhere in the U.S. every year and has severe impacts on economy, environment, and society. The estimated average annual damage is approximately $6-8 billion with significant year-to-year variations (Wilhite 2000). For example, the 1988 drought caused an economic loss of $40 billion in the U.S. (American Meteorology Society 1997). The U.S. Great Plains (GP), one of the main agricultural regions and rangelands in North America, have been affected by a number of major droughts of the 20th century (Namias 1991). The impacts of droughts on GP agriculture and rangeland are numerous and well documented in early ecological research, for example, as a result of 1930s drought (Albertson et al. 1957; Weaver and Albertson 1936). The recent 2006 drought had widespread impacts across the GP, including damage to rangelands that has taken two years to recover (National Climate Data Center 2007). Therefore, drought is considered to be the most significant factor limiting agricultural production in the GP. Accurately predicting the interannual rainfall variation in the GP is critical to agricultural management and production.

Much of the research on interannual summer rainfall variation in the GP has been focused on external teleconnections including tropical Pacific sea surface temperatures (SST) variations (Hu and Feng 2001a; Ting and Wang 1997) and variations in the low-level southerly flow from the Gulf of Mexico (Hu and Feng 2001b; Paegle et al. 1996).

This dissertation follows the style of *Journal of Hydrometeorology*.

It has also been demonstrated that land surface processes are important factors that affect the climate because of the relatively long “land memory”, or persistence of the interactions between the surface and atmosphere (Shukla and Mintz 1982). However, little is known about land-atmosphere interactions in the GP because of the lack of long-term soil moisture observations. For the GP, understanding soil moisture-atmosphere interactions is particularly important since one of the main sources of atmospheric moisture for summer precipitation is from local land surface feedback (Laird et al. 1996). In addition, Koster et al. (2004) identified the Great Plains as one of the regions (hot spots) where soil moisture and precipitation are strongly coupled. Schubert et al. (2004) investigated the causes of the droughts in the Great Plains using ensembles of long-term NASA Seasonal-to-Interannual Prediction Project (NSIPP1) atmospheric general circulation model (AGCM) forced with observed SSTs and found that approximately two-thirds of the low-frequency rainfall variance can be explained by the soil moisture-precipitation interactions and the remaining variance can be attributed to the SST anomalies. However, there are very few studies that have examined the relationship between spring/winter soil moisture and summer precipitation in the GP due to the lack of soil moisture observations.

In this research, we will examine the role of local soil moisture anomalies and Niño SST anomalies in modulating summer precipitation and evaluate their relative significance in climate in the GP. The soil moisture anomalies and SST anomalies are defined as deviations from soil moisture climatology and SST climatology, respectively.

1.2 Objectives of the research

The objectives of this research are to answer three key questions:

1. What is the strength and nature of the relationship between antecedent soil moisture conditions and summer precipitation in the GP?
2. What is the strength and nature of the relationship between remote forcings (e.g., SSTs) and summer precipitation in the GP?
3. What are the physical mechanisms through which regional soil moisture anomalies influence summer precipitation?

To answer questions 1 and 2, statistical correlation analysis will be conducted including Pearson's correlation analysis, moving correlation, the lagged spatial correlation, and significance tests. The persistence of soil moisture memory and SSTs will also be investigated by calculating the correlation of spring soil moisture anomalies and SSTs with summer precipitation. These investigations will identify the length of soil moisture memory and examine the interacting effect of soil moisture and SSTs on summer precipitation in the GP. To answer question 3, NCAR Community Atmosphere Model and Community Land Model (CAM3-CLM3) will be used to identify the physical mechanisms through which soil moisture affects summer precipitation and how sensitive the climate system is to changes in the magnitude and spatial pattern of soil moisture anomalies. Completion of this research will improve our understanding of the roles of soil moisture and SSTs in climate which can further enhance the prediction of summer precipitation in this region. This is critically important since the GP is one of

main agricultural belts of North America and extreme summer moisture conditions can affect not only agriculture but also the economy of the region.

2. LAND-ATMOSPHERE INTERACTIONS*

2.1 Land surface processes

Land surface processes are considered to be important predictors of seasonal precipitation along with global sea surface temperatures (Hu and Feng 2004) and upper-troposphere circulation (Quiring and Papakyriakou 2005; Zhu et al. 2005). Snow cover and soil moisture are two of the most important indicators of land surface conditions. The persistence of snow cover and surface soil moisture anomalies is often called land memory, and it can last up to several months (Pielke et al. 1999; Vinnikov et al. 1996). Previous studies have demonstrated that snow cover anomalies can influence precipitation in India (Dickson 1984; Fasullo 2004; Hahn and Shukla 1976; Wu and Qian 2003), North America (Ellis and Hawkins 2001), Korea (Kripalani et al. 2002), and China (Qian et al. 2003). Other studies have shown that there is a link between Eurasian snow cover extent and summer air temperature in the United States (Qian and Saunders 2003). Like snow cover, soil moisture can also have a strong impact on the climate (Koster et al. 2003; Zheng and Eltahir 1998). Studies demonstrate that soil moisture can play an important role in summer climate predictions in the mid-latitudes where the influence of sea surface temperatures (SST) are typically weaker (Conil et al. 2007). However, the linkages between land surface processes and climate are strongly affected

---

* Part of this section is reprinted with permission from "Observed Observation relationship of sea surface temperatures and precedent soil moisture with summer precipitation in the U.S. Great Plains" by Meng and Quiring, 2009. *International Journal of Climatology*, **in press**, Copyright [2009] by Royal Meteorological Society.

by the persistence of strong external forcings, such as SST anomalies (Hu and Feng 2004). For example, Hu and Feng (2004) demonstrated that winter precipitation has a stronger impact on summer rainfall in southwestern United States when the influence of SST anomalies is weakened.

Soil moisture anomalies alter the local climate by modifying surface energy and water fluxes (Eltahir 1998). Anomalously wet soils lead to increased evaporation, decreased surface temperature, and enhanced convective precipitation. However, the strength of the relationship between antecedent spring soil moisture and summer precipitation is not uniform (i.e., it varies spatially and temporally) (Meehl 1994; Zhu et al. 2005). Zhu et al. (2005) examined the role of antecedent land surface conditions on North America Monsoon rainfall variability and found a statistically significant inverse relationship between monsoon precipitation in Arizona and western New Mexico and antecedent winter precipitation in the southwestern United States. Although soil moisture conditions play a major role in increasing summer precipitation in the southwestern United States, their influence is modulated by tropospheric circulation.

2.2 Strength of land-atmosphere coupling

Research has demonstrated that the strength of the soil moisture and precipitation coupling varies from place to place and from time to time. As mentioned above, Koster et al. (2004) identified that subsurface soil moisture and precipitation are strongly coupled in the transition zones, such as those found in the central Great Plains of North America, the Sahel, equatorial Africa, and India, but not in wet and dry climates. The spatial variation in the land-atmosphere interaction has also been documented in several

other studies (Guo et al. 2006; Koster et al. 2006). Recently, Zhang et al. (2008) used precipitation analysis and soil moisture from the Global Land Data Assimilation System (GLDAS) to assess the land-atmosphere coupling in boreal summer and found that regions of strong land-atmosphere coupling are mainly in arid to semiarid transition zones. These studies generally agree that soil moisture can have a significant impact on summer precipitation over mid-latitude land areas including the central United States. Within the regions of strong coupling, studies suggest that the feedback between soil moisture and precipitation is most significant in summer because this is when convective precipitation dominates. Using observed soil moisture and rainfall data in the state of Illinois, Findell and Eltahir (1997) found that soil moisture had a significant correlation with subsequent precipitation in the summer and little or no correlation for the rest of year. Therefore, the strong feedback between soil moisture and precipitation in summer is because soil moisture anomalies primarily influence convective precipitation, which is only dominant in summer.

The nature of the soil moisture-precipitation feedback also depends on the timing of initial soil moisture anomalies. Pal and Eltahir (2001) found the greatest soil moisture-rainfall sensitivity during June and July in NCAR regional climate model (RegCM). Oglesby (1989) imposed desert-like soil moisture anomalies on May 1st and March 1st in NCAR Community Climate Model and found that the initial soil moisture anomalies on May 1st persisted through summer while those imposed on March 1st did not. Recently, Kim and Wang (2007) investigated how summer precipitation responded to initial soil moisture anomalies imposed in spring and summer months and found a

significant difference in terms of magnitude. Summer precipitation response to dry soil moisture anomalies initialized on April 1st was larger than the response to wet soil moisture anomalies applied on the same date. This was reversed when soil moisture anomalies were imposed on August 1st.

2.3 Simulation of land-atmosphere interactions

To fully understand the physical mechanisms underlying the impact of antecedent soil moisture conditions on summer precipitation, General Circulation Models (GCMs) are often used by experimenting with different initial soil moisture conditions. For instance, using the National Center for Atmospheric Research (NCAR) Community Climate Model (CCM1), Olgesby and Erickson (1989) examined the role of soil moisture in prolonging and amplifying North American drought by testing different initial soil moisture conditions. They found that drier soils lead to increases in surface temperature, decreases in surface pressure, and decreases in precipitation. Similarly, Meehl (1994) used a number of GCMs (e.g., NCAR CCM0 and CCM1) to study the soil moisture–precipitation feedback associated with the Asian monsoon. Meehl (1994) found that increased soil moisture led to increases in monsoon precipitation. Recently, Chow et al. (2007) used a regional climate model (RCM) to examine the local effect of the initial spring soil moisture on summer precipitation over the Tibetan Plateau (TP) and the Yangtze River region of eastern China. They found that TP spring soil moisture has a positive relationship with summer precipitation over the TP and the Yangze River region and a negative relationship with summer precipitation in southern China. Georgescu et al. (2003) used the Regional Atmospheric Modeling System (RAMS) to

study the sensitivity of summertime precipitation over the Mississippi River Basin to initial soil moisture patterns and found that the precipitation response is most pronounced in the dry regime when heterogeneous soil moisture patterns were applied compared to homogeneous soil moisture patterns. In summary, atmospheric models have played a significant role in investigating the physical mechanisms in the land and climate systems.

Overall, previous research has shown that soil moisture can play an important role in climate, but that the strength of the influence is modulated by external atmospheric and oceanic forcings. In other words, the linkage between soil moisture and precipitation varies over space and time. In the GP, the relative significance of these factors and their influences on summer climate conditions as well as the nature of land-atmosphere interactions are not well understood.

In this study, I will examine the temporal and spatial variations in soil moisture/SST and summer precipitation in the U.S. Great Plains and investigate the physical mechanisms through which soil moisture anomalies affect summer precipitation.

3. DATA AND METHODOLOGY*

3.1 Study area

The U.S. Great Plains (GP), as defined in this study, include North Dakota, South Dakota, Nebraska, and portions of Minnesota, Montana, Wyoming, Colorado, Iowa, Kansas, Oklahoma, New Mexico, and Texas (Figure 3.1). This area, which has sometimes been referred to as the breadbasket of North America, is one of the most farming-dependent regions in the United States. Agricultural products in the northern part of GP worth more than $41.5 billion according to 2002 Census of Agriculture. The GP climate is characterized by a strong north-south temperature gradient and a strong east-west precipitation gradient (Ojima et al. 1999). Annual precipitation ranges from less than 200 mm in the west to over 1100 mm in the east of GP, but large season-to-season and year-to-year fluctuations are frequent and July and August are often hot and dry (Miller et al. 2002; Nuttonson 1965; Padbury et al. 2002). The GP experienced a number of major droughts during 20th century (Namias 1991). The 1930s and 1950s droughts were the most extensive and long lasting (Schubert et al. 2004). The impact of droughts on agriculture and rangeland in the GP are numerous and well documented in

---

* Part of this section is reprinted with permission from "A comparison of soil moisture models using Soil Climate Analysis Network observations" by Meng and Quiring, 2008. *Journal of Hydrometeorology*, 9, 641-659, Copyright [2008] by American Meteorological Society and with permission from "Observed Observation relationship of sea surface temperatures and precedent soil moisture with summer precipitation in the U.S. Great Plains" by Meng and Quiring, 2009. *International Journal of Climatology*, in press, Copyright [2009] by Royal Meteorological Society.

early ecological research (Albertson et al. 1957; Weaver and Albertson 1938). The drought of 1995-1996 resulted in about $5 billion in losses in the agricultural regions of the southern GP (National Assessment Synthesis Team, 2000, available at http://www.usgcrp.gov/usgcrp/Library/nationalassessment/overviewwater.htm). This is an example of how precipitation variability can have a major economic impact on the GP.

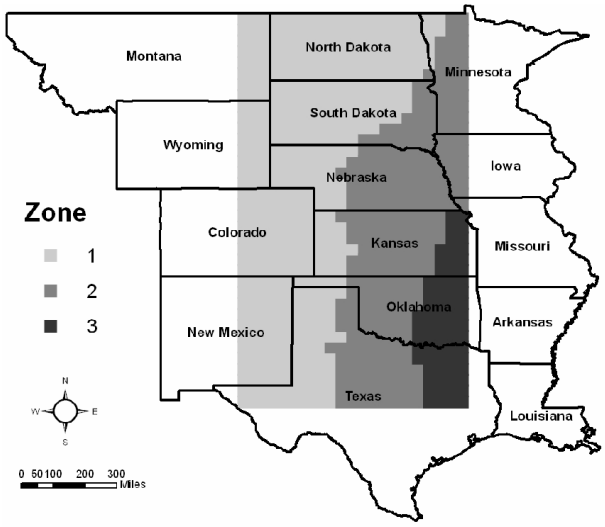

Figure 3.1 Great Plains study region and three zones based on annual precipitation. Zone 1 is the driest zone with mean annual precipitation of 419 mm; zone 2 is the moderate zone with mean annual precipitation of 668 mm; and zone 3 is the wettest with mean annual precipitation of 1010 mm.

3.2 Data

3.2.1 Observational soil moisture data

Observed soil moisture data were obtained from three Soil Climate Analysis Network (SCAN) sites (Bushland (35° 10' N, 102° 6' W) and Prairie View (30° 5' N, 95°

59' W), Texas and Powder Mill (39° 1' N, 76° 51' W), Maryland) and from three Oklahoma Mesonet sites (Butler (Butl) (35° 35'N, 99° 16'W) in Custer County, Kingfisher (King) (35° 52'N, 97° 54'W) in Kingfisher County, and Wister (Wist) (34° 59'N, 94° 41'W) in LeFlore County). For convenience, hereafter we use BL, PV, and PM to represent the Bushland, Prairie View, and Powder Mill sites, respectively, and use Butl, King, and Wist to represent the Butler, Kingfisher, and Wister sites, respectively.

BL is located in the Texas High Plains where the climate can be defined as continental steppe. This climate type is typical of interiors of continents and it is associated with relatively dry conditions. The average annual precipitation is approximately 482 mm and the wettest months occur between July and October (Larkin and Bomar 1983). BL is native, undisturbed rangeland that has never been plowed. The dominant vegetation is blue grama and buffalograss and the dominant soil type is well-drained dark brown silt clay (fine, montmorillonitic, mesic Typic Argiudolls). This site is relatively flat (1% slope).

PV is located in eastern Texas and it has a subtropical climate with humid, hot summers (Larkin and Bomar 1983). The average annual precipitation is roughly 1062 mm and May is the wettest month. This SCAN site is in an agriculture field that grows watermelons and the dominant soil type is a moderately well-drained fine sandy loam (fine-loamy, siliceous, thermic Typic Paleudalfs). PV is a relatively flat (1% slope) site.

PM is located in the coastal plains of Maryland and it has a continental climate with average annual precipitation of approximately 1100 mm (Quiring 2004). July and August are the wettest months. This site is covered by mixed grasses and the dominant

soil type is a well-drained dark brown sandy loam (coarse-loamy, siliceous, mesic Typic Paleudults). PM is a moderately sloped (4%) site.

The three Oklahoma Mesonet sites are located in different climate divisions, namely the West Central (Butl), Central (King), and Southeast (Wist) climate division. The average annual precipitation in West Central, Central, and Southeast climate divisions is 748 mm, 828 mm, and 1246 mm, respectively (source: http://climate.mesonet.org/county_climate/Products/Choose_By_County_Page.html). All of the three Mesonet sites are covered by mixed grass and the dominant soil type at these sites is silt clay loam (Butl), loam (King), and silt loam (Wist).

All of the Natural Resources Conservation Service SCAN sites use Hydra Probe sensors to measure soil water content. The Hydra Probe sends an electromagnetic signal (50 Mhz) into the soil. The reflected wave is associated with the electrical properties of the soil and can be used to determine the soil water content, conductivity, and salinity of the soil (www.stevenswater.com). The measured response (or dielectric permittivity) of the soil is related to soil water content using a calibration equation (Bosch 2004; Seyfried and Murdock 2004). A number of studies have evaluated the accuracy of the calibration equations and the Hydra Probe's inter-sensor variability (Seyfried and Murdock 2004; Seyfried et al. 2005). For example, Bosch (2004) demonstrated that the Hydro Probe measurements using lab-calibrated equations were within 0.04 $cm^3\ cm^{-3}$ of the observed water content and Seyfried et al. (2005) found that average difference in soil moisture content varies from 0.027 (silt) to 0.053 $cm^3\ cm^{-3}$ (clay) between soil specific calibrations and a general multi-soil calibration. Seyfried et al. (2005) also

examined inter-sensor variability by testing 30 sensors in four different fluids and found that the maximum coefficient of variability (CV) is 1.5% for individual sensor measurements. These studies indicate that the Hydra Probe can provide reliable and accurate measurements of soil water content under a variety of soil types and surface conditions (Seyfried et al. 2005).

The soil moisture sensor installed at Oklahoma Mesonet sites is a heat-dissipation sensor manufactured by Campbell Scientific, Incorporated (CSI) and is often called the CSI 229-L heat-dissipation sensor. This particular sensor was also used in the Department of Energy's Atmospheric Radiation Measurement network and the U.S. Department of Agriculture/Agricultural Research Service network (Schneider et al. 2003). The advantages of this sensor are its ease of use, minimal soil disturbance during installation, small size, ease of automation, and absence of potentially harmful radiation (Illston et al. 2008). A full description of this sensor and its installation procedures at Oklahoma Mesonet sites can be found in Illston et al. (2008). A series of the quality assurance (QA) procedures are applied to the observations and only data that passed the QA tests were used (Shafer et al. 2000).

The SCAN soil moisture data are measured hourly at 5, 10, 20, 50, and 100 cm depths (available at http://www.wcc.nrcs.usda.gov/scan/). These hourly measurements were aggregated to a daily mean value. In total, four years of observational data from BL and PM were used for evaluating the VIC and DSSAT models (e.g., 2004 and 2005 for BL; 2002 and 2004 for PM). For convenience, 2004BL, 2005BL, 2002PM, and 2004PM are used to refer to the four simulations for the VIC and DSSAT models. The monthly

averaged data (1997–2004) from PV and BL were only used for evaluating the CWB model since it simulates soil moisture using a monthly time step. For VIC and DSSAT, daily simulated soil moisture was compared to the in situ measurements. Both of the model-simulated and observed soil moisture data were aggregated to compare soil moisture in the top 50 cm of the soil. The measured soil moisture in the top 50 cm was calculated by averaging the observations at 5, 10, 20, 50 cm. For DSSAT and VIC, weighted soil moisture in the top 50 cm was calculated assuming that soil moisture is vertically homogeneously distributed within each layer. This method has been applied in other similar studies (Robock et al. 2003). A preprocessing procedure was used to remove all possible outliers in the soil moisture measurements. In addition, the first two years (1995 and 1996) SCAN data from PV and BL were eliminated due to instrumental problems.

Soil moisture data at Oklahoma Mesonet sites are collected at depths of 5, 25, 60, and 75 cm every 30 minutes. The soil moisture data were aggregated to daily values for use in this study. In total, 6 yr of observational data from these Mesonet sites were used for evaluating VIC models (2006 and 2007 for Butl; 2005 and 2007 for King; 2001 and 2002 for Wist). Only top 50 cm soil moisture from observations and model simulations was compared to provide model performance statistics. The Oklahoma Mesonet data were only used for validating VIC model.

3.2.2 Precipitation and temperature

The VIC model was driven using station-based measurements of daily maximum and minimum temperatures and precipitation. Additional meteorological and radiative

forcings, such as vapor pressure, shortwave radiation, and net longwave radiation, were derived using established relationships with maximum and minimum temperatures, daily temperature range, and precipitation (Kimball et al. 1997; Thornton and Running 1999).

The DSSAT model also requires daily precipitation, and minimum and maximum temperature data and these data were obtained from the same weather stations as VIC. The modeled solar radiation data used in the VIC model were also used in the DSSAT model. Thus, VIC and DSSAT were driven by the same meteorological and radiative forcing data.

Only monthly precipitation and minimum and maximum temperature data are required to run the CWB model and these data were obtained from the Parameter-elevation Regressions on Independent Slopes Model (PRISM) dataset (Daly et al. 1994). The PRISM data are available at: http://prism.oregonstate.edu/. The dataset contains 110 years of monthly precipitation and temperature data at ~4 km resolution (1895–present).

The 1-month SPI was calculated using the same PRISM precipitation data. In this study, the summer season is defined as June, July, and August (JJA). The average of the 1-month SPI values for June, July and August are used to represent summer precipitation conditions. The SPI is interpolated to 0.5° × 0.5° grid to match the resolution of VIC soil moisture data. Positive values of SPI indicate greater than median precipitation, while negative values indicate less than median precipitation (McKee et al. 1993; McKee et al. 1995).

3.2.3 Soil and vegetation characteristics

Soil characteristics, including saturated hydraulic conductivity, porosity, soil water content at field capacity and wilting point, soil depths, and available water capacity (AWC), were available from the NRCS and the Oklahoma Mesonet network. These soil characteristics can also be calculated from soil texture and organic content data using the Rawl and Brakensiek (1985) method. Table 3.1 shows measured (from NRCS) and calculated (using Rawl and Brakensiek (1985)) field capacity, wilting point, and available water holding capacity at Bushland, TX and Powder Mill, MD. Previous studies have demonstrated that proper parameterization of soil properties, such as hydraulic conductivity and wilting point, has a large impact on the accuracy of the model simulations (Xue et al. 1996; Xue et al. 1997). To account for the uncertainties in the soil parameters, four different runs were conducted at BL and PM, namely VIC-1 (using calculated soil parameters), VIC-2 (using measured soil parameters), DSSAT-1 (using calculated soil parameters), and DSSAT-2 (using measured soil parameters). All of the parameters required for VIC and DSSAT were set to be as identical as possible.

The additional soil parameters required by VIC, such as variable infiltration curve parameter and maximum velocity of flow were obtained from the calibrated regional simulations performed by Maurer et al. (2001, 2002). They selected a number of basins where observed streamflow data was available and then calibrated the VIC-simulated streamflow by adjusting soil parameters describing soil depth, baseflow drainage and infiltration capacity of the soil layers (Maurer et al. 2001; Maurer et al. 2002). This procedure is described in greater detail by Maurer et al. (2001, 2002).

Table 3.1 Measured versus calculated field capacity, wilting point, and available water holding capacity (AWC) at Bushland, TX and Powder Mill, MD.

Layer	Measured field capacity (%)*	Measured wilting point (%)*	Measured AWC*	DSSAT Calculated field capacity (%)	DSSAT Calculated wilting point (%)	Calculated AWC
Bushland, TX (Silty Clay)						
0-18 cm	24.4	12.6	11.8	34.5	17.9	16.6
18-61 cm	28.8	17.5	11.3	36.5	23.2	13.3
61-94 cm	25.6	15.2	10.4	33.3	20.1	13.2
94-127 cm	27.1	14.5	12.6	30.0	18.2	11.8
127-160 cm	27.2	14.5	12.7	27.5	17.1	10.4
160-183 cm	22.0	10.1	11.9	31.2	18.5	12.7
183-229 cm	22.6	11.1	11.5	33.9	20.0	13.9
Powder Mill, MD (Sandy loam)						
0-14 cm	13.4	3.5	9.9	18.5	8.0	10.5
14-29 cm	9.8	2.7	7.1	15.9	6.5	9.4
29-46 cm	10.6	2.5	8.1	16.0	6.0	10.0
46-83 cm	7.9	3.6	4.3	13.9	6.9	7.0
83-129 cm	6.8	3.0	3.8	11.2	6.3	4.9

* indicates gravimetric water content

The initial soil moisture for all of the model runs was set at field capacity. Land cover and vegetation parameters were derived using the global vegetation classification developed by Hansen et al. (2000). Since the vegetation at the BL and PM SCAN sites is mixed grass, the DSSAT grass module (CROPGRO-Bahia) was used.

3.2.4 Sea surface temperatures

The extended reconstructed sea surface temperature data (ERSST) v.3 (Smith et al. 2008) were used to calculate monthly SST anomalies over Niño 3, Niño 4, and Niño 3.4 regions. The anomalies are computed with respect to the 1971-2000 climatology (Xue et al. 2003).

3.3 Model descriptions

Three soil moisture models and one general circulation model were used in this study. The descriptions of these models are as follows.

3.3.1 VIC hydrological model

The Variable Infiltration Capacity (VIC) hydrological model was first developed as a single-layer land surface model by Wood et al. (1992) and it was later expanded to a two-layer model by Liang et al. (1994). The VIC model is a semi-distributed hydrological model that is capable of representing subgrid-scale variations in vegetation, available water holding capacity, and infiltration capacity (Liang et al. 1994). The influence of variations in soil properties, topography, and vegetation within each grid cell are accounted for statistically by using a spatially varying infiltration capacity. VIC utilizes a soil-vegetation-atmosphere transfer scheme (SVATs) that accounts for the

influence of vegetation and soil moisture on land-atmosphere moisture and energy fluxes and the fluxes are balanced over each grid cell (Andreadis et al. 2005). The model has been utilized in basin-scale hydrological modeling (Abdulla et al. 1996), continental-scale simulations associated with the North American Land Data Assimilation System (NLDAS) (Wood et al. 1997), and global-scale applications (Nijssen et al. 2001). A thorough evaluation of VIC was undertaken as part of NLDAS and the results indicated that soil moisture is generally well-simulated by the VIC model (Robock et al. 2003).

The model divides the subsurface into three soil layers. Each layer is characterized by a variety of parameters, such as bulk density, infiltration capacity, saturated hydraulic conductivity, soil layer depths, soil moisture diffusion parameters. The land surface is described by approximately 11 land-cover types. The vegetation types are characterized by their leaf area index (LAI), canopy resistance, and relative fraction of roots in each of the soil layers. Roots can extend to layer 1 (usually ~10 cm) or deeper layers depending on vegetation and soil type. Bare soil (no vegetation cover) can also be simulated by the model.

The evapotranspiration from each land-cover type is simulated using vegetation-class specific potential evapotranspiration (ET_p), canopy resistance, aerodynamic resistance to the transfer of water, and architectural resistance coefficients. In this model, the ET_p includes evaporation from the canopy layer of each vegetation class, transpiration from each vegetation class, and evaporation from bare soil. Total evapotranspiration (ET_p) over each grid cell is calculated as the area-weighted sum of these three components for each vegetation class. For each land-cover type, there is a

single canopy layer and three soil layers. The top layer is the most dynamic layer of the soil column and it rapidly responds to daily weather (e.g., precipitation and temperature). Soil moisture in the lower layers of the soil varies more slowly (e.g., they have a lagged response to weather). A detailed description of the VIC model is provided by Liang *et al.* (1994, 1996a, 1996b). The water balance mode of the VIC model was used in this study.

3.3.2 DSSAT soil moisture model

The soil water module in the Decision Support System for Agrotechnology Transfer (DSSAT) crop model was developed originally by Ritchie and Otter (1985) for CERES-Wheat model and was incorporated into all of the DSSAT v3.5 and newer crop models. The one-dimensional water model computes the daily changes in soil moisture due to rainfall and irrigation infiltration, vertical drainage, unsaturated flow, soil evaporation, and root water uptake. The water module in the DSSAT can be represented as follows

$$\Delta S = P + I - T - E - R - D \tag{3.1}$$

where, P is precipitation, I is irrigation, T is plant transpiration, E is soil evaporation, R is runoff, D is drainage. These processes directly affect the water content in the soil profile.

DSSAT requires information about the soil water content for the lower limit of plant water availability (e.g., the lowest volumetric water content at which plants can extract water (corresponds closely to the permanent wilting point)), the drainage upper limit (e.g., the highest volumetric water content of a soil after thorough wetting and gravity drainage (closely related to field capacity)), and field saturation (e.g., the

volumetric water content of a soil when all pores of the soil are filled with water) to calculate processes such as root uptake, drainage, and soil evaporation. These soil parameters are necessary for all layers of the model due to the heterogeneity in the subsurface. The depth for each layer must be specified. In general, each layer should be approximately 20 cm deep for the top layers and approximately 30 cm for lower layers, with a total number of layers between 7 to10 layers (Ritchie 1998). Several of the soil inputs are only required for the soil surface; these include the albedo of the soil, the limit of first stage soil evaporation, the runoff curve number and drainage coefficient. These variables are used to calculate the various components of the water balance in equation (3.1) (Ritchie 1998).

Daily runoff is computed in the DSSAT model using a modifiedf USDA-Soil Conservation Service curve number method (Williams et al. 1984). Soil water drainage is estimated based on a 'tipping bucket' approach. The amount of drainage is calculated using the drainage coefficient, layer depth, volumetric water content, and the drainage upper limit of soil water content. Upward unsaturated flow is approximated using a normalized soil water diffusion equation operating on a daily time-step (Ritchie 199*8*).

Evaporation from the soil surface, root water uptake, and plant transpiration are based on methods developed by Ritchie (1972). Potential evapotranspiration (PE) can be calculated using one of four options within DSSAT (Sau et al. 2004). The Priestley and Taylor (1972) method was employed in this research. Once PE has been calculated, it is partitioned into potential soil evaporation and potential plant transpiration based on the faction of solar energy reaching the soil surface and the LAI (Jones et al. 2003).

Calculation of actual soil evaporation is based on a two-stage process: free soil evaporation and soil-limiting evaporation stages. The actual soil evaporation is the minimum of the free soil evaporation and soil-limiting evaporation on a daily basis. The actual plant transpiration is considered to be the minimum of the potential plant transpiration and potential root water uptake. The potential root water uptake is estimated by calculating a maximum water flow to roots in each layer and summing these values.

3.3.3 Climatic water budget (CWB)

A modified version of a well-established climatic water budget (CWB) model (Mather 1978; Thornthwaite 1948; Thornthwaite and Mather 1955) is the third method used to simulate soil moisture in the study area. The CWB is a one-dimensional model that calculates the daily or monthly changes in soil moisture storage due to evaporation, precipitation, infiltration, and runoff. The CWB assumes that the subsurface can be represented as a single soil layer. Soil moisture storage will increase whenever precipitation exceeds climatic demand for water (e.g., PET). When the climatic demand is greater than precipitation, then soil moisture storage will be depleted. Thus, the difference between precipitation and actual evapotranspiration is the estimated soil moisture change for a specific period of time.

The CWB model requires precipitation and temperature data as well as data for describing soil properties. Among the soil properties, the available water capacity data (AWC) of the soil is a key component in calculating soil moisture since it represents the maximum amount of water that can be held in the soil due to capillary. AWC represents

the difference between field capacity (FC) and permanent wilting point (PWP). PWP is a function of soil porosity and pore size and it represents the lower limit of plant-available soil moisture (Miller and White 1998).

Potential evapotranspiration (PE) is calculated using the Thornthwaite method which estimates PE based on temperature and the number of hours of daylight (Thornthwaite 1948). If potential evapotranspiration exceeds precipitation, a soil moisture loss function developed by Willmott et al. (1985) is applied to calculate soil moisture depletion. When calculated soil moisture is greater than FC, surplus water (S_i) is calculated as the difference of soil moisture and FC. Runoff generated from surplus water is calculated as (Mather 1978)

$$Q = 0.5(S_i + Q_{i-1}) \quad (3.2)$$

where Q_{i-1} is the runoff from the previous time step. This model assumes that half of the surplus in a given time step is converted into stream flow and the other half is held over to the next time step where it is added to the surplus for that period of time. In this study, CWB is run on a monthly time step.

3.3.4 CAM3.0

The stand-along mode of the Community Atmosphere Model (CAM3) was developed by the National Center for Atmospheric Research (NCAR) through collaboration with scientists in the academic community. In its stand-along mode, CAM3 is integrated with the Community Land Model version 3 (CLM3) (Bonan et al. 2002; Oleson et al. 2004), a thermodynamic sea ice model, and a data ocean or optional slab ocean model (Collins et al. 2006). The formulation of the physics and dynamics of

CAM3 is described by Collins et al. (2004, 2006). In this study, CAM3 is forced with prescribed climatological observed sea surface temperature and sea ice coverage. The dynamics of the atmosphere in CAM3 include Eulerian spectral, semi-Lagrangian dynamics, and finite-volume (FV) dynamics (Lin 2004). In this study, we employed the FV dynamical core with a horizontal resolution of 2° latitude by 2.5° longitude and a total of 26 levels in the vertical direction.

CLM3 simulates energy, moisture, and momentum fluxes between land and atmosphere. It has 10 unevenly vertical soil layers, up to 5 snow layers, and 1 vegetation layer (Dai et al. 2003). Spatial land surface heterogeneity in CLM3 is represented as a nested subgrid hierarchy in which grid cells are composed of multiple land units, snow/soil columns, and plant functional types (PFTs). The specific land units within each grid are glacier, lake, wetland, urban, and vegetated. The vegetated land unit consists of a single column with up to four PFTs. The snow/soil column is represented by 10 unevenly vertical layers for soil and up to 5 layers for snow depending on snow depth. The details of CLM3 can be found in Oleson et al. (2004).

3.4 Methods

3.4.1 Methods for validating soil moisture models

Error analysis

Model performance was evaluated using the root mean square error (RMSE), mean absolute error (MAE), Pearson's correlation coefficient (r), and the coefficient of efficiency (E) (Legates and McCabe 1999). It has been suggested that MAE should be used instead of RMSE for evaluating model performance since it is an unambiguous

measure of average error magnitude (Willmott and Matsuura 2005). In this research, both RMSE and MAE are provided for ease of comparison with previous studies. The coefficient of efficiency (E) represents the degree of fit between modeled and observed soil moisture and is calculated as follows:

$$E = 1.0 - \frac{\sum_{i=1}^{N}(O_i - P_i)^2}{\sum_{i=1}^{N}(O_i - \overline{O})^2} \tag{3.3}$$

where the overbar denotes the mean for the entire time period of the evaluation, *P* is model-simulated data, *O* is the observed data, *N* is the number of days in a year. E ranges from -∞ to 1.0, a value of 1 indicates perfect agreement between the modeled and observed data and a value less than zero indicates that the observed mean is a better predictor than the model.

Sensitivity analysis

The accuracy of the soil moisture simulations are influenced by the soil parameter estimates (Xue et al. 1996; Xue et al. 1997). Undoubtedly these parameters are associated with a variety of errors and uncertainties. A sensitivity analysis was employed to quantify the impact of parameter uncertainty on model performance. A sensitivity analysis is useful for determining how model parameters influence model results and for identifying parameters that have the greatest influence on model performance (Gebremichael and Barros 2006; Yildiz and Barros 2007). The first stage of the sensitivity analysis involved varying each parameter independently of the others and measuring how it influences model performance. A total of 16 parameters were selected

from each model for the sensitivity analysis and each parameter was varied by an arbitrary constant ±20%. Based on simulations at BL and PM using data from 2004, the five most significant parameters were further examined using a factorial analysis approach. Rather than employ the traditional "change one parameter at a time" approach, the factorial design method was employed (Box et al. 1978). This method of sensitivity analysis accounts for the interacting effects of model parameters (Gebremichael and Barros 2006; Yildiz and Barros 2007). Compared with Monte Carlo simulations, this method is simpler and less computationally intensive. It has been applied to many different environmental models (Barros 1996; Liong et al. 1995). The half-fraction factorial design of 5 parameters (2^5) was employed which resulted in 16 simulations for each model.

3.4.2 Methods for analyzing the soil moisture-precipitation relationship

Ward's method of cluster analysis was used to divide the GP into three relatively homogeneous precipitation regions based on long-term (1910-2007) mean annual precipitation. These regions are referred to as low (mean precipitation = 419 mm), median (mean precipitation = 668 mm), and high (mean precipitation = 1010 mm) and they comprise 56%, 35%, and 9% of the GP study region, respectively.

An index of SST persistence was calculated to represent the persistence of SST anomalies in the Niño 3, Niño 4, and Niño 3.4 regions (Chao et al. 2000; Hu and Feng 2004). Here SST persistence is defined as the lagged correlation of the SST anomaly (SSTA) in spring (April) versus summer (June-August) and measures whether the SSTA

pattern persists from spring to summer. The lagged spatial correlation r(*t0*, *t1*) at time *t0* with respect to the time lag *t1* is calculated by:

$$r(t0,t1) = \frac{\sum_x \sum_y (T(x,y,t0) - \overline{T(x,y,t0)})(T(x,y,t1) - \overline{T(x,y,t1)})}{\sqrt{\sum_x \sum_y (T(x,y,t0) - \overline{(T(x,y,t0))})^2 \sum_x \sum_y (T(x,y,t1) - \overline{T(x,y,t1)})^2}} \quad (3.4)$$

Here *T(x, y, t)* is the SST anomaly at location *(x, y)* and time *t0*, $\sum_x \sum_y$ represents the double sum with respect to *(x, y),* and the overbar represents the mean anomaly averaged over the domain. Persistence (or the lagged spatial correlation) ranges from -1 to 1 with a value of 1 indicating that the spatial pattern of SST anomalies at *t0* is identical to that at *t1*. An examples of SST anomaly patterns in a year with strong positive persistence (r = 0.89) is shown in Figure 3.2 and its corresponding histograms in Figure 3.3. Figure 3.4 and Figure 3.5 show SST anomaly patterns and histogram in a year with negative persistence. It can be seen that in a high persistence year the spatial pattern of SST anomalies in April is similar to that in JJA (Figure 3.2). Figure 3.3 suggests that the differences in SST anomalies in April versus JJA are mostly (e.g., approximately 40% of the domain) between -1 and 0. In a low persistence year, the spatial pattern of SST anomalies in April is quite different from the pattern in JJA (Figure 3.4). A dominant cool region in April shifted to the southwestern corner and a much warmer region developed over the eastern part of the domain. Figure 3.5 shows that the majority of the differences between the SST anomalies in April and JJA are between -2 and -1 (e.g., 27% of the domain). Comparing Figure 3.2 and Figure 3.4 illustrates that years with strong positive persistence are associated with a static spatial patterns of SST anomalies, while years with low or negative persistence are associated with large changes in the

spatial pattern of SST anomalies. The lagged spatial correlation method has been previously applied in both atmospheric studies (Mo and Ghil 1987) and oceanographic studies (Chao et al. 2000) to describe shifts of circulation regimes and climate variations. In this study this method will be applied to both the SST and soil moisture data to describe the relative stability of the spatial patterns of SST and soil moisture (SM) anomalies. SM persistence is defined as the lagged spatial correlation of soil moisture anomalies on May 1st versus summer (JJA).

3.4.3 Methods for simulating the effect of soil moisture on precipitation

Experiment design

Due to the lack of observed soil moisture data, a soil moisture climatology (normal soil moisture conditions) was created using an 8-year model simulation driven with climatological SSTs. After the 8-year simulation, the soil moisture difference between the current year and previous years are relatively small, thus we assume that soil moisture has reached equilibrium. This model-based soil moisture climatology is used to initialize the model in subsequent simulations. This method was used by Kim and Wang (2007).

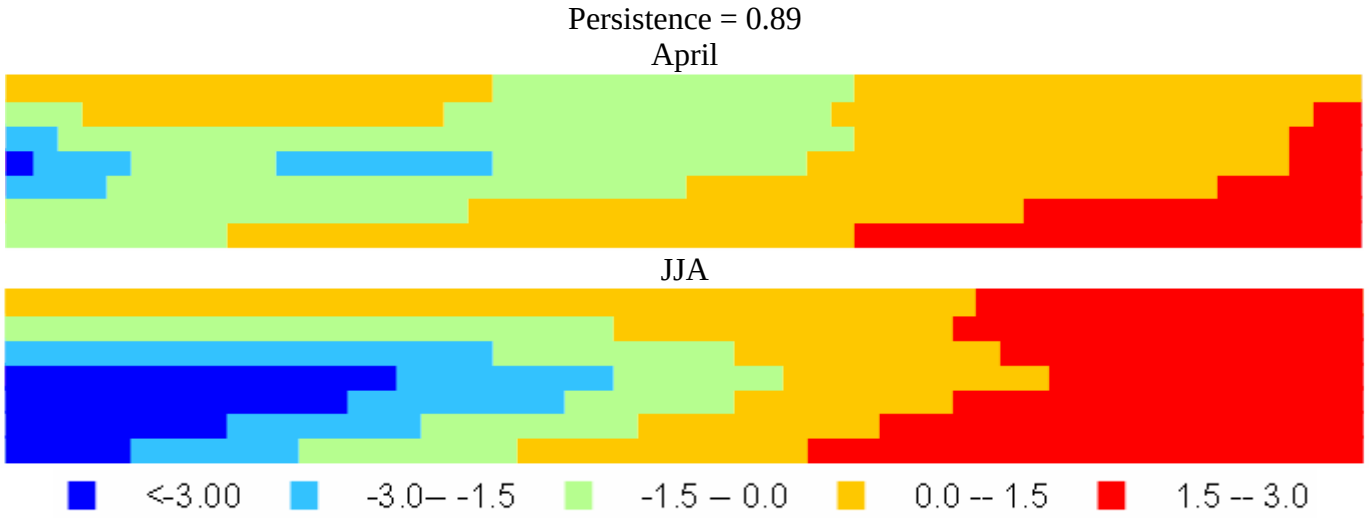

Figure 3.2 Spatial distributions of SST anomalies in a high persistence (0.89) year from April (top) to JJA (bottom).

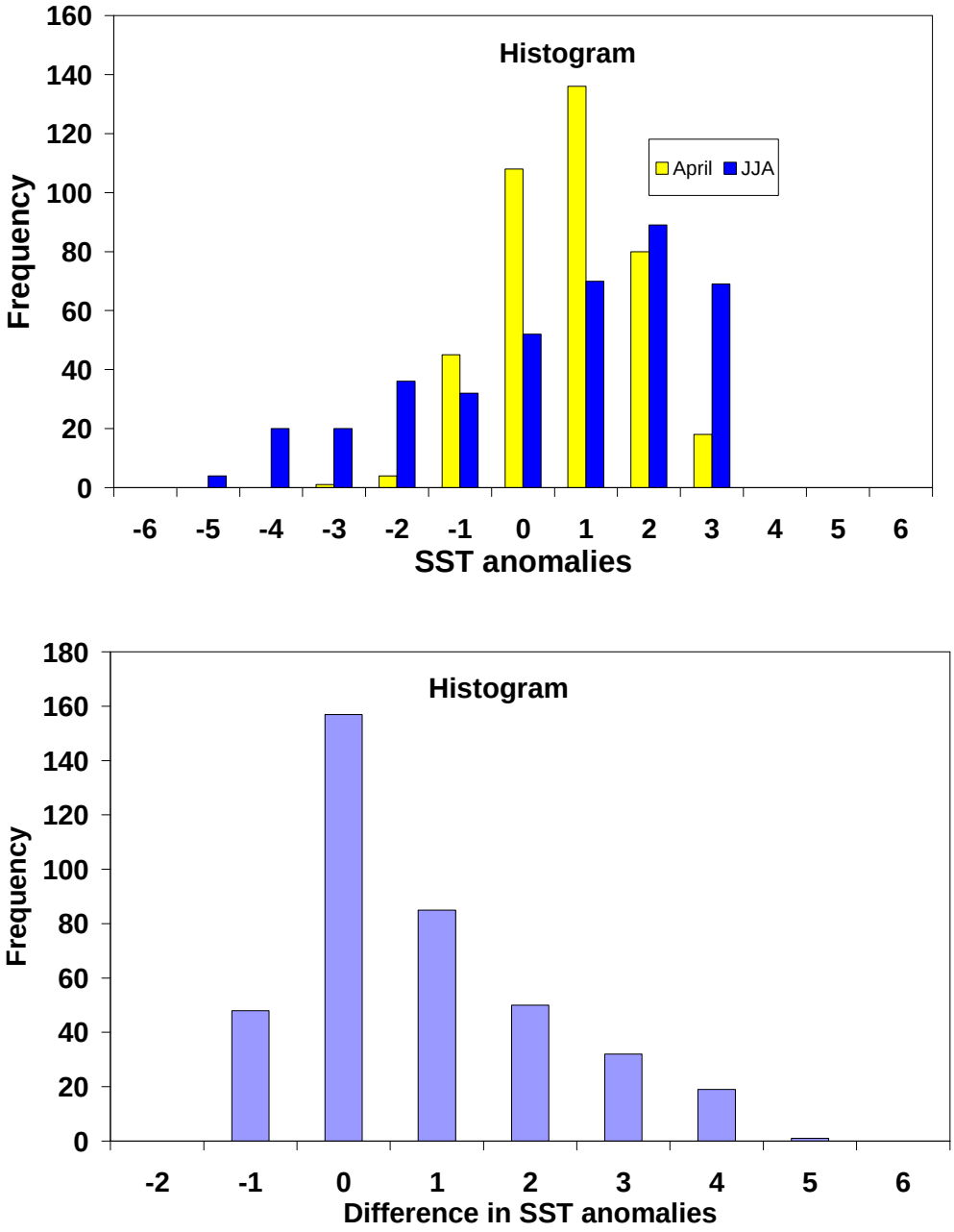

Figure 3.3 Histograms of SST anomalies in April and JJA (top) and the differences in SST anomalies between April and JJA (bottom) in Figure 3.2.

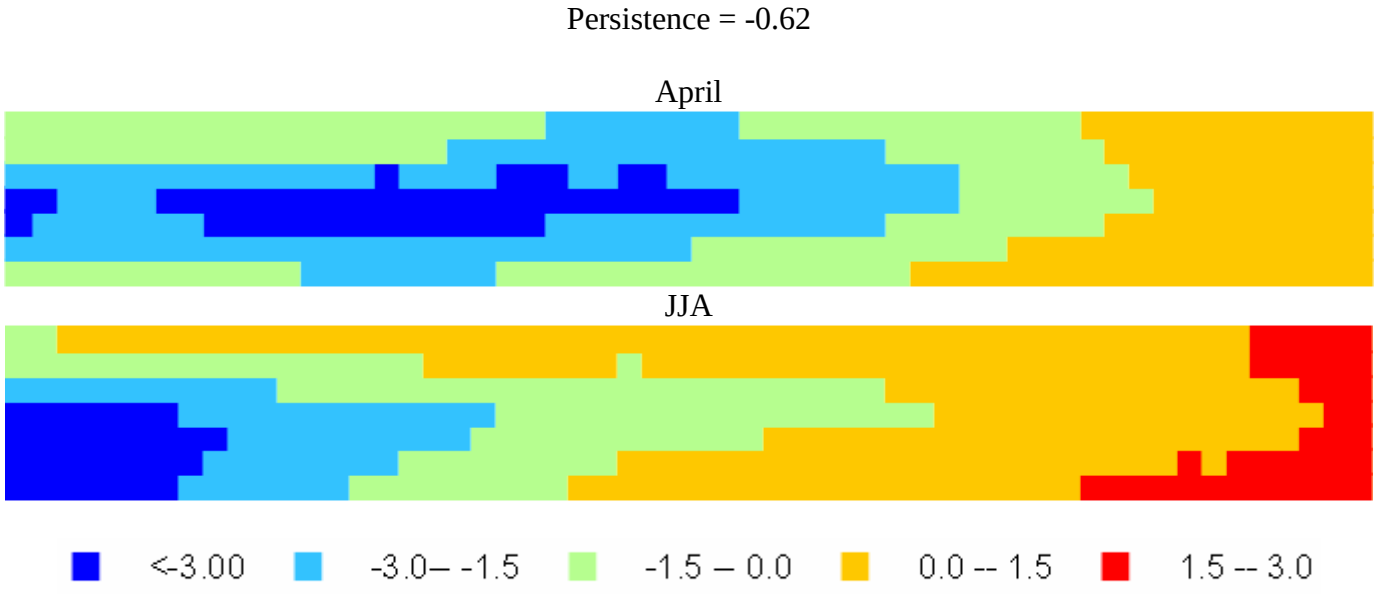

Figure 3.4 Spatial distributions of SST anomalies in a low persistence (-0.62) year from April (top) to JJA (bottom).

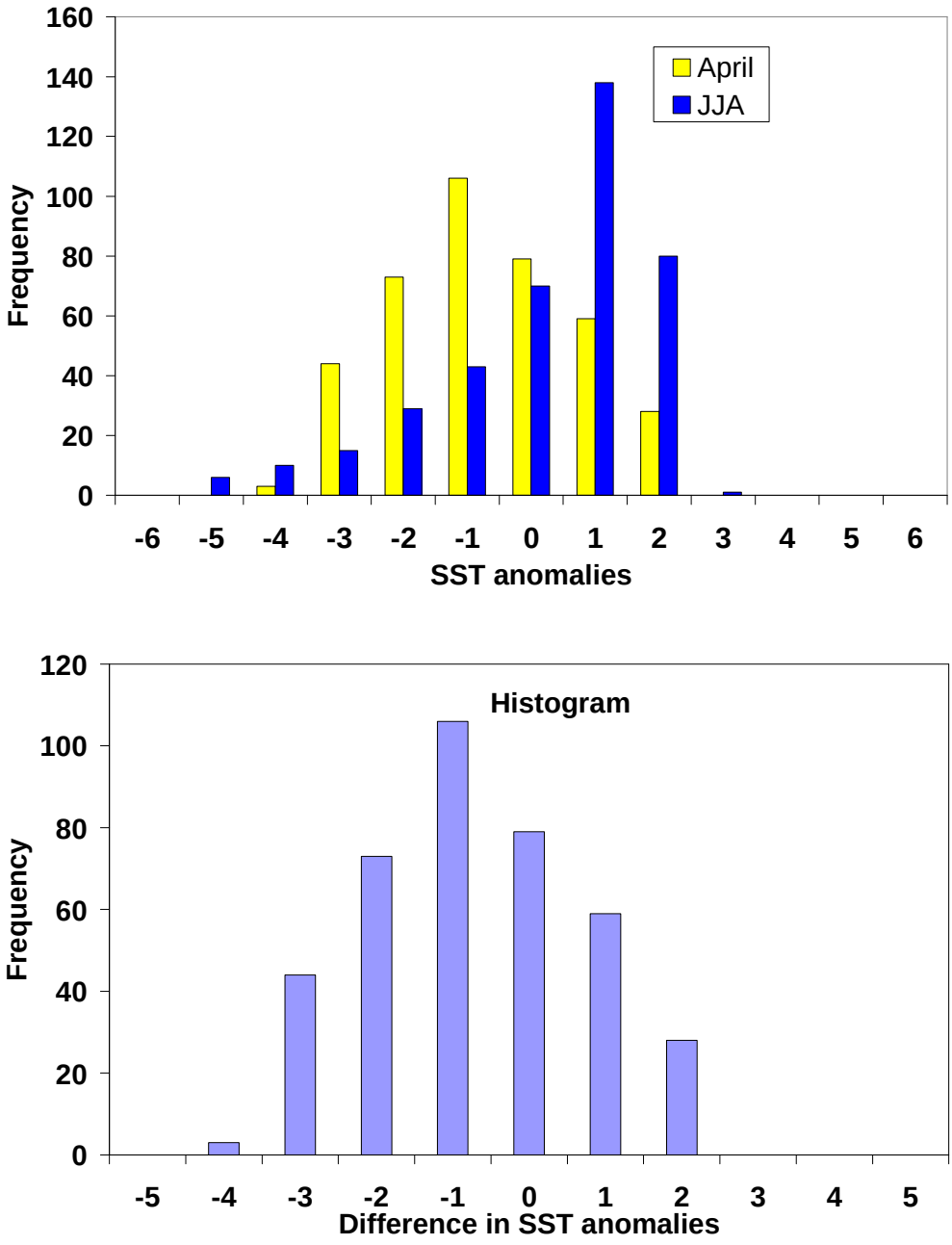

Figure 3.5 Histograms of SST anomalies in April and JJA (top) and the differences in SST anomalies between April and JJA (bottom) in Figure 3.4.

A series of sensitivity experiments were performed to investigate the influence of spring soil moisture anomalies on summer precipitation in the GP. Due to the model's non-linear response, five-member ensemble simulations were conducted in each experiment and the average of the five-member ensemble was used to interpret the results. Five experiments were conducted including a control experiment, dry experiment, dry persistence experiment, wet experiment, and wet persistence experiment (see Table 3.2 for experiment descriptions and abbreviations). For the control (Con), dry (D01), and wet (W01) experiments, our experimental design follows Kim and Wang (2007). In the control experiment, the spring soil moisture is set at a level close to the model climatology on the first day of the simulation (at 100%, 99%, 98%, 97%, and 96% of the climatological soil moisture respectively). In the wet/dry experiment, the spring soil moisture in each simulation is higher or lower than its counterpart in the control ensemble by the same amount (e.g., set to 20%, 19%, 18%, 17%, and 16% of the climatological soil moisture, respectively, for the ~80% dry anomaly case). Initial soil moisture anomalies are applied as a percentage increase or decrease of soil moisture climatology on the first of May 1st. To be consistent with our previous observational analysis (Meng and Quiring 2009a), initial soil moisture on May 1st is used to represent spring season soil moisture conditions. For the dry persistence (D30) and wet persistence (W30) experiments, a fixed soil water content is applied to the 10 soil layers for the first entire month to examine how the persistence of soil moisture anomalies affects summer precipitation. Soil moisture contents of 0.05 and 0.36 mm^3/mm^3 at all grid cells are used to represent the dry soil moisture anomaly and wet soil moisture anomaly in the

persistence cases since they approximately represent an 80% decrease and 80% increase in mean soil water content, respectively. The focus of this study is on the GP (30°-50°N, 95°-105°W) which we define as including North Dakota, South Dakota, Nebraska, and portions of Minnesota, Montana, Wyoming, Colorado, Iowa, Kansas, Oklahoma, New Mexico, and Texas. This region has been described in detail in Section 3.1 (Meng and Quiring 2009a).

Table 3.2 Description of all of the CAM3 soil moisture experiments described in this study.

Experiment Name	**Start Date**	**Initial Soil Moisture** (% of climatology)	**Description** (all experiments are based on 5 ensemble members and use climatological SSTs)
Con_May	May 1st	100, 99, 98, 97, 96	Control experiment initialized with climatological soil moisture on May 1
Con_Apr	April 1st	100, 99, 98, 97, 96	Control experiment initialized with climatological soil moisture on April 1
D01_May	May 1st	20, 19, 18, 17, 16	Dry soil moisture anomalies were applied on May 1
D30_May	May 1st	20, 19, 18, 17, 16	Dry soil moisture anomalies were applied and May 1 and held constant for the rest of May
W01_May	May 1st	180, 179, 178, 177, 176	Wet soil moisture anomalies were applied on May 1
W30_May	May 1st	180, 179, 178, 177, 176	Wet soil moisture anomalies were applied and May 1 and held constant for the rest of May
D01_Apr	April 1st	20, 19, 18, 17, 16	Dry soil moisture anomalies were applied on April 1
W01_Apr	April 1st	180, 179, 178, 177, 176	Wet soil moisture anomalies were applied on April 1

Bootstrap technique

The bootstrap method is used to test the significance of the difference between the control and perturbed runs (Efron and Tibshirani 1993). The bootstrap is a computer-based resampling procedure for drawing statistical inferences. It is used to determine the sampling distribution of a parameter or test statistic and to provide a method for estimating the standard error that parameter (Efron and Tibshirani 1993; Sklut 2005). The advantage of using the bootstrap is that it only requires independent samples and it can be used the when sampling distribution is unknown. The bootstrap algorithm repeatedly samples with replacement from the original dataset of size n and produces a large number (B) of independent bootstrap samples of size n. Then each of the bootstrap samples is used to calculate a new estimate of the parameter. When B is very large, the standard error of the estimate becomes very stable. In this study, 200 samples were generated from repeatedly sampling (with replacement) from the 5 difference fields that were created by comparing the perturbed model runs with the control. The 200 samples were then sorted at each of the grid points. The upper and lower 90% limits, which correspond to the 190^{th} and 10^{th} bootstrap samples, were selected to test the significance of the differences observed in the perturbed runs. The differences are classified as statistically significant if they appear in both the 190^{th} and 10^{th} bootstrap samples.

4. VALIDATION OF SOIL MOISTURE MODELS*

4.1 Introduction

Due to the lack of field measurements, models are often used to monitor soil moisture conditions. Therefore, it is important to find a model that can accurately simulate soil moisture under a variety of land surface conditions. In this section, three models of varying complexities (Variable Infiltration Capacity (VIC), Decision Support System for Agrotechnology Transfer (DSSAT) and Climatic Water Budget (CWB)) that are commonly used for simulating soil moisture were evaluated and compared using soil moisture data (1997-2005) from three Soil Climate Analysis Network (SCAN)) sites (Bushland, TX, Prairie View, TX, and Powder Mill, MD). The VIC soil moisture simulations were further evaluated using soil moisture data from three Oklahoma Mesonet sites (Butler (Butl) in Custer County, Kingfisher (King) in Kingfisher County, and Wister (Wist) in LeFlore County). The purpose of this section is to evaluate model performance and select the most suitable model for simulating long-term soil moisture for analyzing land-atmosphere interactions in the GP.

4.2 VIC and DSSAT soil moisture simulations

Since both VIC and DSSAT models were run on a daily time step, the performance of these two models can be directly compared at Bushland (BL) and

---

* Part of this section is reprinted with permission from "A comparison of soil moisture models using Soil Climate Analysis Network observations" by Meng and Quiring, 2008. *Journal of Hydrometeorology*, **9**, 641-659, Copyright [2008] by American Meteorological Society.

Powder Mill (PM) (Figure 4.1 and Figure 4.2). DSSAT and VIC both did well in simulating the annual cycle of soil moisture and daily patterns of the wetting and drying in response to weather conditions, as evidenced by the relatively strong correlations. The correlation between the model-simulated and measured soil moisture ranged from 0.51 to 0.95, with an average of 0.76 (Table 4.1).

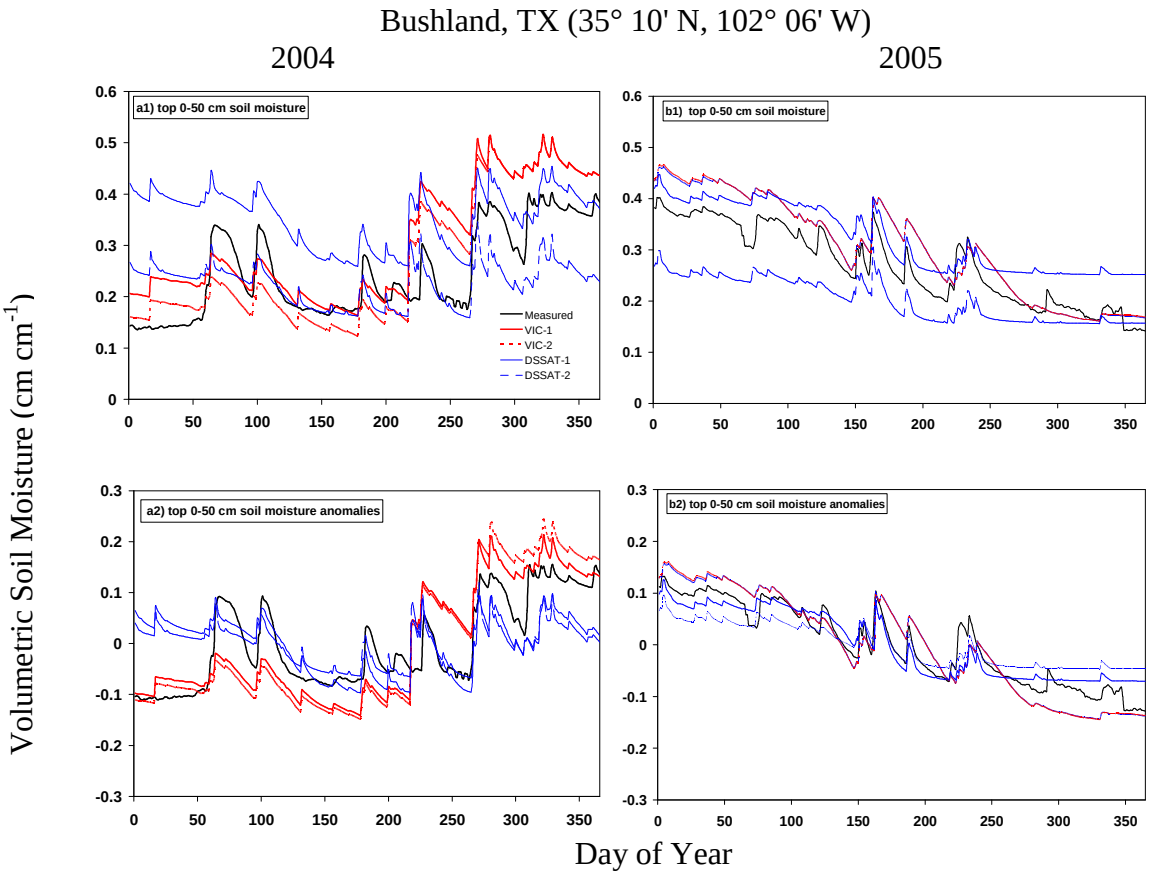

Figure 4.1 Measured (black) and modeled (DSSAT (blue) and VIC (red)) daily soil moisture (top) and soil moisture anomalies (bottom) at Bushland, TX in 2004 (left) and 2005 (right).

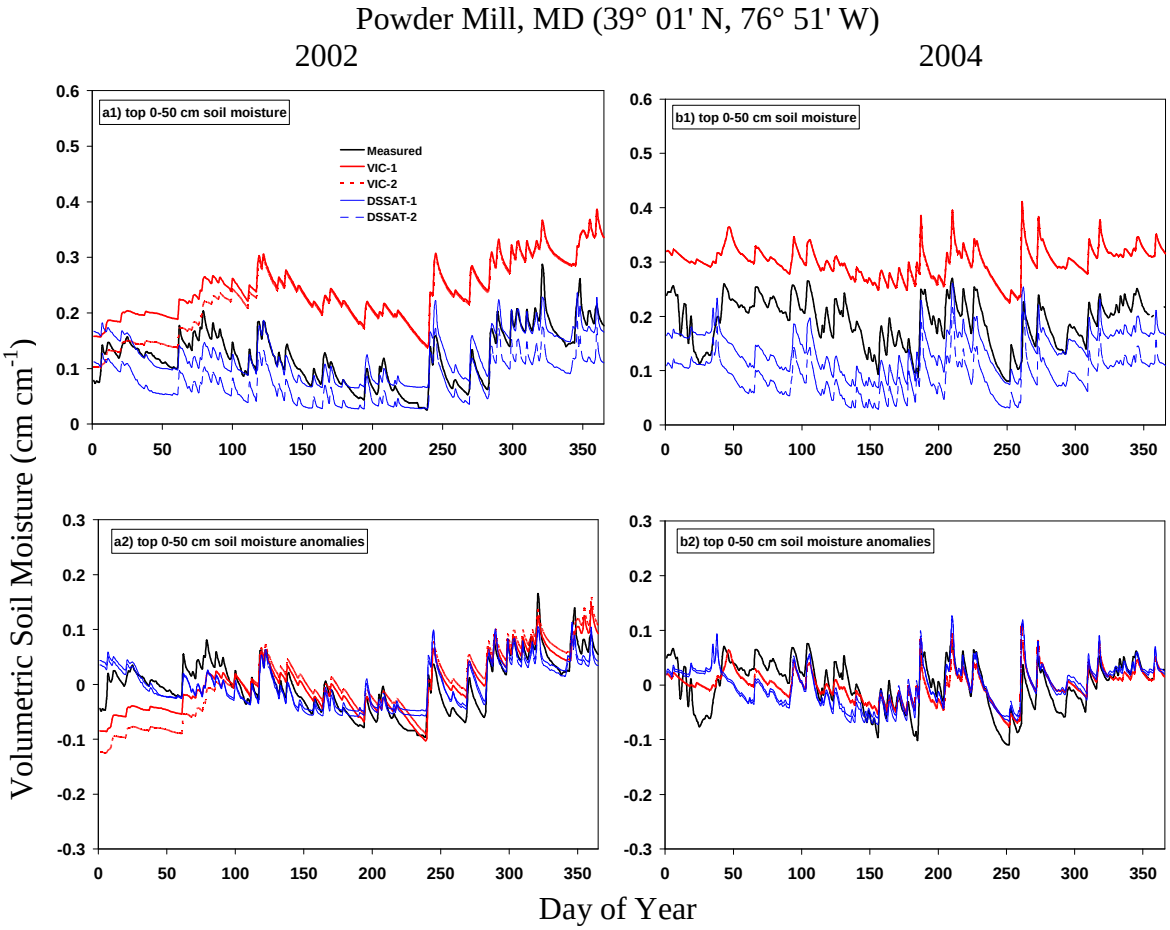

Figure 4.2 Measured (black) and modeled (DSSAT (blue) and VIC (red)) daily soil moisture (top) and soil moisture anomalies (bottom) at Powder Mill, MD in 2002 (left) and 2004 (right).

Table 4.1 Model performance statistics for VIC, DSSAT, and CWB soil moisture models.

PM	2002 DSSAT-1	2002 DSSAT-2	2002 VIC-1	2002 VIC-2	2004DSSAT-1	2004DSSAT-2	2004 VIC-1	2004 VIC-2	CWB PV
Correlation (r)	0.85	0.85	0.78	0.59	0.55	0.56	0.75	0.75	0.74
RMSE	0.03	0.05	0.13	0.12	0.06	0.11	0.12	0.11	0.10
MAE	0.02	0.05	0.12	0.11	0.06	0.10	0.11	0.11	0.09
E	0.73	-0.17	-5.54	-4.70	-1.08	-5.02	-5.94	-5.82	-0.61
BL	2004 DSSAT-1	2004 DSSAT-2	2004 VIC-1	2004 VIC-2	2005 DSSAT-1	2005 DSSAT-2	2005 VIC-1	2005 VIC-2	CWB BL
Correlation (r)	0.51	0.53	0.80	0.81	0.94	0.95	0.95	0.94	0.55
RMSE	0.14	0.08	0.09	0.08	0.06	0.08	0.05	0.05	0.09
MAE	0.11	0.06	0.07	0.07	0.05	0.07	0.04	0.05	0.08
E	-1.50	0.23	-0.04	0.12	0.41	-0.03	0.56	0.56	-0.26

Figure 4.1 and Figure 4.2 show that all simulations produce similar daily variations in soil moisture, but the absolute magnitude of simulated soil moisture is quite different. DSSAT was slightly more accurate than VIC in simulating the actual soil water content in the top 50 cm of soil since it had a lower MAE and a higher E for 3 of 4 simulations (2002PM, 2004PM, and 2004BL). The coefficient of efficiency (E) was negative for 5 of 8 VIC simulations which indicates that the observed mean soil moisture value was a better predictor of soil moisture conditions than VIC. VIC overestimated the actual soil water content in 7 of 8 simulations. This systematic bias has been found in other studies (Robock et al. 2003; Sheffield et al. 2003). However, VIC was more strongly correlated with observed soil moisture than DSSAT in 6 of the 8 simulations and it had a higher average correlation (0.80 versus 0.72).

At both BL and PM, the two VIC simulations (VIC-1 and VIC-2) are nearly identical, while the two DSSAT simulations (DSSAT-1 and DSSAT-2) differ from each other. In fact, changing the soil parameters did not significantly change VIC simulated soil moisture in the top 50 cm of the soil, only simulated soil moisture below 50 cm was slightly different (not shown). This suggests that DSSAT is more sensitive to the specified soil parameters than VIC.

The results also demonstrate that there is significant interannual and spatial variability in model performance. At PM, the 2002 and 2004 mean measured (mean VIC) soil moisture at PM was 0.122 (0.294) and 0.189 (0.320), respectively. VIC overestimated the magnitude of soil moisture by more than 100% and this is reflected in

the low E values -5.94 (2004 VIC-1) and -5.54 (2002 VIC-1) (Table 4.1). However, VIC was much more accurate in simulating the soil water content at BL (particularly in 2005). This spatial variability in VIC model performance has also been observed in other studies (Guo and Dirmeyer 2006). It can partially be attributed to differences in soil texture at BL and PM sites. At the PM site the soil is sandy loam which has higher hydraulic conductivity and lower field capacity and wilting points (Table 3.1 in section 3) than the clay loam soil at the BL site. As a result, the observed soil moisture content at PM is significantly lower than at BL. This difference in soil water content between the two sites is not well-captured by VIC.

The DSSAT soil moisture simulations using the calculated soil parameters (DSSAT-1) generally simulated the observed soil moisture more accurately than those using measured soil parameters. Table 4.1 shows that DSSAT-1 simulated soil moisture most accurately at PM in 2002. This simulation had the highest E 0.73 and the lowest MAE 0.02. A more detailed examination of the results revealed seasonal differences in the accuracy of the model simulations. In particular, DSSAT simulated soil moisture more accurately during the growth season than during other seasons (not shown). This is likely because DSSAT was primarily designed for simulating soil moisture for agricultural applications and therefore it has been extensively tested and evaluated using growing season data.

Like VIC, DSSAT model performance also varied significantly from year to year. Model performance during 2005BL simulation was significantly better than the 2004BL simulation, especially in terms of the strength of the correlations. At the PM

site, the differences in model performance between 2002 and 2004 may be due to the antecedent moisture conditions since 2003 was one of the wettest years on record in Maryland (Quiring 2004).

4.3 CWB soil moisture simulations

As can be seen from Figure 4.3, the soil moisture for both BL and PV were poorly simulated by CWB model. CWB model simulated monthly soil moisture and treated the whole soil profile as a homogeneous unit, which is not practical given the heterogeneity of soil characteristics (Table 3.1 in Section 3). The annual cycle of soil moisture can be predicted in most cases by the CWB model as evidenced by the correlations (> 0.5). The scatter of points shows that CWB model tends to underestimate the soil moisture content in the wettest months (Figure 4.4). This might be caused by the constraint of the upper limit of soil moisture (field capacity). Results show that the highest observed soil moisture content exceeds the field capacity specified in the model. Changing field capacity might allow the model to more closely replicate actual soil moisture conditions. Another cause of the poor model performance is that the model assumed that half of the surplus water (difference between FC and soil water content) was converted to streamflow and half was held over to the next time step (e.g., month). This simple method of handling runoff and storage is not physically realistic and has a negative impact on the accuracy of the model simulations. The CWB also does not account for net ground water fluxes, which might be an important factor for upward or download flow recharge. Therefore, the poor simulation of soil moisture is not

surprising. Our results suggest that the CWB is not an appropriate model for simulating soil water content.

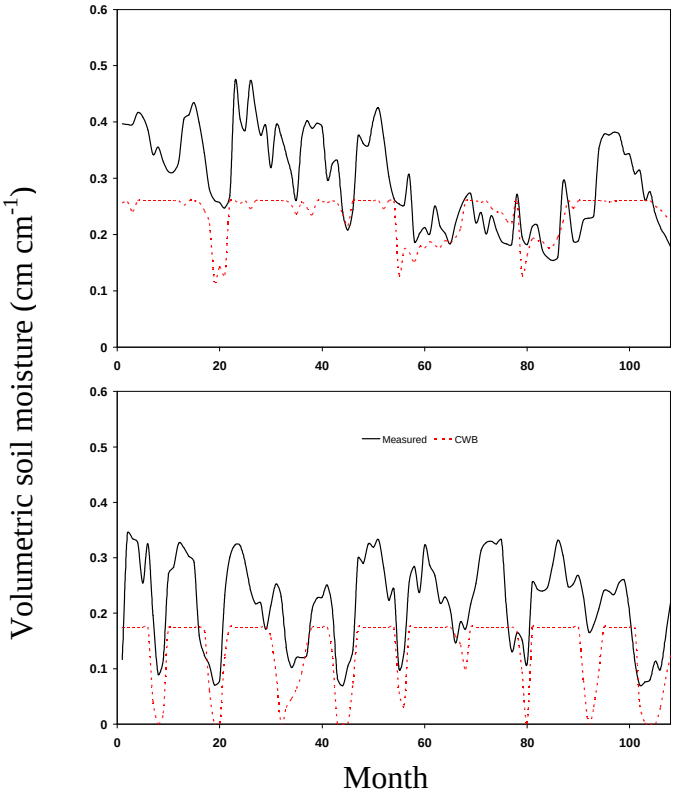

Figure 4.3 Measured (black) and CWB (red) monthly soil moisture from 1995-2005 at Bushland (top) and Prairie View (bottom), TX.

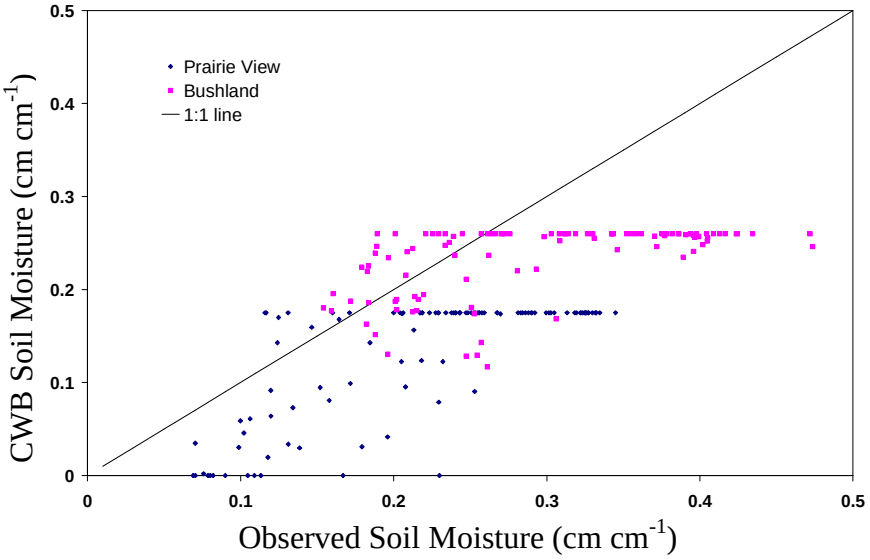

Figure 4.4 Scatter plot of measured and CWB monthly soil moisture.

4.4 Comparison of VIC, DSSAT, and CWB model performance

Soil moisture simulations from three different models were evaluated and compared to determine which model simulates soil water content most accurately. All of these models have been used for simulating soil moisture, but they vary in regards to their data requirements and level of complexity. VIC model is the most complex and data intensive of the land surface models that were evaluated in this study since it accounts for sub-grid scale variability in vegetation and infiltration. VIC is commonly used for simulating hydrology and land surface processes at basin to global scales. DSSAT is a model of moderate complexity that is commonly used for simulating crop growth and evaluating the impact of various agricultural management decisions at field to regional scales. CWB is a simple model that is used to simulate the water balance at basin, regional, and global scales.

Of the three models, DSSAT and VIC simulated soil moisture in the top 50 cm at BL and PM with similar levels of accuracy (Table 4.1). Due to the small sample size, a paired t-test demonstrated that the differences in the model performance statistics (E, MAE, r) between VIC and DSSAT are not statistically significant. Therefore, although there are some differences in model performance between VIC and DSSAT, both models demonstrated similar skill in simulating soil moisture in the upper 50 cm of the soil and the performance of both models varied significantly in time and space.

CWB was able to simulate the annual cycle and interannual variability of soil moisture. However, it could not accurately simulate the actual soil water content as demonstrated by the large MAE and negative E at both PV and BL sites. These performance issues, coupled with the coarse temporal resolution (e.g., monthly) and vertical resolution (e.g., a single layer) make CWB, despite its simplicity, the least desirable of the three models. Therefore, CWB was excluded from further consideration and the sensitivity analysis and detailed examination of model differences will focus on VIC and DSSAT.

4.5 VIC and DSSAT evapotranspiration simulations

Insights into the differences in model performance between VIC and DSSAT can be gained by examining the other components of the water balance. Although both models were driven using the same meteorological and radiative forcing data, the evapotranspiration rates for the two models are quite different. Figure 4.5 shows the monthly actual evapotranspiration rate for BL and PM. It is evident that the DSSAT-simulated evapotranspiration is in good agreement with VIC-simulated

evapotranspiration at PM. However, there are significant differences between DSSAT and VIC estimated evapotranspiration at BL. For the BL site in 2005, the DSSAT-simulated evapotranspiration rate peaked in June, while the VIC evapotranspiration rate was highest in April. VIC-simulated evapotranspiration was much less than DSSAT evapotranspiration for 2004BL. The estimated annual evapotranspiration also shows remarkable intermodel differences (Table 4.2). These differences can be attributed to the different schemes used by the two models to calculate evapotranspiration. DSSAT uses the Priestly-Taylor equation while VIC uses the Penman-Monteith equation. Previous studies have suggested that the performance of evapotranspiration equations varies in space (Sau et al. 2004). This is in good agreement with Desborough et al. (1996) who found that the difference between model-estimated soil evaporation rates is due to the different methodologies used to calculate it. Since VIC and DSSAT also utilize different methodologies to partition potential evapotranspiration into soil evaporation and plant transpiration, this influences the vertical distribution of the simulated soil moisture. Ideally the DSSAT and VIC evapotranspiration rates should be compared with observed data to evaluate model performance, however, the lack of observed data makes it impossible in this study.

Table 4.2 Annual drainage, runoff, and evapotranspiration (all in mm) simulated by DSSAT and VIC at Bushland, TX and Powder Mill, MD.

	2004 BL		2005 BL		2002 PM		2004 PM	
	DSSAT	VIC	DSSAT	VIC	DSSAT	VIC	DSSAT	VIC
Precipitation	715.20	715.20	377.90	377.90	897.40	897.40	1387.50	1387.50
Drainage	13.97	9.96	15.00	11.30	192.29	96.40	234.76	336.06
Runoff	44.07	20.09	14.60	12.01	30.38	63.25	255.64	225.82
Evapotranspiration	759.79	433.56	596.10	614.57	675.30	510.29	897.74	849.58

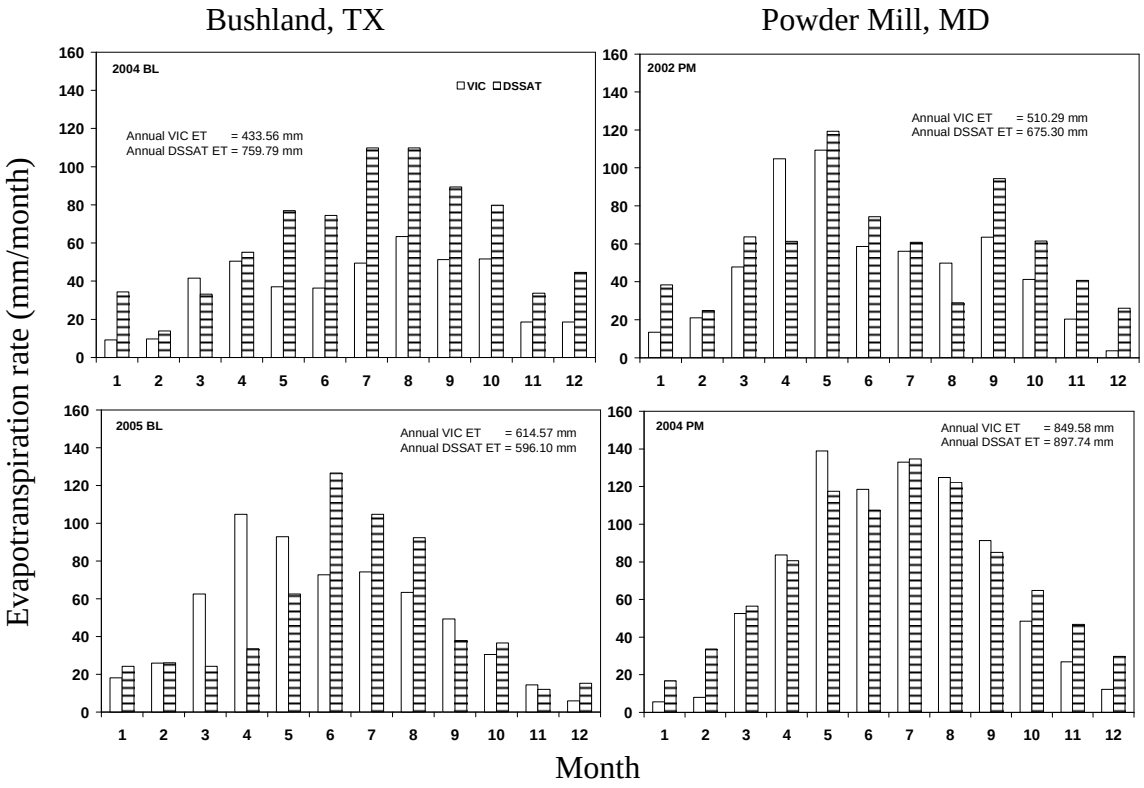

Figure 4.5 DSSAT and VIC simulated monthly evapotranspiration at Bushland, TX (left) and Powder Mill, MD (right).

4.6 VIC and DSSAT drainage and runoff simulations

Table 4.2 shows the estimated annual drainage (subsurface flow) and runoff (overland flow). It is clear that there are large differences in modeled drainage and runoff at the two SCAN sites (Figure 4.6 and Figure 4.7, Table 4.2). At BL drainage and runoff combined account for less than 10% of annual precipitation. This indicates that most precipitation infiltrates the soil and very little water drains out the bottom of the soil profile. Drainage and runoff do not have a major impact on soil water content at this location. However, drainage and runoff are more important at PM since together they account for between 18% and 40% of annual precipitation. Both models generally simulated more runoff at PM than at BL (Table 4.2). This is due to a combination of factors including differences in the amount of precipitation, precipitation intensity, soil type (hydraulic conductivity), and slope.

Generally both DSSAT and VIC produced a similar pattern of monthly runoff, although the amount of runoff differed between the two models (Figure 4.6). Although DSSAT and VIC-estimated annual runoff varied by more than a factor of two in some years, the absolute difference in mean annual runoff between the two models was less than 35 mm for all simulations. Both models simulated more drainage at PM than at BL (Table 4.2). The differences in drainage can be attributed to differences in the depth of the soil profile, soil texture, and annual precipitation. The soil is much shallower at PM (129 cm) than at BL (229 cm) and it has a coarser texture (sandy loam) than BL (silty clay). PM also received more precipitation than BL. These factors help explain why annual drainage at PM was approximately 10 times greater than at BL. Generally both

DSSAT and VIC produced a similar pattern of monthly drainage pattern, except for 2004PM (Figure 4.7). The absolute difference between DSSAT and VIC-estimated annual drainage was relatively small at BL (<18 mm) and it was relatively large at PM (~100 mm).

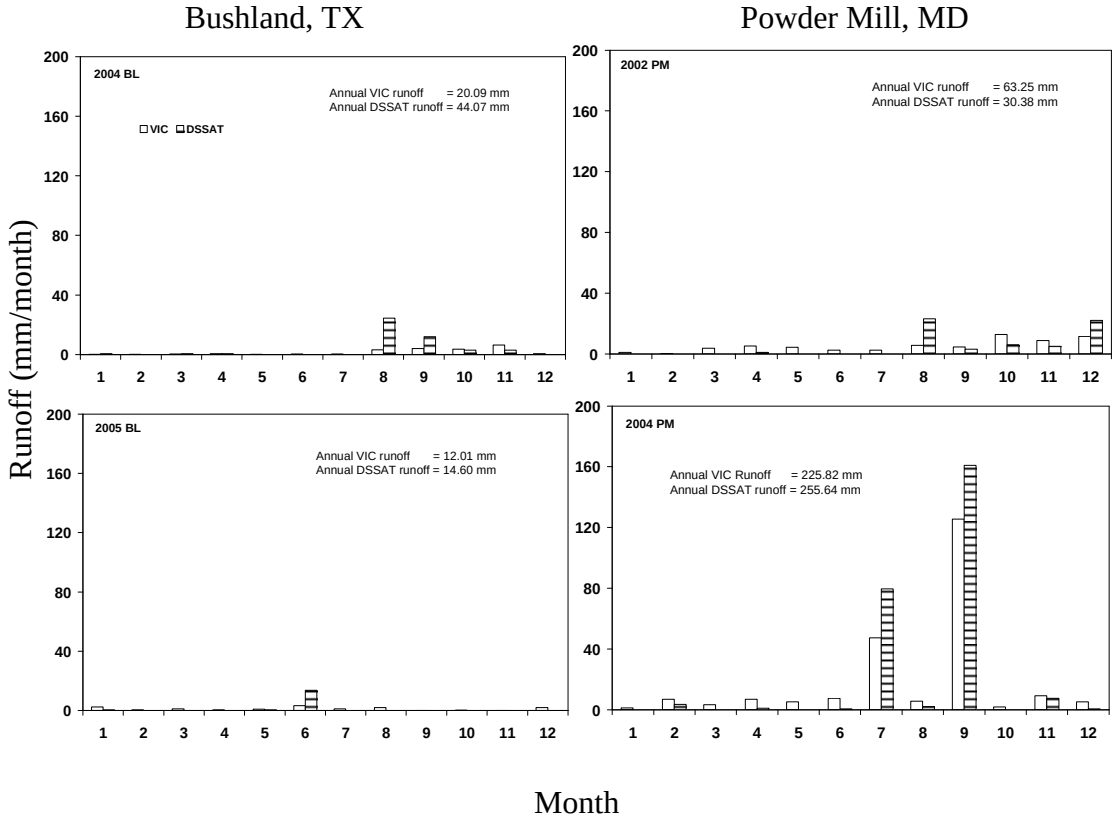

Figure 4.6 DSSAT and VIC simulated monthly runoff at Bushland, TX (left) and Powder Mill, MD (right).

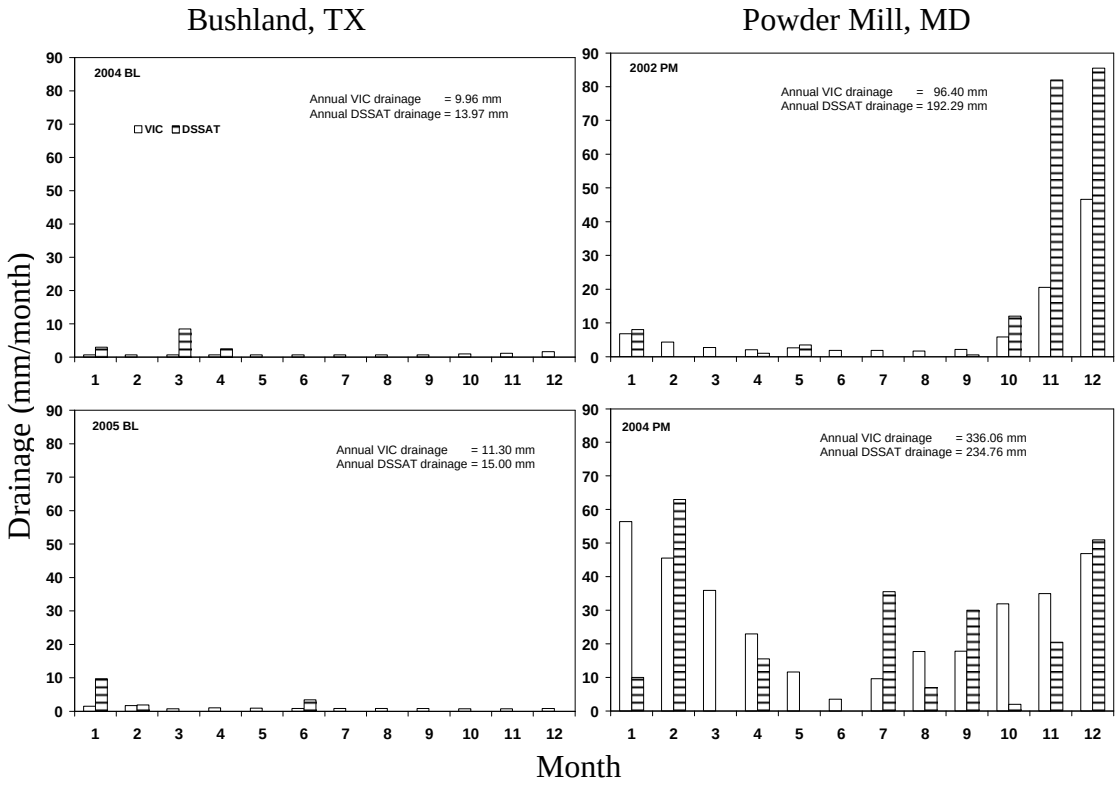

Figure 4.7 DSSAT and VIC simulated monthly drainage at Bushland, TX (left) and Powder Mill, MD (right).

Although there are significant differences in the amount of drainage and runoff simulated by the models (especially at PM), no consistent pattern was evident. During some simulations, DSSAT predicted higher amounts of runoff (drainage) than VIC and during others VIC simulated more runoff (drainage) than DSSAT. Accurate simulation of drainage and runoff processes is necessary to get the soil water balance right, but the lack of observational data makes it impossible to evaluate how well the models are doing.

4.7 VIC and DSSAT sensitivity analysis

4.7.1 VIC

Uncertainty in model parameters can have a significant impact on the response of the model. A total of 16 VIC soil parameters were selected for the sensitivity analysis, namely: b_{infilt} (variable infiltration curve parameter), D_{smax} (maximum velocity of baseflow), D_s (fraction of D_{smax} where non-linear baseflow begins), W_s (fraction of maximum soil moisture where non-linear baseflow occurs), K_{sat} (saturated hydraulic conductivity), expt 1, expt 2, expt 3 (parameters describing the variation of K_{sat} with soil moisture), Wcr_Fract 1, Wcr_Fract 2, Wcr_Fract 3 (parameters describing the fractional soil moisture content at the critical point), Wpmp_Fract 1, Wpmp_Fract 2, and Wpmp_Fract 3 (parameters describing the fractional soil moisture content at the wilting point). Each parameter was varied by an arbitrary ±20%. The model was run once using the upper value of the parameter (+20%) and once using the lower value of the parameter (-20%). Table 4.3 shows the difference in the mean annual soil water content between the simulations using the upper value and lower value of each parameter. In the

majority of simulations, varying a parameter from 120% to 80% of its prescribed value produced a chance in mean soil moisture of less than 1%. Note that even though the differences in mean soil moisture are small, they are statistically significant because of the even smaller standard deviation in the differences. Generally the sign and magnitude

Table 4.3 VIC factorial analysis for Bushland and Powder Mill sites.

Parameter name	Parameter values		$\Delta*10^2$			
	BL	PM	BL	(%)	PM	(%)
1. infilt	0.03	0.10	-0.19	(-0.7)	-0.29	(-1.0)
2. Ds*	0.01	0.05	-0.65	(-2.4)	-0.80	(-2.7)
3. Dsmax*	11.22	10.00	-0.65	(-2.4)	-1.51	(-5.1)
4. Ws*	0.50	0.40	0.71	(+2.6)	2.86	(+9.7)
5. expt 1*	19.69	12.00	0.28	(+1.0)	0.34	(+1.1)
6. expt 2*	19.69	12.00	-0.44	(-1.6)	0.99	(+3.3)
7. expt 3	19.69	12.00	0.00	(+0.0)	0.00	(+0.0)
8. Ksat 1	163.20	621.60	-0.05	(-0.2)	-0.05	(-0.2)
9. Ksat 2	14.40	621.60	0.13	(+0.5)	-0.13	(-0.4)
10. Ksat 3	42.40	621.60	0.00	(+0.0)	0.00	(+0.0)
11. Wcr_Fract 1	0.43	0.19	0.01	(+0.1)	0.00	(+0.0)
12. Wcr_Fract 2	0.42	0.16	0.56	(+2.0)	0.00	(+0.0)
13. Wcr_Fract 3	0.37	0.13	0.18	(+0.7)	0.08	(+0.3)
14. Wpmp_Fract 1	0.22	0.08	0.02	(+0.1)	0.00	(+0.0)
15. Wpmp_Fract 2	0.27	0.06	1.62	(+6.0)	0.00	(+0.0)
16. Wpmp_Fract 3	0.23	0.07	2.37	(+8.7)	0.17	(+0.6)

Here, Δ is the change in simulated mean soil moisture ($cm\,cm^{-1} * 100$) caused by increasing the parameter from 80% of the estimate to 120% of the estimate. Non-zero denotes significant difference in the mean at 5% level. b_{infilt} is variable infiltration curve parameter; D_s is fraction of D_{smax} where non-linear baseflow begins; D_{smax} is maximum velocity of baseflow, W_s is fraction of maximum soil moisture where non-linear baseflow occurs, K_{sat} is saturated hydraulic conductivity; *expt* is parameter describing the variation of K_{sat} with soil moisture; *Wcr_Fract* is fractional soil moisture content at the critical point; *Wpmp_Fract* is fractional soil moisture content at the wilting point; number in parameter names indicates layers. * indicates the five most significant parameters that are common for both sites and these parameters are used for the further factorial analysis.

of the changes in mean soil moisture were relatively consistent across both sites, although PM tended to be more sensitive to changes in the parameters than BL. The five most significant parameters for both sites were D_s, D_{smax}, W_s, expt 1 and expt 2. These parameters were selected for further sensitivity analysis using the factorial analysis approach (Box et al. 1978).

Table 4.4 shows the design of the half-fraction factorial analysis and the resulting mean soil moisture. The "+" denotes the prescribed value of a parameter plus 20% and the "-" denotes the prescribed value of a parameter minus 20%. The largest decrease in mean soil moisture was obtained from simulation 4 for each site, the concurrent increase of D_s and D_{smax}, and decrease of W_s, expt 1 and expt 2. Simulation 4 decreased mean soil moisture by 6% at BL and 13% at PM. The largest increase in mean soil moisture was obtained from simulation 13, the concurrent decrease of D_s and D_{smax}, and increase of W_s, expt 1 and expt 2 (the opposite of simulation 4). Simulation 13 increased mean soil moisture by 4% and 10% at BL and PM sites, respectively. Three of these parameters are related to how the model simulates baseflow (D_s, D_{smax}, W_s) and the other two parameters (expt 1 and expt 2) control how the unsaturated hydraulic conductivity in the top two layers of the soil changes as a function of soil water content. In general, the values of D_s, D_{smax}, and W_s control the threshold below (above) which linear (nonlinear) baseflow occurs according to the Arno model conceptualization (Franchini and Pacciani 1991). Accordingly, the decrease of D_s and D_{smax} and the increase of W_s will lower the threshold value which will eventually decrease the rate of baseflow and increase the soil moisture content. The expt 1 and expt 2 are the Brooks-Corey exponents for layer 1 and

layer 2 which control the soil water retention curve. Higher values of expt 1 and expt 2 will make the soil water retention curve closer to the typical retention curve of clay soil and thereby decrease the rate at which water infiltrates and moves through the soil.

Table 4.4 Design of the 2^4 half-fraction factorial sensitivity analysis for Bushland and Powder Mill sites for VIC-3L model.

simulation runs	Parameter index					Mean soil moisture (cm cm^{-1})			
	D_s	D_{smax}	W_s	expt 1	expt 2	BL	(%)	PM	(%)
1	–	–	–	–	+	0.263	(-3.4)	0.288	(-2.4)
2	+	–	–	–	–	0.261	(-3.9)	0.268	(-9.5)
3	–	+	–	–	–	0.261	(-3.9)	0.263	(-11.2)
4	+	+	–	–	–	0.257	(-5.5)	0.257	(-12.9)
5	–	–	+	–	–	0.264	(-2.9)	0.288	(-2.7)
6	+	–	+	–	+	0.263	(-3.3)	0.299	(+1.2)
7	–	+	+	–	+	0.263	(-3.3)	0.296	(+0.1)
8	+	+	+	–	–	0.261	(-3.9)	0.275	(-7.1)
9	–	–	–	+	–	0.280	(+3.0)	0.295	(-0.3)
10	+	–	–	+	+	0.276	(+1.6)	0.306	(+3.5)
11	–	+	–	+	+	0.276	(+1.6)	0.302	(+2.1)
12	+	+	–	+	–	0.274	(+0.8)	0.281	(-5.1)
13	–	–	+	+	+	0.282	(+3.8)	0.325	(+9.9)
14	+	–	+	+	–	0.280	(+3.0)	0.306	(+3.6)
15	–	+	+	+	–	0.280	(+3.0)	0.302	(+2.3)
16	+	+	+	+	+	0.277	(+1.7)	0.312	(+5.4)
Reference						0.272		0.296	

Columns two-six show parameters names for the five parameters in the analysis. A plus symbol indicates that the parameter was set at 120% of the estimate while a minus indicates 80% of the estimate. The last row as reference shows the resulting mean soil moisture based on the chosen model parameter estimates. The percent values in parenthesis indicate the change relative to the reference values on the last row.

The sensitivity analysis shows that VIC is quite stable since relatively large changes in individual parameters and groups of parameters resulted in relatively small

changes in mean soil moisture (<10%). The results also suggest that the model response is more sensitive at PM than BL site which might be caused by the different climatology. This agrees with Demaria et al. (2007) who found that parameter sensitivity was more strongly controlled by climatic gradients than by changes in soil properties.

4.7.2 DSSAT

The same methodology was used to evaluate the sensitivity of DSSAT. Up to 16 soil parameters were selected for the sensitivity analysis, namely: the Soil Conservation Service (SCS) runoff curve number, drainage coefficient, FC 1 to FC 7 (the soil moisture content at field capacity in layers 1 to 7), and WP 1 to WP 7 (the soil moisture content at the wilting point in layers 1 to 7). Each parameter was varied by an arbitrary ±20%, although since there are only five soil layers at PM site no sensitivity analysis was undertaken for WP 6, WP 7, FC 6 and FC 7 (Table 4.5). The model was run once using the upper value of the parameter (+20%) and once using the lower value of the parameter (-20%). Table 4.5 shows the difference in the mean annual soil water content between the simulations using the upper value and lower value of each parameter. In the majority of simulations, varying a parameter from 120% to 80% of its prescribed value produced a change in mean soil moisture of less than 5%. Generally the sign and magnitude of the changes in mean soil moisture were relatively consistent across both sites, although the changes tended to be larger at PM than at BL (Table 4.5). This is similar to VIC which also showed greater sensitivity at PM. The five parameters that have the largest influence on mean soil moisture are the runoff curve and the field

capacity of soil layers 2, 3, 4 and the deepest soil layer (e.g., layer 5 at PM and layer 7 at BL). These parameters were further evaluated using the factorial analysis approach.

Table 4.6 shows the design of the half-fraction factorial analysis and the resulting mean soil moisture for BL and PM. Results indicate that the largest decrease in mean annual soil moisture at both sites was obtained from simulation 2, which corresponds to a higher runoff curve number and a decrease in the field capacity in four of the soil layers. Simulation 2 decreased soil moisture by 11% and 23% at BL and PM, respectively. The largest increase in mean soil moisture was obtained from simulations 7, 11, and 13. The average soil moisture content of all three simulations was 7% and 11% higher than the reference values at BL and PM sites, respectively. These simulations were associated with a lower runoff curve number and an increase in the field capacity of three of the soil layers. Not surprisingly, increasing the runoff curve number leads to decreases in soil moisture because it reduces the amount of infiltration and increases the amount of overland flow. Decreasing the field capacity of the soil reduces soil moisture because the field capacity directly controls the amount of water that can be held against the pull of gravity in each soil layer.

Table 4.5 DSSAT factorial analysis for Bushland and Powder Mill sites.

	Parameter values		$\Delta*10^2$			
Parameter name	BL	PM	BL	(%)	PM	(%)
1. Runoff curve number*	81	76	-1.73	(-5.2)	-1.87	(-15.2)
2. Drainage rate	0.60	0.60	0.06	(+0.2)	-0.01	(-0.1)
3. FC 1	0.35	0.19	0.10	(+0.3)	0.37	(+3.0)
4. FC 2*	0.37	0.16	1.38	(+4.8)	0.37	(+3.0)
5. FC 3*	0.33	0.16	1.09	(+3.8)	0.92	(+7.5)
6. FC 4*	0.30	0.14	1.00	(+3.5)	0.89	(+7.2)
7. FC 5*	0.28	0.11	1.06	(+3.7)	0.16	(+1.3)
8. FC 6	0.31	N/A	0.99	(+3.5)	N/A	
9. FC 7*	0.34	N/A	1.64	(+5.7)	N/A	
10. WP 1	0.18	0.08	0.43	(+1.5)	0.14	(+1.1)
11. WP 2	0.23	0.07	1.13	(+3.9)	0.11	(+0.9)
12. WP 3	0.20	0.06	0.66	(+2.3)	0.13	(+1.1)
13. WP 4	0.18	0.07	0.61	(+2.1)	0.12	(+1.0)
14. WP 5	0.17	0.06	0.50	(+1.7)	0.14	(+1.2)
15. WP 6	0.19	N/A	0.28	(+1.0)	N/A	
16. WP 7	0.20	N/A	0.07	(+0.2)	N/A	

Here, Δ is the change in simulated mean soil moisture ($cm\ cm^{-1} * 100$) in the total zone by changing the parameter from 120% to 80% of the estimate. *Runoff curve* is the SCS runoff curve number, *Drainage coeff.* is the drainage coefficient, *FC 1* to *FC 7* is the soil moisture content at field capacity in layers 1 to 7, and *WP 1* to *WP 7* is the soil moisture content at the wilting point in layers 1 to 7.

*indicates the five most significant parameters that are common for both sites and these parameters are used in the factorial analysis (note that FC 5 and FC 7 are for PM and BL, respectively).

Table 4.6 Design of the 2^4 half-fraction factorial sensitivity analysis for Bushland and Powder Mill sites for DSSAT model.

simulation runs	Parameter index					Mean soil moisture (cm cm^{-1})			
	Runoff curve	FC2	FC3	FC4	FC5(FC7*)	BL	(%)	PM	(%)
1	–	–	–	–	+	0.284	(-0.9)	0.121	(-1.3)
2	+	–	–	–	–	0.255	(-11.2)	0.095	(-22.4)
3	–	+	–	–	–	0.281	(-2.1)	0.109	(-11.0)
4	+	+	–	–	–	0.266	(-7.3)	0.096	(-22.1)
5	–	–	+	–	–	0.278	(-3.3)	0.115	(-6.4)
6	+	–	+	–	+	0.275	(-4.2)	0.108	(-12.3)
7	–	+	+	–	+	0.308	(+7.4)	0.135	(-9.9)
8	+	+	+	–	–	0.280	(-2.6)	0.100	(-18.8)
9	–	–	–	+	–	0.279	(-3.0)	0.135	(-9.7)
10	+	–	–	+	+	0.276	(-3.9)	0.109	(-11.3)
11	–	+	–	+	+	0.307	(+7.1)	0.135	(-9.7)
12	+	+	–	+	–	0.273	(-5.0)	0.100	(-18.3)
13	–	–	+	+	+	0.304	(-5.9)	0.140	(-14.1)
14	+	–	+	+	–	0.271	(-5.7)	0.104	(-15.6)
15	–	+	+	+	–	0.300	(+4.7)	0.128	(+4.3)
16	+	+	+	+	+	0.301	(+4.7)	0.113	(-7.9)
Reference						0.287		0.123	

*FC5 and FC7 are field capacity in the deepest layers at PM and BL sites, respectively. Others are the same as Table 5. The last row as reference shows the resulting mean soil moisture based on the chosen model parameter estimates.

The sensitivity analysis shows that DSSAT is more sensitive to changes in the model parameters (at least for the subset of parameters that were tested) than VIC since both the sensitivity analysis of the individual parameters and the groups of parameters produced much larger changes (up to 22%) in DSSAT-simulated soil moisture. This finding is also supported by the soil moisture simulations that were previously reported, since there much larger differences between the DSSAT-1 and DSSAT-2 simulations than between VIC-1 and VIC-2 (Figure 4.1 and Figure 4.2). The results also suggest that DSSAT is more sensitive to changes in model parameters at PM than at BL.

4.8 Validation of VIC using Mesonet observations

Our previous model evaluation has shown that VIC is generally quite suitable for simulating soil moisture variations. Therefore, we obtained data from the Oklahoma Mesonet network to further assess VIC model performance in the GP. Overall, VIC was able to accurately produce the soil moisture variation as demonstrated by the strong correlations (Table 4.7). The correlations between model simulations and observations ranged from 0.56 to 0.81 with an average of 0.70. This compares very well with the model performance at SCAN sites (Table 4.1). However, VIC was unable to simulate the magnitude of measured soil moisture. The coefficient of efficiency E was negative for 5 of 6 VIC simulations indicating that the observed mean soil moisture value was a better predictor of soil moisture contents than VIC. The systematic bias has been found in the simulations at SCAN sites and other places in other studies (Robock et al. 2003; Sheffield et al. 2003). The systematic bias can be reduced by removing the long-term mean values in the simulations. Figs. 4.8, 4.9, and 4.10 compared the modeled and measured soil moisture anomalies at the three Mesonet sites. In general, there is a better agreement between modeled and measured soil moisture anomalies. The three Mesonet sites are in different climatic divisions and represent dry (Butl), normal (King), and wet (Wist) climates. It can be seen from Table 4.7 that model performance is comparable at the three Mesonet sites. This means that VIC can simulate the wetting and drying cycle of soil moisture at an acceptable level of accuracy under different climate conditions. The lowest E values at Butl site are because VIC tended to underestimate the observed soil moisture as seen in Figure 4.8. Further examination of the comparison between

modeled and measured soil moisture reveals that VIC can better simulate soil moisture variations during growth season (Figs. 4.8, 4.9, and 4.10).

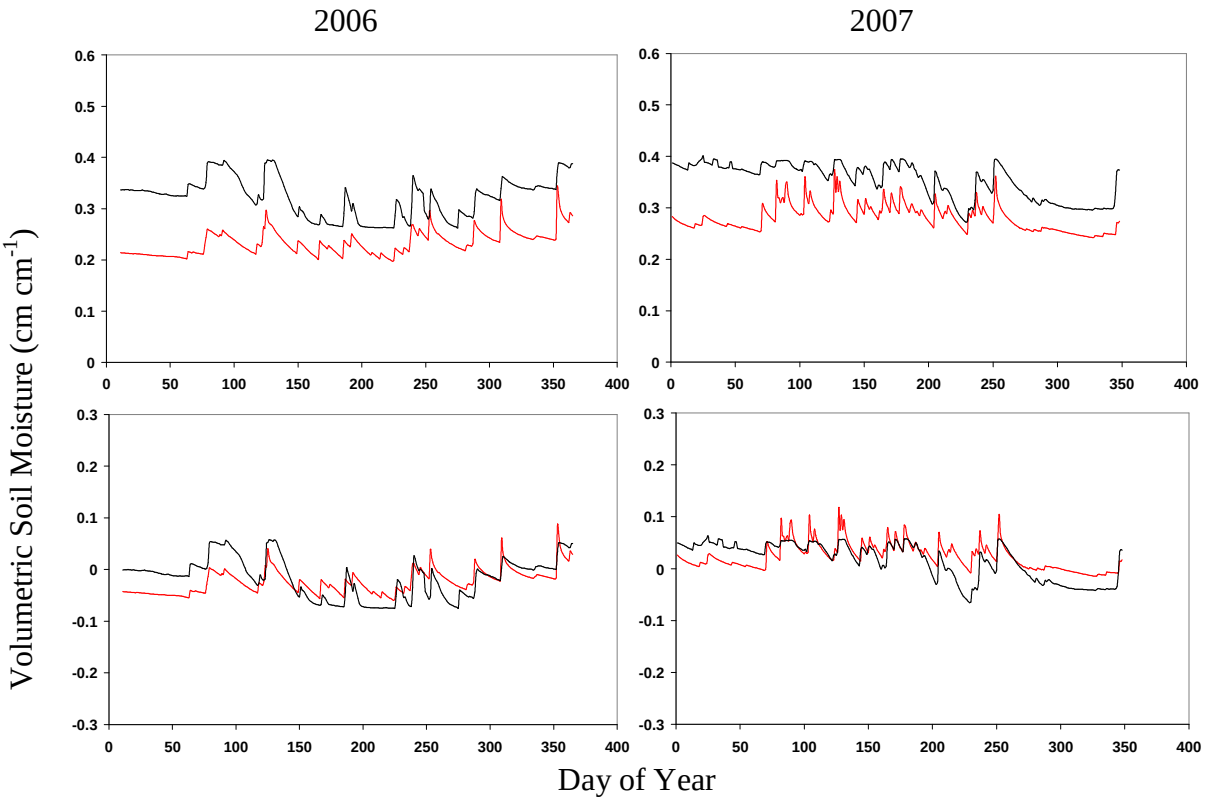

Figure 4.8 Measured (black) and VIC modeled (red) daily soil moisture (top) and soil moisture anomalies (bottom) at BUTL in 2006 (left) and 2007 (right).

Table 4.7 Model performance statistics for VIC model using Oklahoma Mesonet observations.

	2006Butl	2007Butl	2005King	2007King	2001Wist	2002Wist
Correlation (r)	0.56	0.65	0.79	0.58	0.80	0.81
RMSE	0.09	0.08	0.04	0.03	0.09	0.08
MAE	0.09	0.07	0.03	0.03	0.08	0.07
E	-14.88	-8.47	-0.51	0.04	-1.38	-0.71

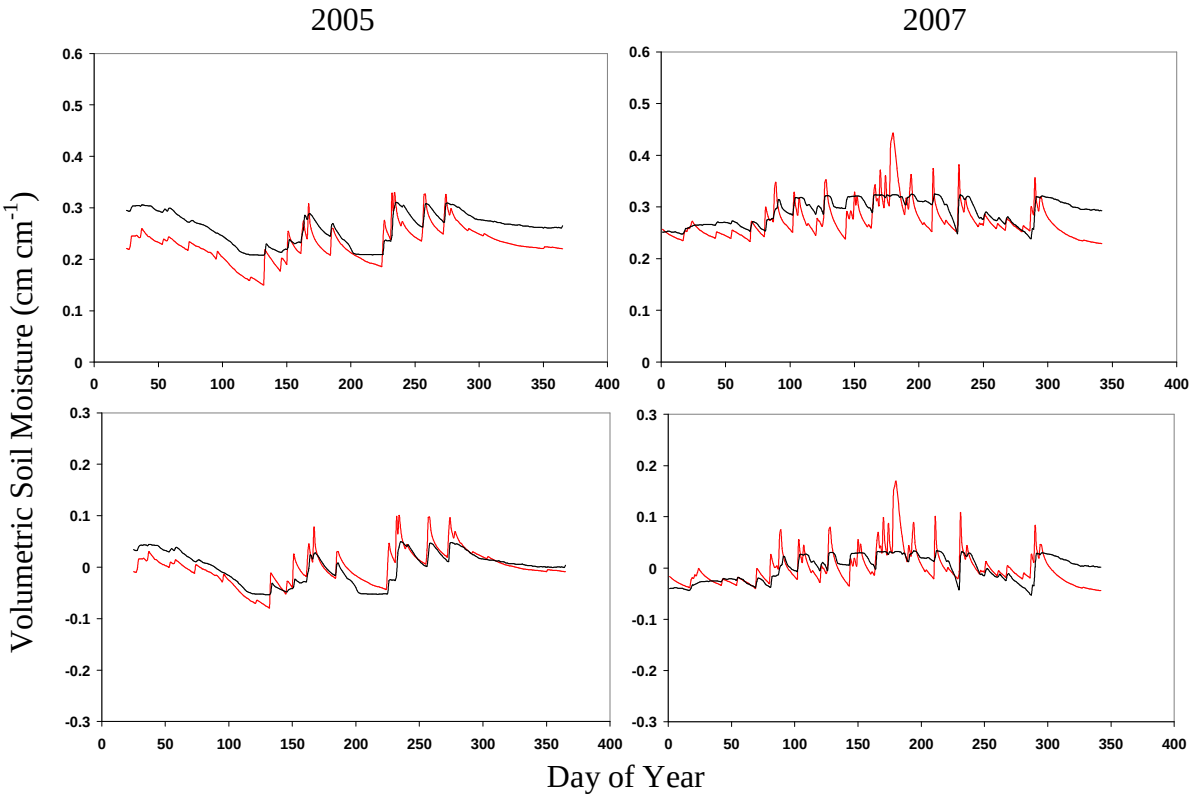

Figure 4.9 Measured (black) and VIC modeled (red) daily soil moisture (top) and soil moisture anomalies (bottom) at KING in 2005 (left) and 2007 (right).

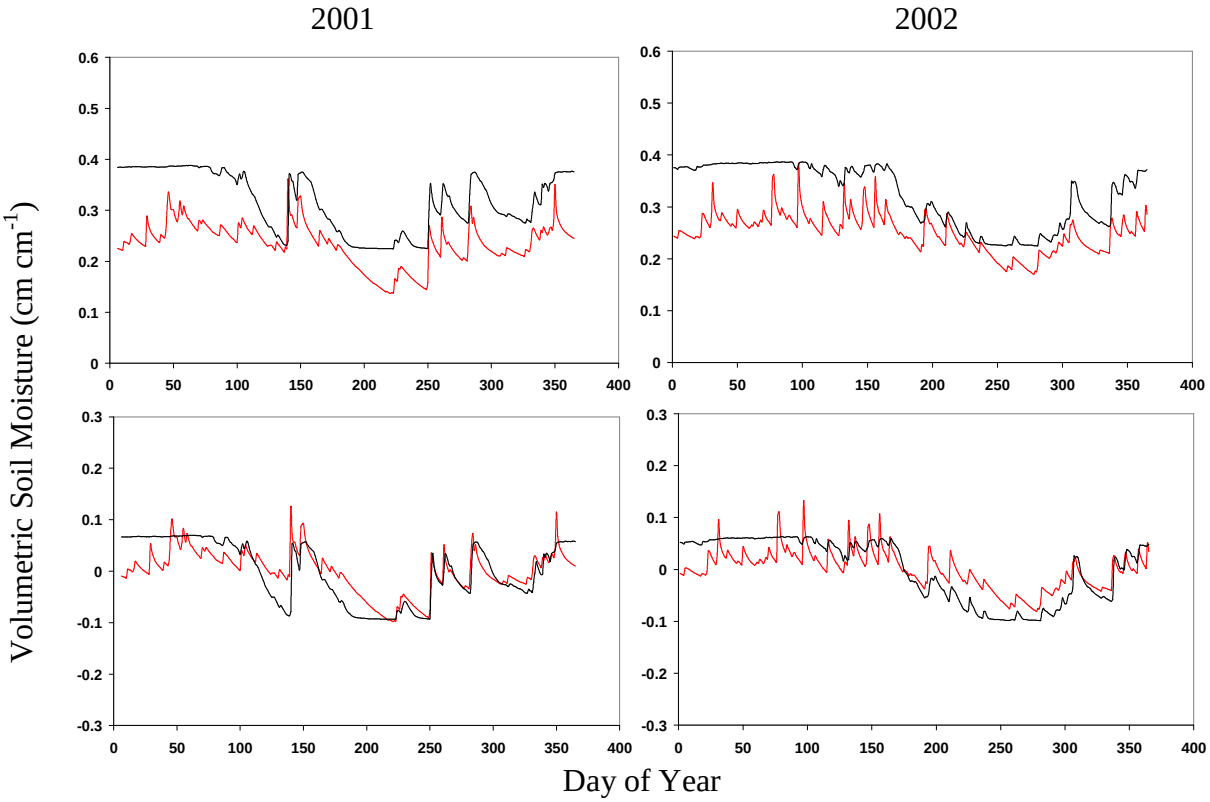

Figure 4.10 Measured (black) and VIC modeled (red) daily soil moisture (top) and soil moisture anomalies (bottom) at WIST in 2001 (left) and 2002 (right).

4.9 Conclusions

The results of this study indicate that DSSAT and VIC more accurately simulate soil moisture than CWB. The overall accuracy of VIC and DSSAT soil moisture simulations, as measured by the correlation coefficient and RMSE, compare favorably with the values reported in other model intercomparison studies (*cf.* Guo and Dirmeyer *2006*). In this study, model complexity was not a perfect predictor of model performance, although the limitations of the least complex model (e.g., CWB) were

readily apparent, the performance of the model of moderate complexity (e.g., DSSAT) was statistically indistinguishable from the more complex model (e.g., VIC).

The analysis revealed significant spatial variations in model performance. For example, VIC simulated soil moisture more accurately at BL than at PM. These spatial variations in model performance have been identified in other studies (Dirmeyer et al. 2004; Guo and Dirmeyer 2006). Model performance also varied significantly from year-to-year. Both VIC and DSSAT simulations at BL were significantly accurate in 2005 than in 2004. In 2005, the correlation between DSSAT soil moisture and the observations increased approximately 80% and E increased from 0.23 to 0.41. In addition, DSSAT also exhibited intra-annual variations in model performance since it tended to simulate soil moisture more accurately during the growing season. These variations in model performance demonstrate that it is difficult to develop a model that can accurately simulate soil moisture under a variety of edaphic and climatic conditions.

The primary cause of differences in model performance is the different land surface scheme used by each model. For example, although VIC and DSSAT were run using the same meteorological and radiative forcing data, there was significant inter-model variability in the simulated evapotranspiration, drainage, and runoff. These differences are important since the models need to be able to simulate all aspects of the soil water balance in order to accurately predict soil water content. However, given the lack of observation data it was only possible to verify the accuracy of the DSSAT and VIC soil moisture simulations. Previous studies have also demonstrated that differences

in model formulation and land surface schemes have a significant impact on simulated soil moisture (Dirmeyer et al. 2004; Robock et al. 2003).

Some of the variation in model performance is also likely due to model-to-model differences in the number of soil layers and the layer depths. Soil properties can change dramatically over short distances. The one-layer CWB model does not account for any of the vertical changes in soil properties, which greatly reduces model performance. VIC and DSSAT used the same soil properties obtained directly from soil surveys conducted at the SCAN sites. DSSAT can divide the subsurface into up to 10 layers, while VIC only uses three layers. This allows DSSAT to more accurately account for the vertical heterogeneity in soil properties. In addition, DSSAT was designed for agricultural applications and therefore it has been extensively tested and evaluated at sites similar to those used in this study. VIC was primarily designed for hydrological applications and therefore previous evaluations have emphasized the accurate simulation streamflow.

The sensitivity analysis focused on examining the sensitivity of VIC and DSSAT to a selection of soil parameters required by each model because soil parameters have a large and direct influence on the soil moisture simulations and because soil properties are extremely spatially heterogeneous. In addition, these models are often applied in areas where detailed soil surveys are not available and therefore the soil parameters must be estimated from relatively coarse datasets (e.g., NRCS STATSGO). The sensitivity analysis demonstrated that both models are sensitive to changes in the model parameters (VIC was most sensitive to changes in D_s, D_{smax}, W_s, expt 1 and expt 2, while DSSAT was most sensitive to changes in the runoff curve number and field capacity in four of

the soil layers), although it appears that, overall, DSSAT is more sensitive than VIC. The factorial analysis revealed that changing a number of parameters simultaneously can have a greater influence on the model than varying an individual parameter. Our results also showed that model sensitivity varied by location, the sensitivity analysis produced larger changes in soil moisture at PM than at BL. Therefore model sensitivity is not just a function of the changes in soil parameters, but also changes in the climate. Generally, the results of the sensitivity analysis demonstrated that a portion of the systematic error in the soil moisture simulations may be attributable to uncertainties in the model parameters. However, the sensitivity analysis did not attempt to quantify the uncertainty in each of the parameter estimates (an arbitrary change of ±20% was applied to all parameters).

Further validation of VIC model using the Oklahoma Mesonet observations suggests that VIC model is suitable to simulate soil moisture variations in different climate regions. Overall, our results suggest that VIC model is able to simulate soil moisture variations in the GP. Therefore, VIC model simulated soil moisture will be used for investigating soil moisture-precipitation interaction in the next section.

5. OBSERVATIONAL RELATIONSHIP BETWEEN SOIL MOISTURE AND SUMMER PRECIPITATION*

5.1 Introduction

This section will examine the nature and strength of the relationship of fall/spring soil moisture conditions and remote forcings with summer precipitation. The persistence of soil moisture anomalies and SSTs anomalies will be calculated to examine the interacting effects of the two factors in affecting summer precipitation in the GP. Here the persistence (or lagged spatial correlation) of soil moisture anomalies from May 1st to JJA is an indicator of soil moisture memory (e.g., does the pattern of soil moisture anomalies present on May 1st persist through JJA). High persistence indicates that the spatial pattern of soil moisture anomalies is relatively constant from May 1st to JJA. This research will be the first to investigate the role of antecedent soil moisture conditions in modifying summer precipitation in the GP using long-term soil moisture data. Understanding the role of soil moisture in climate, coupled with other external teleconnections (e.g., SST) will further enhance the prediction of summer precipitation in this region.

5.2 Spatial variations in the soil moisture-precipitation relationship

Although fall soil moisture anomalies (1920-2007) are not strongly correlated

---

* Part of this section is reprinted with permission from "Observed Observation relationship of sea surface temperatures and precedent soil moisture with summer precipitation in the U.S. Great Plains" by Meng and Quiring, 2009. *International Journal of Climatology*, **in press**, Copyright [2009] by Royal Meteorological Society.

with summer precipitation, as measured by JJA SPI, in the GP (not shown), there are statistically significant positive correlations between spring soil moisture and regional summer SPI in 25% of the GP (Figure 5.1). There is a great deal of spatial variation in the relationship between spring SM and summer SPI in the GP. The locations with positive correlations are generally concentrated in the eastern half of the study region, specifically the northeastern corner. A positive correlation suggests that when spring soil moisture is above (below) normal in these locations, GP summer precipitation tends to be above (below) normal. This region is comparable to the high feedback efficiency zone in the central U.S. identified by Zhang et al. (2008) (their Figure 4). In addition to being identified as a region of efficient moisture recycling, it is also possible that the higher correlations are present because the available water holding capacity of the soils in the northeastern GP are generally higher than in the rest of the GP. Therefore, for example, it takes more precipitation to replenish dry soils than in the rest of the GP. The statistically significant correlations are primarily located in zone 2 where, as demonstrated in Section 3.3, SM persistence is always higher than the rest of the GP.

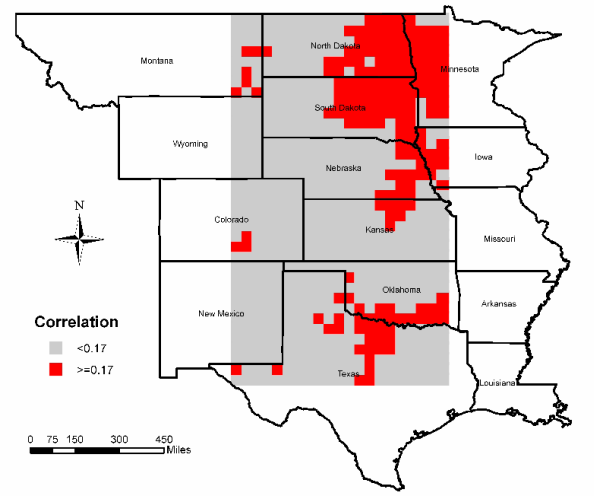

Figure 5.1 Spatial distribution of the correlation between spring soil anomalies in each grid and averaged JJA SPI in the GP. [Red grids indicate correlation significance at 90% confidence level].

Although a detailed examination of the physical mechanisms that are responsible for the patterns shown in Figure 5.1 is beyond the scope of this research, we hypothesize that spring SM is physically linked to GP precipitation in two ways:

1) Energy and water fluxes. May 1st SM anomalies cause local and regional anomalies in the energy and water fluxes that can persist for a number of months. Many of the locations that have statistically significant correlations between SM and summer SPI are located in the portion of the GP with the greatest SM persistence (e.g., longest 'memory'). The observed positive correlations suggest that May 1st SM anomalies increase GP precipitation by, for example, increasing surface evaporation and convective instability. Brubaker et al. (1993) suggested that soil moisture processes and precipitation recycling are most significant in the central U.S. and they found that the ratio of locally evaporated precipitation to total precipitation was high as 0.4 during the summer. The influence of the soil moisture anomalies is generally limited to the region

directly surrounding the anomalies and downwind locations that are influenced by water vapor transport (Schar et al. 1999).

2) Atmospheric circulation. It has been demonstrated that soil moisture anomalies can have significant non-local impacts on precipitation in regions that are far removed from the soil moisture anomalies due to modifications in regional atmospheric circulation (Zhang and Frederiksen 2003). Therefore May 1st SM anomalies in the GP may influence precipitation patterns both upstream and downstream of their location by altering atmospheric circulation patterns. Changes in upper-level circulation can modify the strength and location of the storm tracks and patterns of atmospheric moisture convergence/divergence (Hu and Feng 2001b; Ruiz-Barradas and Nigam 2006). Therefore, regions that are far removed from the soil moisture anomalies can still experience significant changes in summer precipitation. For example, Zhang and Frederiksen (2003) found that local moisture recycling only accounted for a limited portion of the variation in East Asian monsoon rainfall and that changes in horizontal water transport and regional atmospheric circulation were more important.

It is important to interpret these results with care because it is not realistic to suggest that spring soil moisture from an individual grid cell can cause summer rainfall anomalies in the entire GP. This analysis is only meant to illustrate that spring SM in the GP is statistically related to summer precipitation and that this relationship is spatially variable. The true nature of the relationship between spring SM and summer precipitation can not be determined using these data.

5.3 Temporal variations in the soil moisture-precipitation relationship

A 15-yr sliding correlation between fall/spring SM anomalies and summer precipitation (SPI) was calculated for the three GP precipitation zones (Figure 5.2a, 5.2b). Statistically significant correlations (at 90% significant level, and thereafter, unless indicated) between spring SM anomalies and summer precipitation are evident only during 1920s-1930s and they weaken or disappear in other periods. This suggests that the strength of the land-atmosphere coupling is not consistent over time in the GP. The temporal variation in the correlation supports the hypothesis that several different and competing processes are responsible for summer precipitation variability in the GP (Namias 1991) and, therefore, no persistent linear relationships between precipitation and soil moisture anomalies are present (Hu and Feng 2004; Zhu et al. 2005). The highest correlations between spring SM and summer SPI are approximately 0.6-0.8 for the three zones indicating that approximately 36%~64% of summer SPI variations can be attributed to antecedent SM conditions. These numbers are consistent with the peak correlations ($r^2 > 0.4$) between spring SM and summer precipitation calculated by Findell and Eltahir (1997) using observational data in Illinois. These values are also comparable to the ratio of locally evaporated precipitation to total precipitation during the summer (JJA) in the central U.S. calculated by Brubaker et al. (1993).

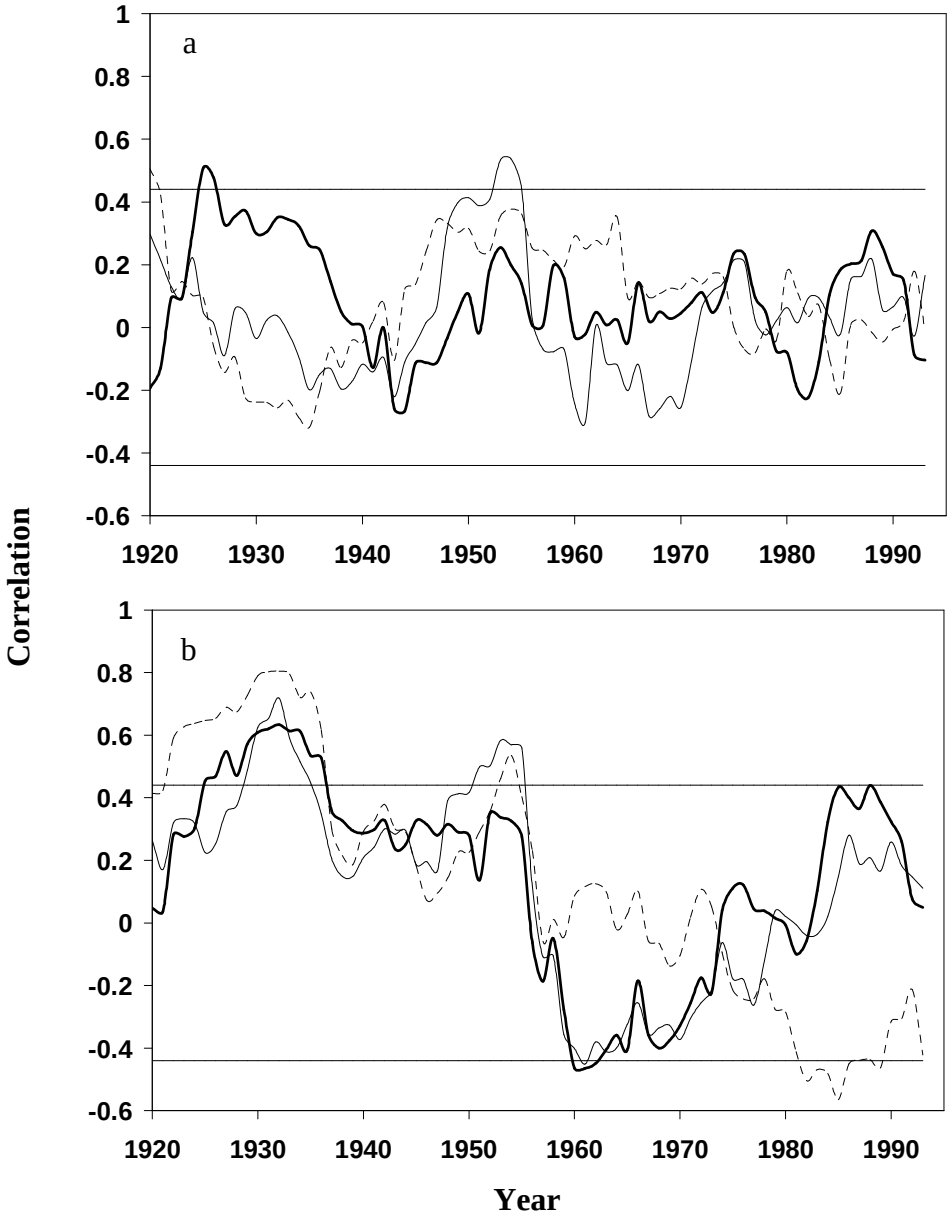

Figure 5.2 Temporal variations in the 15-year sliding correlation between fall (a) and spring soil moisture (b) and summer SPI in zone 1 (thick line), zone 2 (thin line) and zone 3 (dashed line). [Straight lines indicate correlation significance at 90% confidence level].

Our results also show some interesting intra-regional variability in the temporal correlations (Figure 5.2). It is evident that the correlations for zone 1 and zone 2 have similar patterns, while zone 3 is different from zones 1 and 2. The correlations in zone 3 have decreased since 1950s from positive to negative. This might be attributable to the different climatic region where zone 3 is located. Zone 3 is located on the southeastern edge of the GP and has annual mean precipitation that is about two times and three times greater than that in zone 1 and zone 2, respectively. Therefore, zone 3 has a different climatology from zone 1 and zone 2 and responds differently to antecedent SM conditions. Further examination of the correlation between spring SM anomalies and each individual month (June, July, and August) SPI reveals that the strongest correlations are present in the early period (1920s-1930s). During this period, the impact of spring SM anomalies tended to persist for at least three months in the three zones, as demonstrated by the significant correlations in Figure 5.2b. After 1950, spring SM conditions do not account for much of the variance in summer precipitation in the GP, indicating that SM memory is no longer a dominant factor affecting summer precipitation. When comparing Figure 5.2a and Figure 5.2b, it is clear that spring SM (1-3 month lead) generally has stronger correlations with summer precipitation than fall SM (> 8 months lead). Fall SM anomalies have not had a statistically significant influence on summer precipitation during any period since 1920. This indicates that fall SM anomalies do not persist long enough to affect subsequent summer precipitation.

5.4 Persistence of spatial patterns in SM anomalies

The variations in the relationship between SM anomalies and summer precipitation are possibly associated with the persistence of SM anomalies. Strong persistence of SM anomalies indicates longer land memories resulting in a larger influence on atmospheric circulation (Koster and Suarez 2001). It has been suggested that the persistence of SM anomalies depends on several factors including climatic region (Arora and Boer 2006; Wu and Dickinson 2004), soil depth (DeLiberty and Legates 2008), and vegetation type (Dong et al. 2007). In this study, the GP are divided into three different climatic regions based on monthly precipitation climatology. The persistence of spatial patterns in SM anomalies from May 1st to summer (JJA) is shown in Fig 5.3. Overall, there are strong temporal variations in the persistence of SM anomalies. Zone 1 and zone 2 have similar patterns of SM persistence with slightly higher values in zone 2. This is possibly due to the fact that zone 1 and zone 2 have similar climatology, but zone 2 is the transition zone between zone 1 (dry zone) and zone 3 (wet zone) (Figure3.1 in section 3) (Koster et al. 2004). The temporal variations in SM persistence are similar to those in SM-precipitation correlations (Figure 5.2b). For example, the highest soil moisture-precipitation correlations during the period of 1920s-1930s are associated with the highest soil moisture persistence during the same period. This suggests that strong SM-precipitation coupling might be due to the persistence of SM anomalies. It also reveals that there is an overall decreasing trend in the SM persistence in each zone (Figure 5.3). This might explain why SM-precipitation correlations were only significant during the early period 1920s-1930s and have

decreased since then. Further comparison of Figure 5.3 with Figure 5.2b suggests that the low SM persistence (< 0.3) in zone 3 during the period of 1970s-1980s might contribute to the strong negative SM-precipitation correlation in the early 1980s.

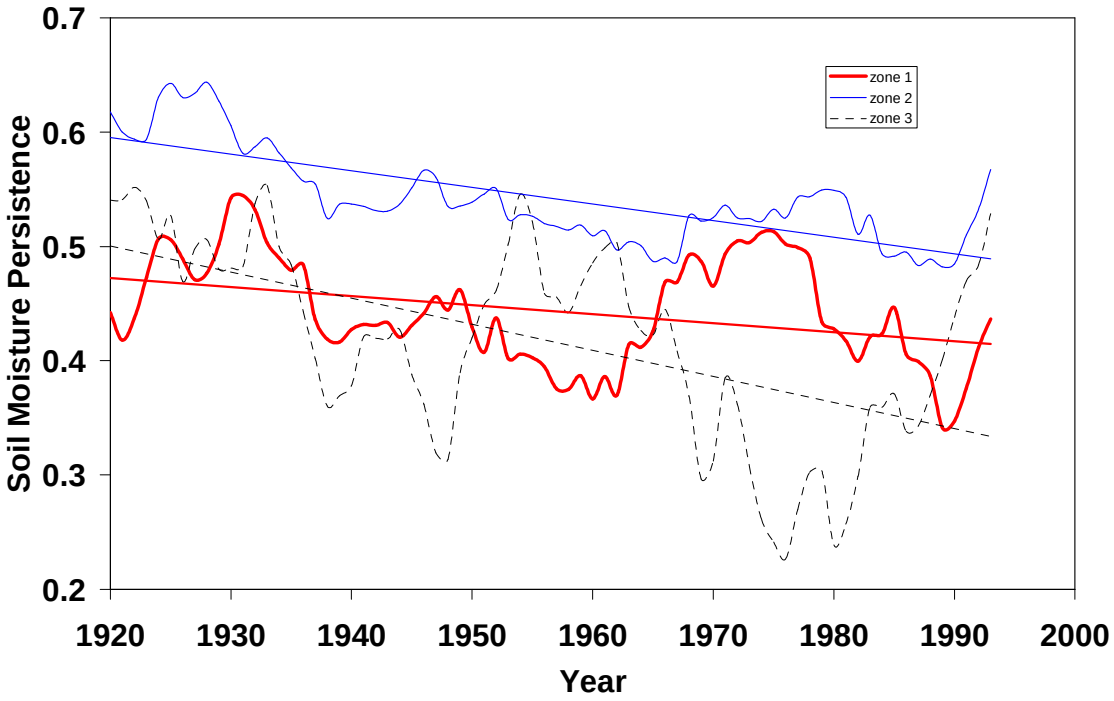

Figure 5.3 Temporal variations in soil moisture persistence in zone 1, zone 2, and zone 3. A 15-yr smoothing was applied to remove the high frequency variations. [Three straight lines indicate the general trends in soil moisture persistence in zone 1, zone 2, and zone 3].

5.5 Temporal variations in the relationship between GP summer precipitation and Niño SSTs

In addition to land-atmosphere interactions, Niño SSTs are also known to have significant influence on summer precipitation in the GP. Our results reveal that the SST anomalies over Niño 3 and Niño 4 (central equatorial Pacific) regions have the strongest correlations with GP summer precipitation. Figure 5.4 shows the temporal variations in

the correlation between the Niño SST anomalies and summer SPI. Significant zone to zone differences in the correlation are apparent. A strong positive correlation only exists in the periods 1950-1980s in zone 1. There are no significant correlations between SST anomalies and JJA SPI in zone 2 and zone 3. This suggests that although ENSO can influence GP summer precipitation, these influences vary greatly over time and space. The dominantly positive correlation between ENSO and summer SPI exists during 1950-1980s which is similar to the period identified by Hu and Feng (2001) (e.g., their Figure 4). The temporal variations in the influence of ENSO on the GP summer precipitation may be caused by the changes in SST anomalies persistence (Hu and Feng 2004) since strong SST anomalies persistence will cause persistent anomalies in the atmospheric circulation in the United States (Namias et al. 1988). The persistence of SST anomalies in Niño 3 and Niño 4 regions from April to JJA was calculated using ERSST.v.3 (Figure 5.5). The average persistence from April to JJA is 0.49 which is comparable to the value calculated by Namias et al. (1998), although our calculation uses a longer record and focuses on a smaller area. It is shown in Figure 5.5 that the SST persistence is strong in the period of 1940s-1980s and the SST persistence is weak before 1940s and after 1980s. A comparison of Figure 5.4 and Figure 5.5 suggests that the highest SST-SPI correlations occur concurrently with the strong persistence of SST anomalies. The weakness of the SST-SPI correlation in the later part of the record is likely associated with the weak SST persistence after 1980s. Further comparison with Figure 5.2 suggests that when the persistence of the SST anomalies in the Niño 3 and Niño 4 regions is

strong, the influence of soil moisture anomalies on summer precipitation tends to be weak.

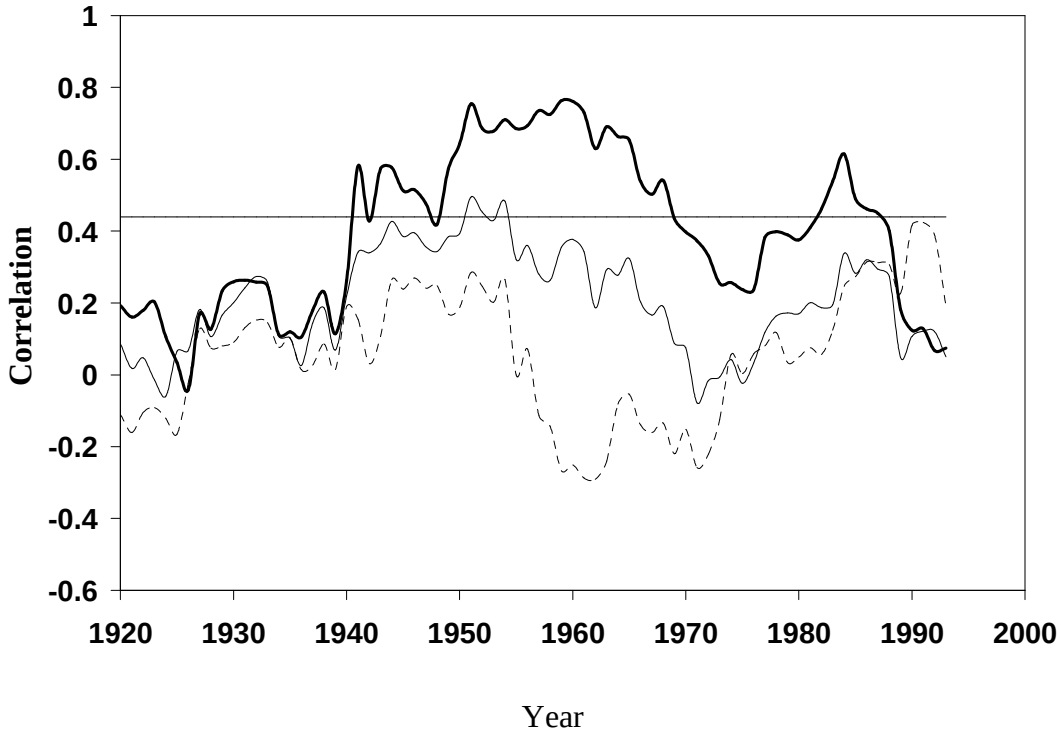

Figure 5.4 15-year sliding correlations between SST anomalies in Niño 3 and Niño 4 regions and summer SPI in zone 1 (thick line), zone 2 (thin line), and zone 3 (dashed line). [Straight line indicates correlation significance at 90% confidence level].

The strong persistence of SST anomalies since the 1940s is associated with weak SM-SPI correlations indicating that the influence of the remote SST forcings is the dominant control. During strong persistence years, SST anomalies play a dominant role and local SM conditions are not important (or at least secondary) in modifying summer precipitation in the GP. When SST anomalies persistence is weak, such as during the period 1920-1940s, the land-atmosphere interaction played a more significant role as

evidenced by strong SM-SPI correlations. This suggests that the apparent weak soil moisture memory after 1940s could be a result of stronger SST persistence. This finding is similar to Hu and Feng *(2004)* who found that land memory had a stronger influence on the North American Monsoon precipitation when the influence of SST anomalies was weak. They also documented that when the persistence of SST in the North Pacific Ocean was strong, the effect of land surface processes on summer monsoon variations tended to be weak.

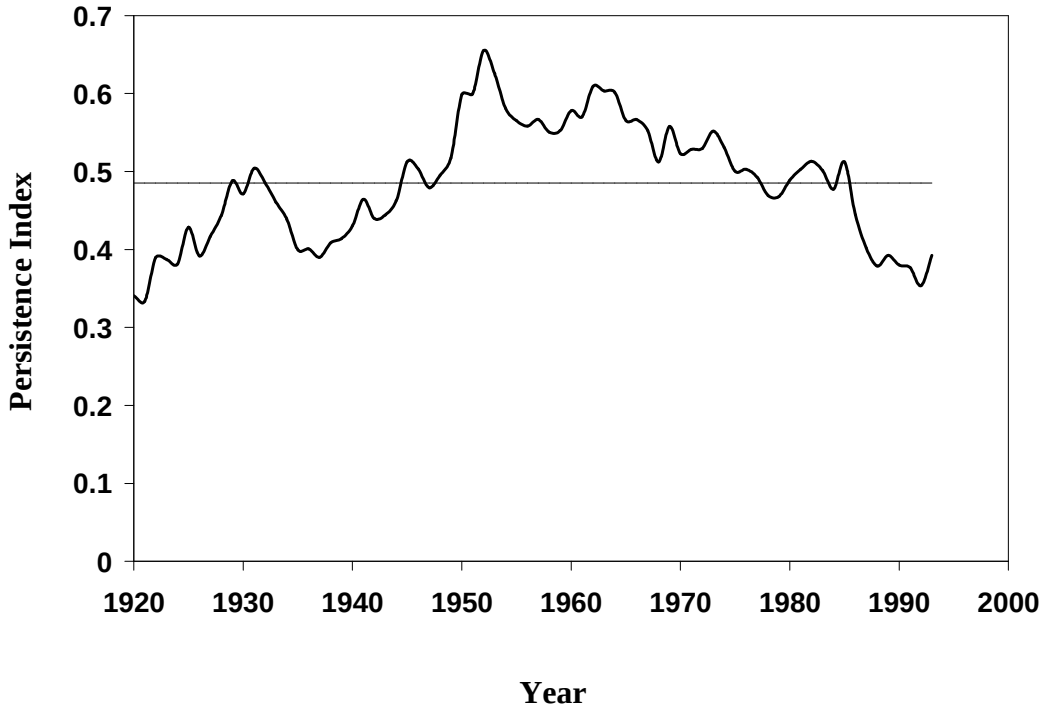

Figure 5.5 Persistence of SST anomalies from April to JJA over Niño 3 and Niño 4 regions. [Straight line indicates the long term mean (0.49)]. A 15-yr smoothing was used to remove the high frequency variations in the persistence variations of the SSTA.

Further analysis was conducted to calculate the spring SM and summer SPI correlation for zone 1 in years with high and low SM/SST persistence to identify how these variations influence summer precipitation. A comparison of Figure 5.2 and Figure 5.5 suggests that the highest correlation between spring SM and summer SPI did not occur concurrently with the lowest SST persistence in 1921. In order to identify the years have the strongest correlation, we ranked the persistence of years from low to high values and then calculated 10 year sliding correlations of corresponding spring soil moisture anomalies and summer SPI which are shown in Figure 5.6. The results suggest that when SST persistence is negative, spring SM anomalies tend to have negative correlations with summer SPI. It also demonstrates that spring SM and summer SPI are highly correlated when SST persistence is less than 0.4. The correlations between SM and SPI are not statistically significant during years when SST persistence is greater than 0.4. These results suggest that the apparent weak correlation between spring SM and summer SPI could be a result of the dominant influence that SST anomalies in the central equatorial Pacific have on the summer precipitation in the GP. To further examine the influence of SST persistence, composite mean monthly SST anomalies were calculated and plotted in Figure 5.7. A clear pattern was identified. During negative persistence (-0.60 to -0.07) years, SST anomalies in the central equatorial Pacific increased significantly from cold phase in winter to warm phase in summer and fall. The pattern in the negative persistence years is opposite to that in the highest persistence (0.48 to 0.94) years and the change in SST in the highest persistence years is even greater than that in the negative years. During the low positive persistence years, we see

a very small change in SST from winter to summer. Previous studies have documented the effects of ENSO and PDO phases on precipitation in the central United States (Kurtzman and Scanlon 2007) and in the southwest United Stated (Guan et al. 2005). These studies generally suggest that ENSO has a large influence on precipitation during either strong El Niño or La Niño years, but not in neutral years. Our study reveals that SST anomalies have significant impacts on summer precipitation in the GP during high persistence years when SST in central equatorial Pacific is switching from warm phase (winter) to cold phase (summer). When there are no significant changes in SST (low positive persistence), SM anomalies explain a statistically significant proportion of the variation in GP summer precipitation. In addition, SM anomalies may have significant negative correlations with summer SPI when Niño SST shifts from cold phase in winter to warm phase in summer. This negative correlation between spring SM anomalies and summer SPI is unexpected. However, previous studies have demonstrated that negative feedbacks may be present under certain conditions (Ek and Holtslag 2004; Pan et al. 1996). For instance, Ek and Holtslag (2004) showed that decreasing soil moisture may increase boundary layer clouds when the stability above the boundary layer is weak. Increased cloud cover can cause more precipitation on a daily time scale. Negative SM-precipitation feedbacks can also exist as demonstrated by Douville et al. (2001) in their numerical simulations of the Asian monsoon. Douville et al. (2001) found that increased SM did not increase rainfall due to a weak moisture convergence suppressed by the increased evapotransporation over India. In our study, positive SM feedbacks dominate,

but negative feedbacks also can occur when SST persistence is below zero. This finding merits further examination with regional/global climate models.

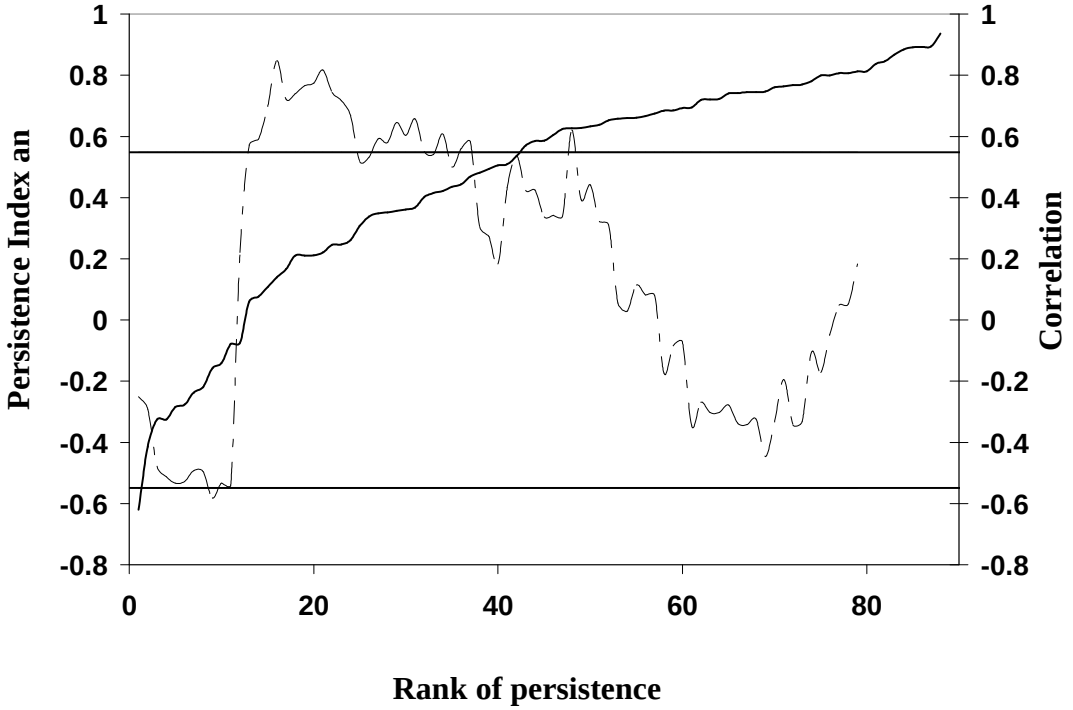

Figure 5.6 Distribution of the ranked SST persistence values (solid line) from lowest to highest and the corresponding ten-year sliding correlations (dashed line) between spring soil moisture and summer SPI. [Straight lines indicate 90% significance level].

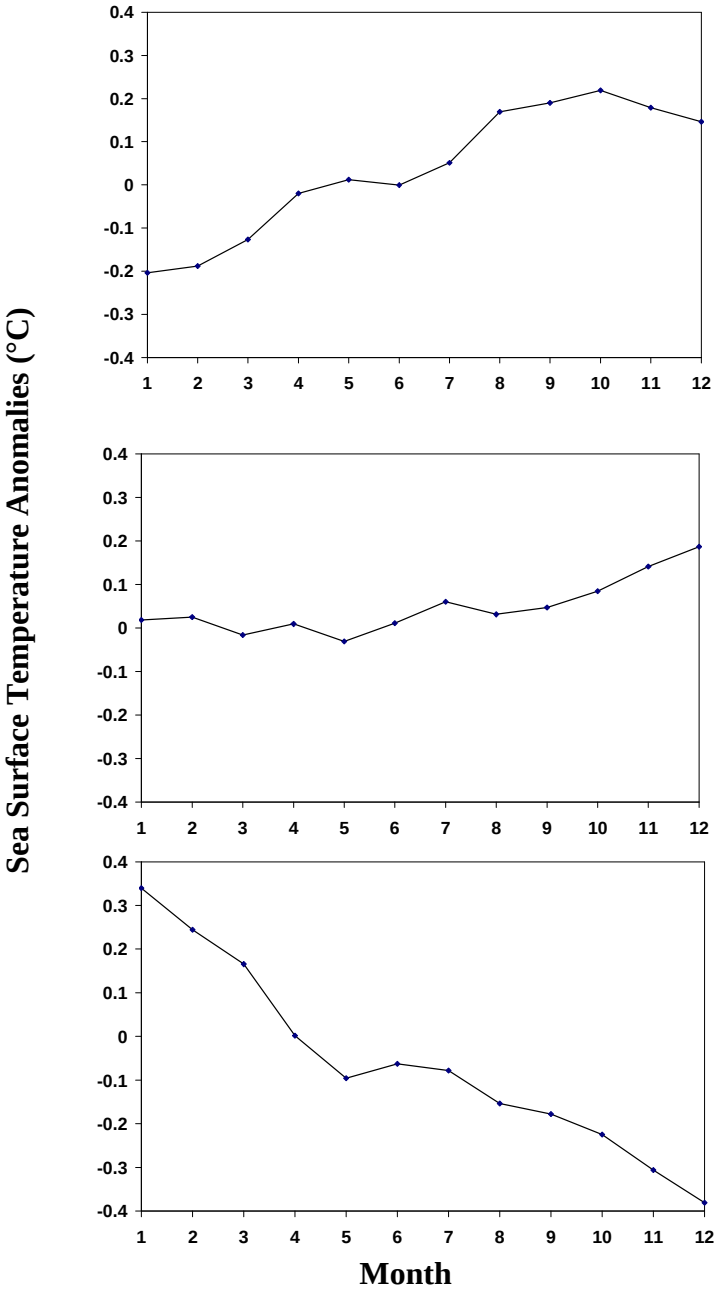

Figure 5.7 Composite mean monthly SST anomalies during 12 negative persistence years (top), 12 low positive persistence years (middle), and 12 high positive persistence years (bottom). The mean persistence is -0.26, 0.18, and 0.86, respectively.

5.6 SST persistence versus SM persistence

To further investigate how SST and SM persistence influences precipitation, we divided each year into one of four categories: low SST and low SM persistence years (LsstLsm), low SST and high SM persistence years (LsstHsm), high SST and low SM persistence years (HsstLsm), and high SST and high SM persistence years (HsstHsm) (Figure 5.8). Here high SST persistence is defined as greater than mean SST persistence and low SST persistence years are those years with lower than mean SST persistence. The same rule applies to define low and high SM persistence years. From each category, 18 years were selected to calculate soil moisture-precipitation correlation. Only the SM-precipitation correlations in zone 1 were examined for this analysis since zone 1 is the only zone in the GP where SST and precipitation are significantly correlated (Figure 5.4). It is shown in Table 5.1 that the highest SM-precipitation correlation is associated with the LsstHsm years and the correlation is weaker during HsstHsm years possibly indicating that SST persistence is the dominant process limiting SM-precipitation interactions (Hu and Feng 2004). Positive correlations were observed during the high SM persistence years and negative correlations were generally found in the low SM persistence years. Interestingly, high SST persistence seems to favor (inhibit) negative (positive) SM-precipitation relationships. For instance, the strongest negative correlation was associated with HsstLsm years.

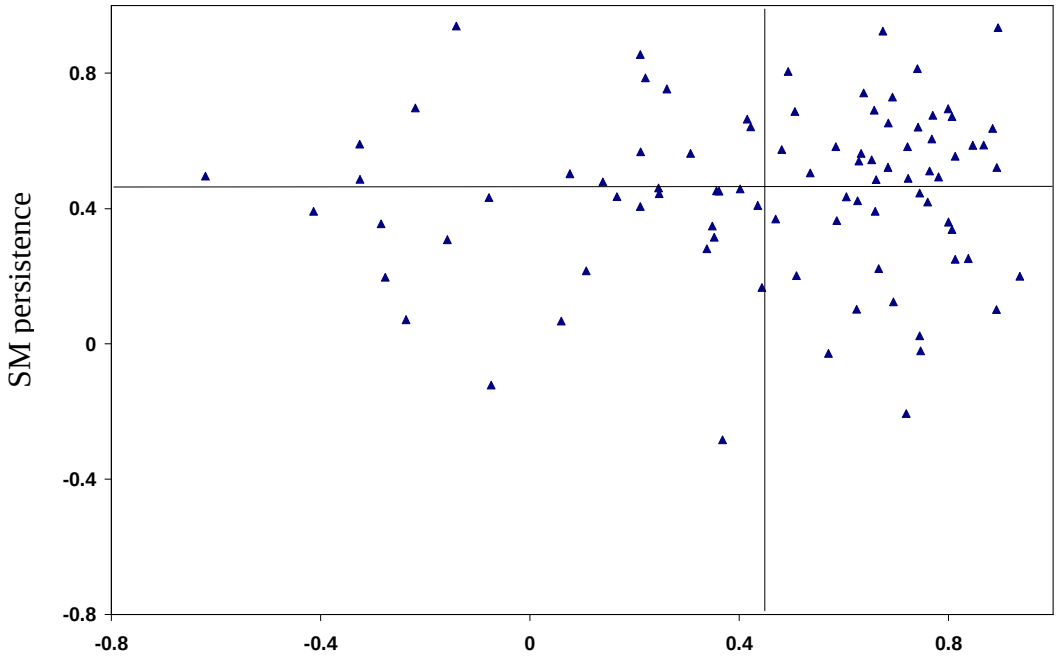

Figure 5.8 Scatter plot of SM and SST persistence in zone 1 during the period of 1920-2007. The mean SM and SST persistence are 0.45 and 0.49, respectively.

Table 5.1 The SM-precipitation correlations in zone 1 during the defined four categories.

	High SM persistence	Low SM persistence
High SST persistence	0.22	-0.31
Low SST persistence	0.35	-0.14

5.7 Conclusions

The temporal and spatial variations in the soil moisture-precipitation relationship were examined using VIC-simulated SM and SPI. In addition, the role of SST

persistence was also investigated to identify how persistence influences the relationship between SM, SST and GP summer precipitation. Our results suggest that there are significant temporal and spatial variations in the correlations between SM and summer precipitation in the GP. Spring SM has a statistically significant influence on summer precipitation in GP and the correlation is stronger in zone 1 than in zones 2 and 3. Generally, SM only plays a significant role in modifying summer precipitation during the periods when the influence of SST anomalies is less important (e.g., 1920s-1930s). When SST anomalies are dominant (e.g., 1940s-1980s), soil moisture anomalies are not a good predictor of GP summer precipitation. The periods when SST anomalies are dominant are usually associated with strong SST persistence (April to summer). In particular, there are strong positive correlations between summer precipitation and Niño SST anomalies during years when SST changes from warmer than normal during winter to colder than normal during summer. Our study also suggests that statistically significant SM-precipitation correlations are associated with strong SM persistence and weak SST persistence. In conclusion, although both local soil moisture and remote SST anomalies influence GP summer precipitation, soil moisture anomalies are of greatest importance when SST persistence is weak.

6. SIMULATION OF THE EFFECT OF SPRING SOIL MOISTURE ON SUMMER PRECIPITATION

6.1 Introduction

General Circulation Models are often used to explore the nature of soil moisture-precipitation interactions and to investigate the physical mechanisms in the soil moisture-precipitation relationship (Oglesby et al. 2002; Pal and Eltahir 2001). In this section, NCAR CAM3.0, a commonly used model, was selected to investigate how soil moisture anomalies affect summer precipitation. The length of land memory and the difference in precipitation response to wet/dry soil moisture anomalies are documented. In addition, the influence of short-lived (1-day) and persistent (1-month) spring soil moisture anomalies on summer precipitation is investigated.

6.2 Influence of initial spring soil moisture anomalies on summer precipitation

6.2.1 D01_May experiment

In the D01_May experiment initial soil moisture on May 1st was modified to investigate how short-lived spring soil moisture anomalies affect subsequent precipitation in the GP. Results indicate that dry soil moisture anomalies on May 1st lead to a substantial decrease in precipitation in the GP during May (-19.6%), June (-11.1%), and July (-35.4%) indicating a positive feedback between soil moisture and precipitation. By August, the magnitude of the precipitation anomalies are greatly reduced indicating a soil moisture memory of approximately 3 months (Figure 6.1). This is consistent with

previous findings (Entin et al. 2000; Liu and Avissar 1999; Oglesby and Erickson 1989; Vinnikov et al. 1996). For instance, Entin et al. (2000) studied the temporal scales of soil moisture using observational measurements in Illinois and Iowa and found that soil moisture memory is approximately 2 months and Vinnikov et al. (1996*)* found that it is about 3 month in Russia. The largest precipitation anomaly in D01_May runs was in July possibly indicating a time-lag effect of soil moisture memory which has also been shown in previous studies (Chow et al. 2008; Koster and Suarez 2001; Pielke et al. 1999). Even though dry soil moisture anomalies of the same magnitude were applied to the whole GP, persistence is greater in the northern part of GP (Figure 6.2). This is possibly due to the fact that the soils in the northern part of GP have a higher field capacity (Figure 6.3) and therefore it takes longer to recharge the depleted soil water content to field capacity. The largest precipitation anomalies were located over the northern GP and to the north/northeast of the study region indicating that the response of precipitation to soil moisture anomalies might be both local and nonlocal. That is, the strong persistent soil moisture anomalies in the northern GP affect not only the precipitation in the same region but also in remote regions as indicated by the large precipitation anomalies in the north/northeast of the GP. This is consistent with Pal and Eltahir (2002) who found that soil moisture anomalies alter precipitation not only locally but also regionally through modifying the large-scale atmospheric circulation (e.g., changing the position of storm tracks). The region of precipitation anomalies is co-located with the region of higher surface temperature which is directly caused by suppression of evaporative cooling due to the dry soil moisture anomalies. Such an

increase in surface heating induces a thermal low pressure at the surface. The increased 500 mb geopotential heights result in an anomalous anti-cyclonic flow (especially in June and July) and less rainfall over the most portion of the GP (Oglesby and Erickson 1989). The bootstrap test suggests that although the differences in precipitation in the GP are not significant in May, they are statistically significant over the northern part of the GP in June and July (Figure 6.4). This time-lag further reveals the influence of soil moisture memory on precipitation. However, the region that experiences significant precipitation differences only encompasses a small portion of the GP.

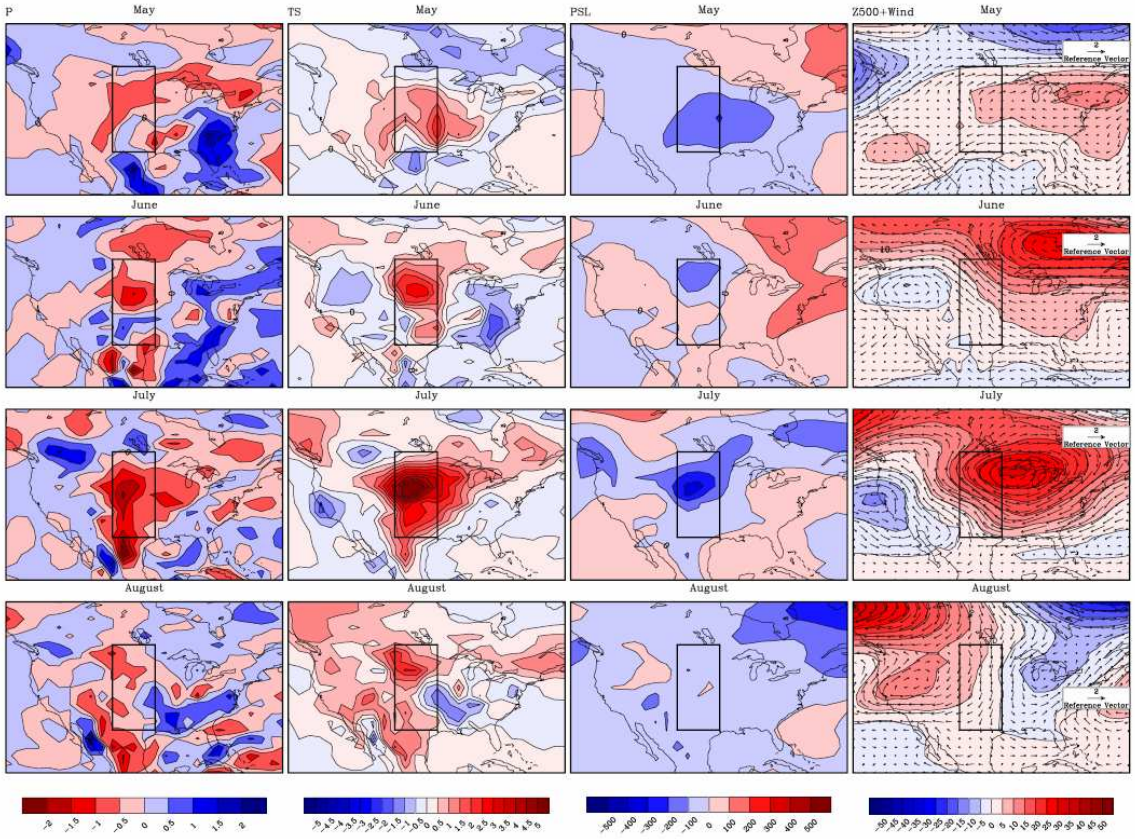

Figure 6.1 Anomalies of precipitation (P, mm day^{-1}), surface temperature (TS, °C), sea level pressure (PSL, mb), 500 mb geopotential heights (m) and 500 mb wind (m/s) (Z500+Wind) in D01_May experiment as compared to Con_May experiment.

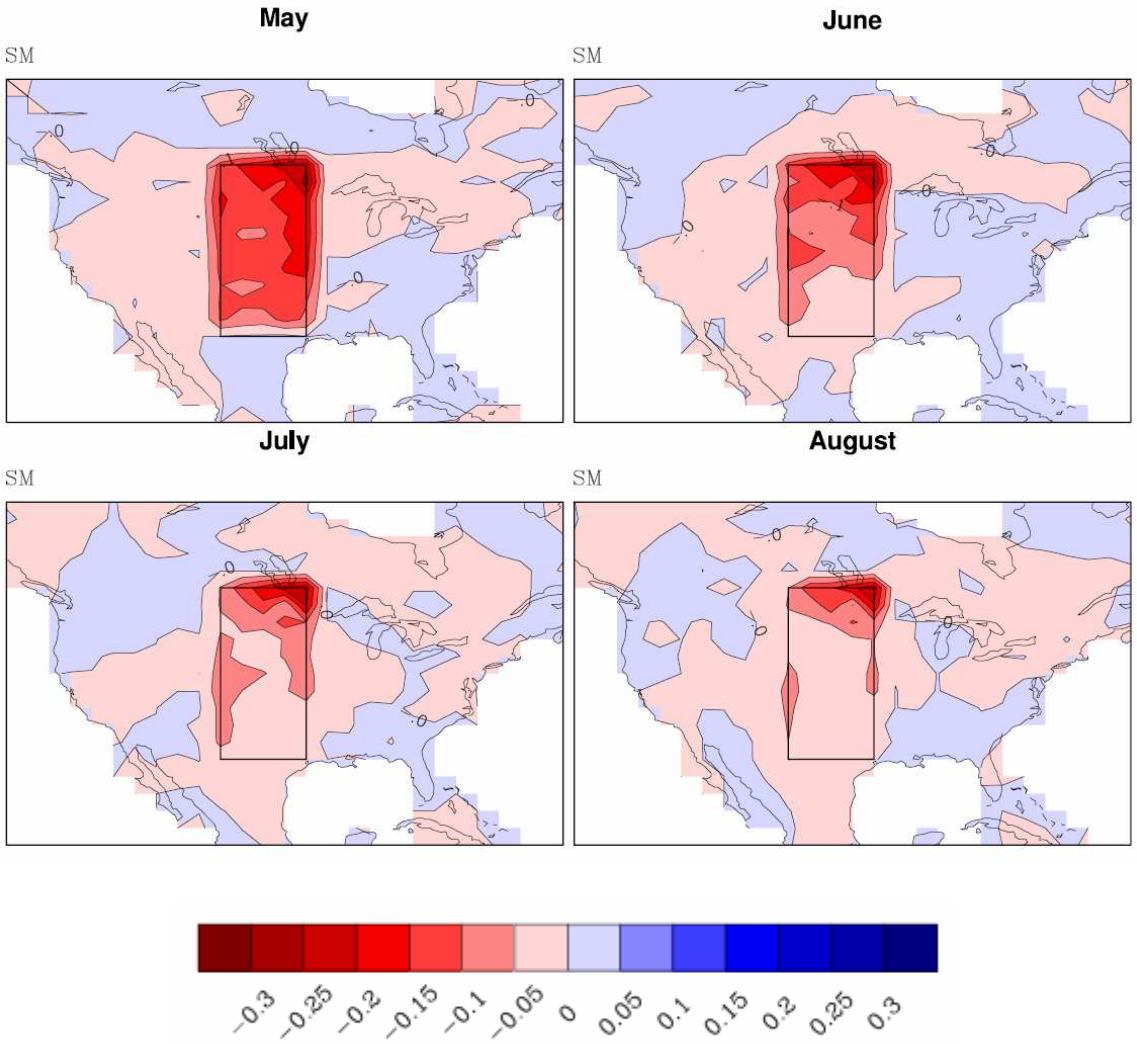

Figure 6.2 Anomalies of soil moisture (SM, mm^3/mm^3) in the D01_May experiment relative to the Con_May experiment in May, June, July, and August.

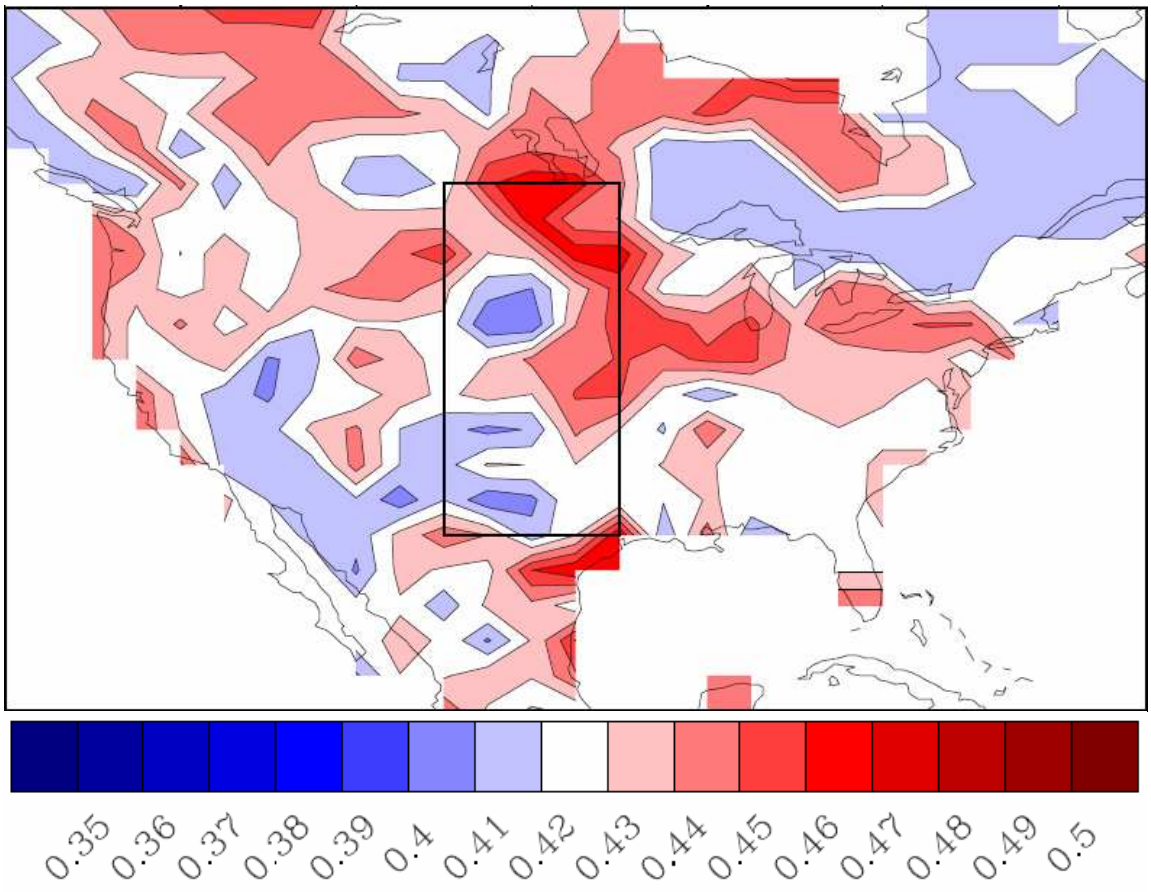

Figure 6.3 Distribution of soil field capacity at approximately 17 cm depth in the U.S.

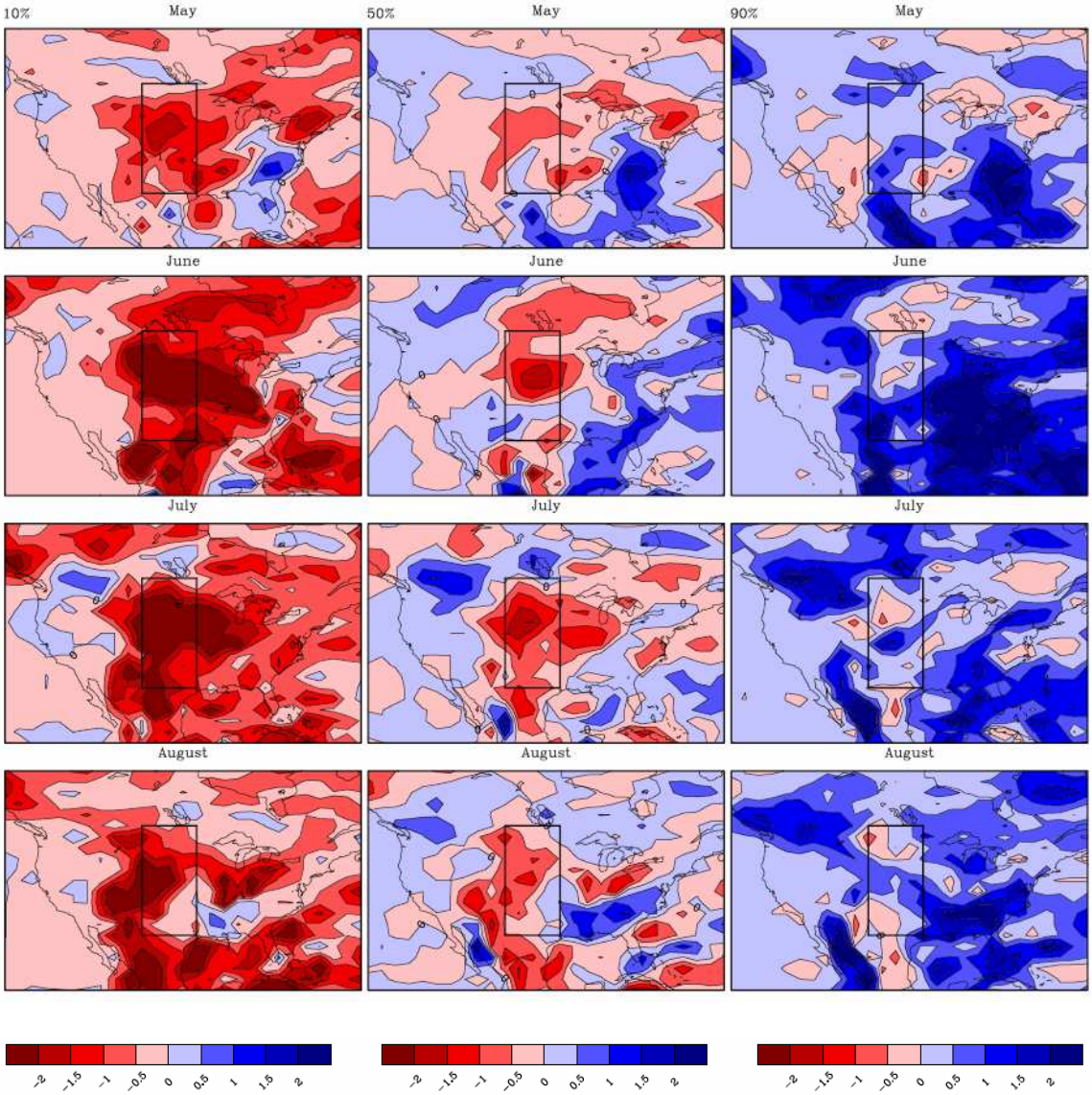

Figure 6.4 Bootstrap precipitation (mm day^{-1}) upper 10% (left), median 50% (middle), and lower 90% (right) confidence fields for May, June, July, and August (from top to bottom)in the D01_May relative to the Con_May experiment.

6.2.2 W01_May experiment

Similarly, short-lived wet soil moisture anomalies also have significant impacts on precipitation in the following months as demonstrated in Figure 6.5. This figure

shows that the largest precipitation increases occur in the central GP in May and the magnitude and spatial extent of these precipitation anomalies gradually decreases from June to August. The increase in precipitation is generally associated with decreased surface temperatures and increased sea level pressure. As the precipitation anomalies weaken from June to August, the anomalies in surface temperature and sea level pressure also weaken. Specifically, the surface cooling observed in May and June in the GP is less apparent in July. However, a large surface cooling is dominant over the northern GP and the western U.S. in August. This cooling is possibly associated with the anomalous cyclonic flow that is present over the western North America in August and the associated increase in advection of airmasses from the Pacific Ocean. The W01_May simulation also produced a low pressure anomaly centered off the western coast of North America resulting in anomalous cyclonic flow and a statistically significant increase in precipitation northwest of the GP during June, July, and August (Figure 6.6). This is an example of the nonlocal influence of wet soil moisture on summer precipitation which has been demonstrated in Pal and Eltahir (2002) and Xue (1996). Pal and Eltahir (2002) suggested that local soil moisture anomalies can affect remote precipitation through modifying the intensity and location of storm tracks. They documented that wet soil moisture anomalies over the southwestern United States resulted in an increase in precipitation of the same region and a decrease in precipitation over the Midwestern United States as well as a widespread low pressure anomaly.

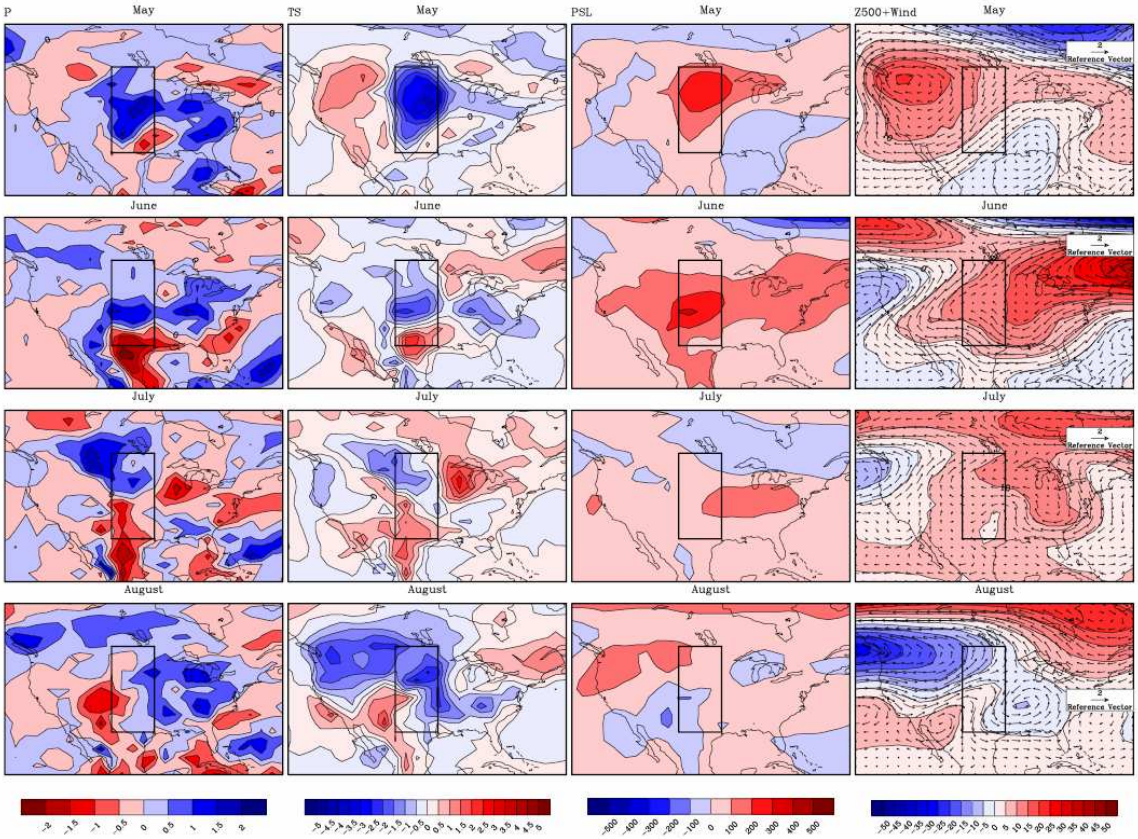

Figure 6.5 Same as in Figure 6.1, but for the W01_May experiment.

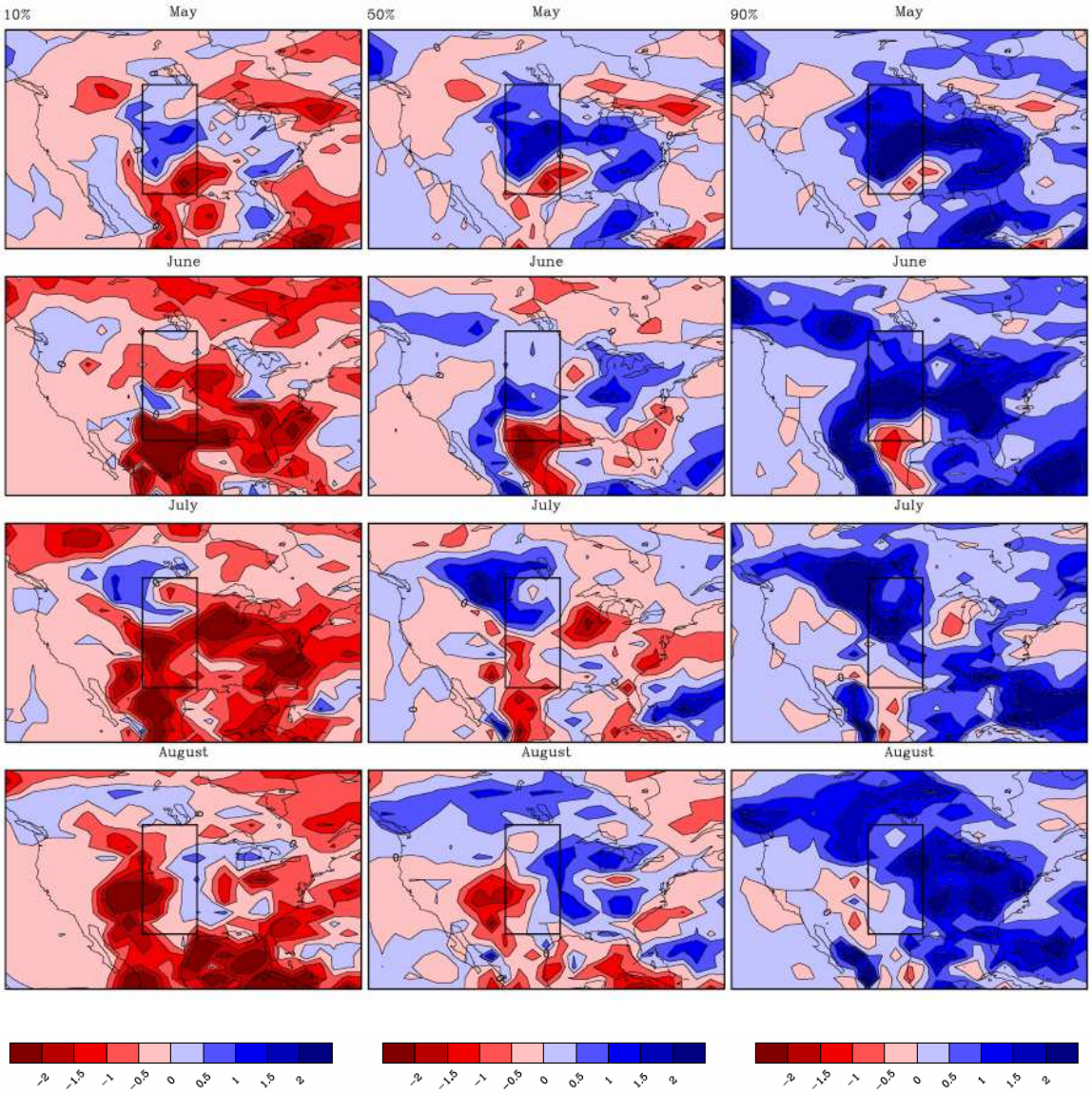

Figure 6.6 Same as in Figure 6.4, but for the W01_May experiment.

It should also be noted that the W01_May simulation produced statistically significant decreases in precipitation over parts of the southern GP in May through July. Decreases in precipitation are also evident in the western/southwestern GP in August.

These decreases in precipitation are associated with anomalous ridging at 500 mb over the southern/southwestern United States.

6.3 Influence of persistent spring soil moisture anomalies on summer precipitation

6.3.1 D30_May experiment

We investigated the influence of the persistence of soil moisture anomalies on subsequent precipitation. Dry and wet experiments were performed in which soil water content was held at fixed level in all ten soil layers for the entire month of May. The D30_May experiment produced substantial decreases in precipitation from May to July over the study region (Figure 6.7). The effect of soil moisture anomalies becomes minimal by August. The largest decreases in monthly precipitation were -1.15 mm/day in June and -0.93 mm/day in July which are roughly 64% and 32% greater, respectively, than the precipitation decreases in May. These decreases in precipitation are associated with anomalous ridging and anticyclonic flow at 500 mb centered to the east of the GP. This geopotential height anomaly is strongest in June and gradually weakens until August, when it is replaced by a zone of anomalous troughing over the central U.S.. The presence of this persistent circulation anomaly inhibits convection and causes a shift in the storm track (Oglesby and Erickson 1989; Pal and Eltahir 2002). The change in precipitation in August is only -0.02 mm/day. This suggests that the influence of the dry soil moisture anomalies has mostly dissipated by this time. Bootstrap tests verify that precipitation patterns observed from May to July, but not August, appear in both the upper and lower 90% confidence limits (Figure 6.8).

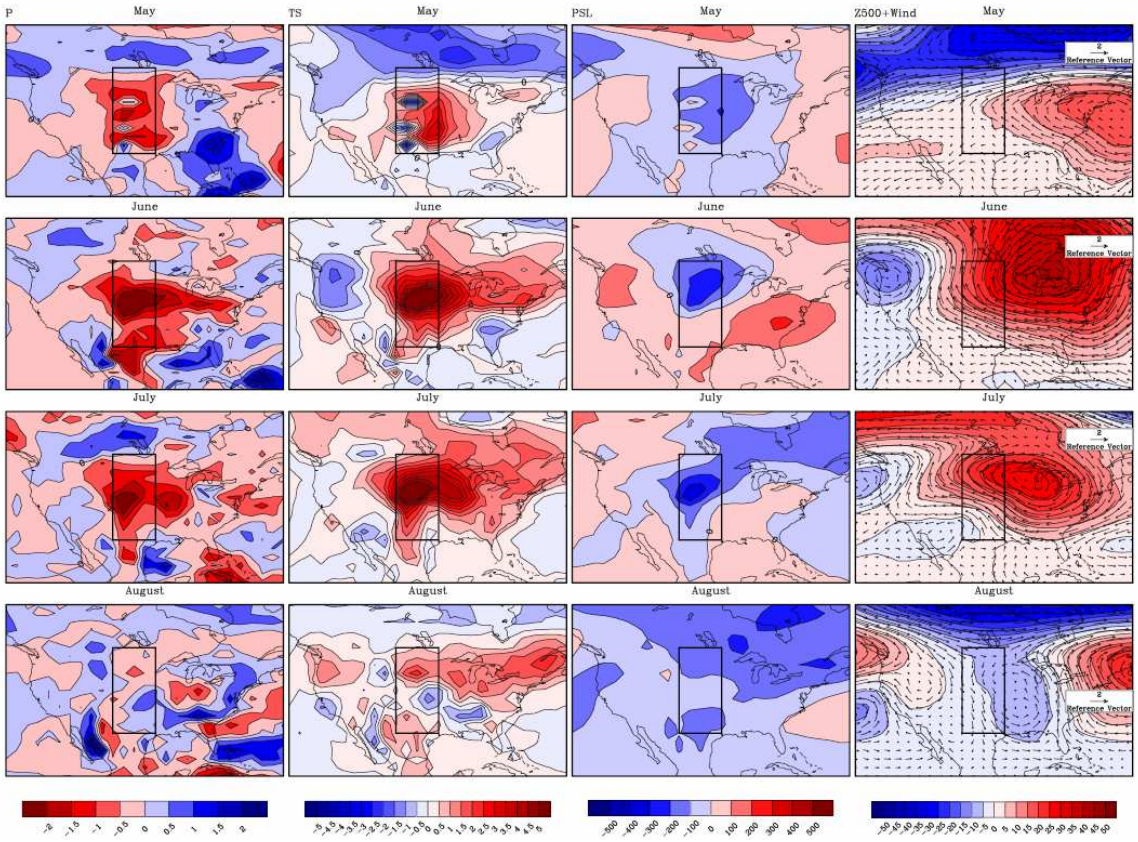

Figure 6.7 Same as in Figure 6.1, but for the D30_May experiment.

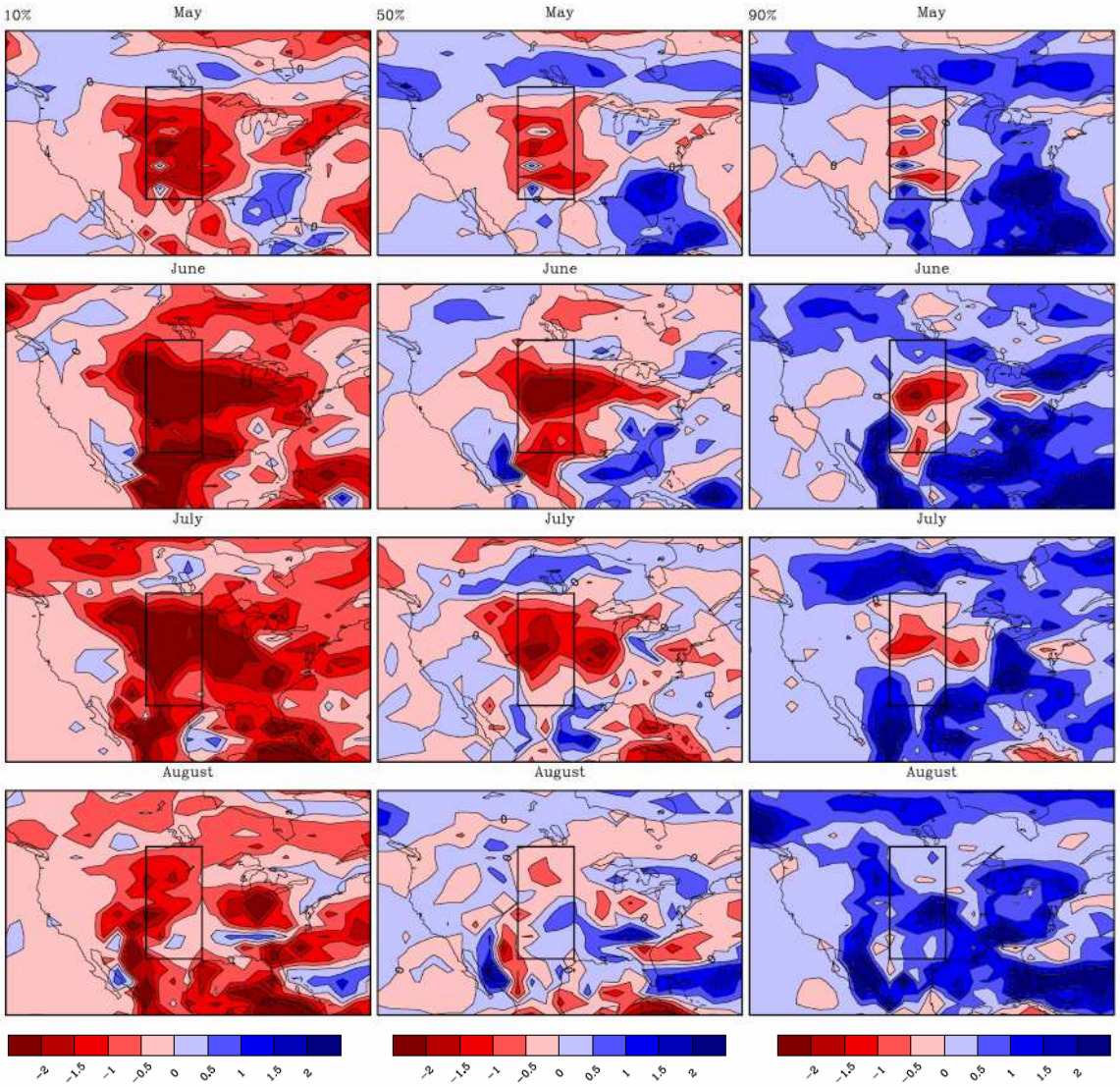

Figure 6.8 Same as in Figure 6.4, but for the D30_May experiment.

6.3.2 W30_May experiment

The persistently wet experiment (W30_May) produced significant increases in GP precipitation in May (1.62 mm/day), June (1.19 mm/day), and July (0.26 mm/day) (Figure 6.9). The precipitation response to the prolonged positive soil moisture anomalies is largest in May and gradually decreases, becoming minimal in August. Not

surprisingly, by this time soil water conditions have returned to normal in all but the lowest layers of the soil (Table 6.1). The above normal precipitation over the GP in June and July is associated with anomalous troughing and cyclonic circulation over the northern U.S. and Canada and anomalous ridging and anticyclonic flow over the southeastern U.S.. The pattern of upper atmospheric circulation in May is notably different than that observed in the other three months. In May anomalous ridging is present over the western U.S. and Canada and this matches the pattern shown in the W01_May simulations. Bootstrap tests confirmed that the increases in precipitation for May, June, and July, as demonstrated in Figure 6.10, are statistically significant.

Table 6.1 Length of time (in days) needed for each soil layer to return to the normal condition (for the period of May to October) based on the D01_May and W01_May experiments.

Response Time (days)	Soil Layer									
	1	2	3	4	5	6	7	8	9	10
D01_May	17	56	57	106	>155	> 155	> 155	> 155	> 155	> 155
W01_May	29	30	31	51	114	140	>155	> 155	> 155	> 155

Note: 1. Units are in days;
2. 155 days are the maximum simulation time.

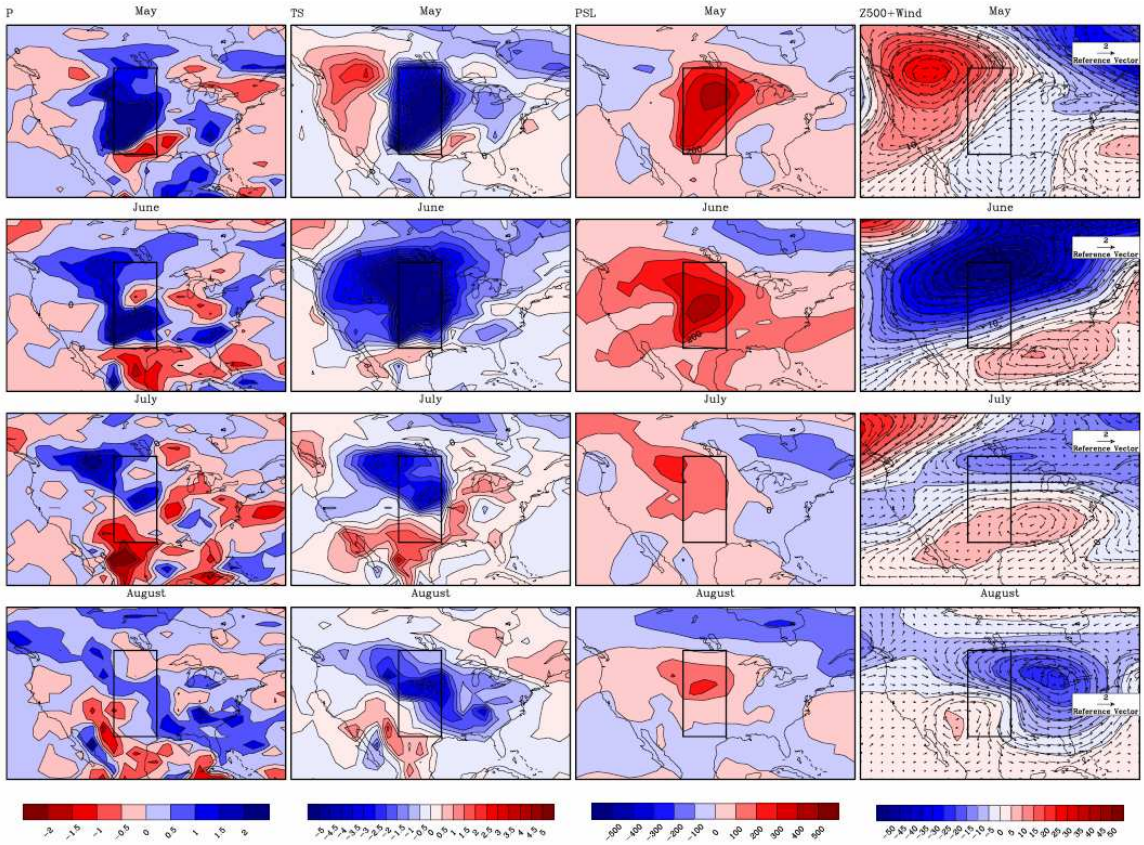

Figure 6.9 Same as in Figure 6.1, but for the W30_May experiment.

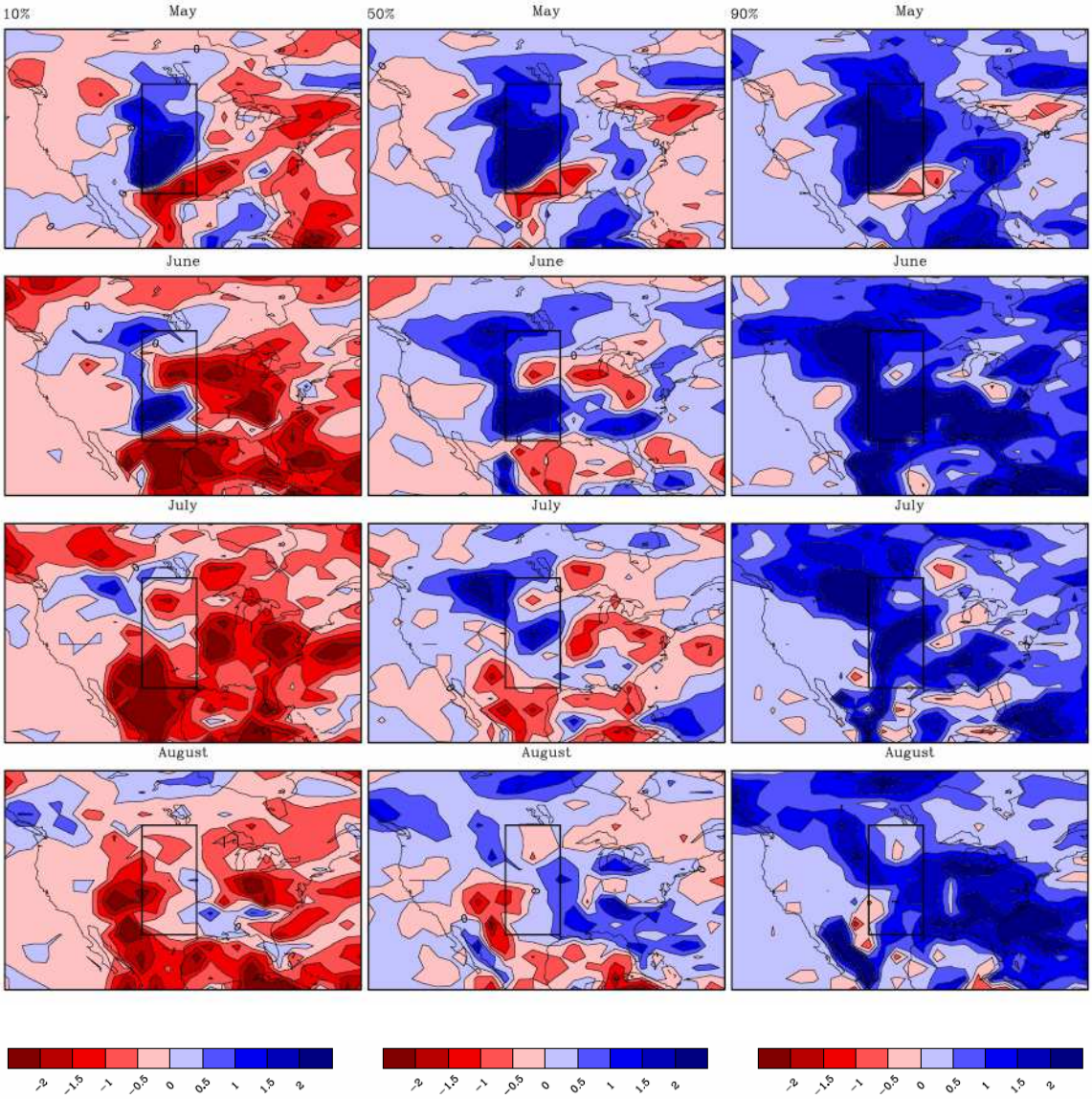

Figure 6.10 Same as in Figure 6.4, but for the W30_May experiment.

6.4 Comparison between dry and wet soil moisture anomalies

6.4.1 Dry experiments vs. wet experiments

Previous studies have shown that there are significant differences in the response of precipitation to dry/wet soil moisture conditions (Kim and Wang 2007; Pal and

Eltahir 2001). For instance, Kim and Wang (2007) demonstrated using CAM3.0 that the precipitation response to wet soil moisture conditions is greater in magnitude but shorter in duration than the response to dry soil moisture conditions. Pal and Eltahir (2001) examined the sensitivity of rainfall to initial soil moisture in the Midwestern U.S. in the NCAR RegCM and documented the greatest soil moisture-rainfall sensitivity in wet conditions. Our results suggest that positive soil moisture anomalies have larger impacts on precipitation than negative soil moisture conditions during the first month (Figure 6.11). They have comparable impacts during the second month and wet anomalies have smaller impacts than dry anomalies in the third month. In other word, the impacts are gradually decreasing in wet experiment and they are increasing in dry experiments until two months later. In the dry experiments, surface temperature anomalies increase in magnitude and area from May to July due to the persistence of the dry soil conditions. On the contrary, the magnitude of the surface temperature anomaly (absolute values) decreases over time in the wet experiments. These differences will be addressed in the next section. In general, when the soil is saturated soil water can be quickly removed through evapotranspiration as well as runoff and drainage. Dry soil moisture anomalies usually take much longer to return to normal because they require precipitation rates to exceed evapotranspiration rates. Thus, dry soil moisture anomalies (and the associated positive surface temperature anomalies) are more resistant to change than wet soil moisture anomalies (and the associated negative surface temperature anomalies). Figure 6.11 also suggests that the precipitation anomalies associated with wet soils are most pronounced in May and June, while the precipitation anomalies associated with dry soils

are largest in July. This indicates that soil moisture memory tends to be at least one month longer for dry soil moisture anomalies than wet soil moisture anomalies.

6.4.2 Short-lived soil moisture anomaly vs. persistent soil moisture anomaly

Our experiments demonstrated that persistent (1-month) soil moisture anomalies have larger impacts on precipitation than short-lived (1-day) soil moisture anomalies. For instance, W30_May experiments produced an increase in precipitation that is almost three times larger than W01_May experiments. This is not unexpected since the persistent wet soil moisture anomalies lead to higher evapotranspiration and thus higher convective precipitation. Similarly, precipitation response to the D30_May experiments was almost doubled as compared to the D01_May experiment (Figure 6.11). This suggests that summer floods or droughts are more likely to occur if spring soil moisture anomalies are persistent.

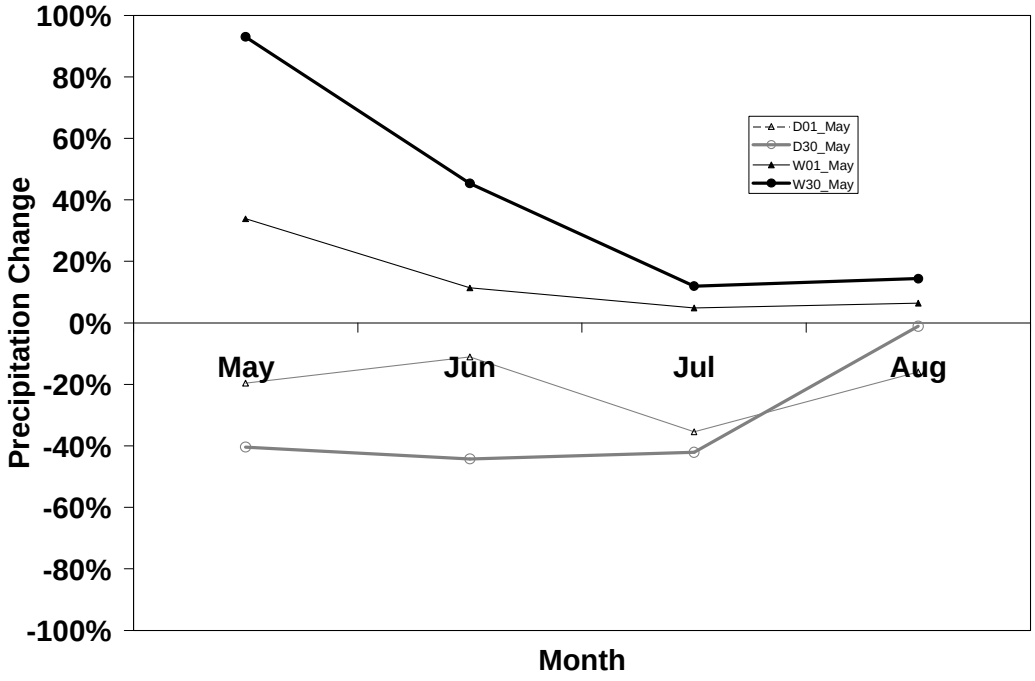

Figure 6.11 Averaged precipitation change (mm day^{-1}) (relative to control ensembles) over the U.S. Great Plains in May, June, July, and August in the four experiments.

Our results also demonstrated that soil moisture memory is not necessarily influenced by the degree of soil moisture persistence. As can be seen in Figure 6.11, the precipitation response to both the short-lived and persistent soil moisture anomalies is generally indistinguishable after three months. This is likely because soil moisture memory is primarily controlled by other factors including climate region (Arora and Boer 2006; Wu and Dickinson 2004), soil depth (DeLiberty and Legates 2008), and vegetation type (Dong et al. 2007).

6.5 Soil moisture response and recovery

Namias (1991) suggested that anomalous soil moisture conditions during spring could induce an anomalous summer precipitation through the modification of local evapotranspiration and large-scale atmospheric circulation. Our results indicate that the magnitude of precipitation response largely depends on the sign and persistence of soil moisture anomalies. In order to quantify the nature of the land-atmosphere interactions the temporal variations of soil moisture are investigated. Overall, significant differences in the temporal variations of soil moisture exist not only between dry and wet experiments but also between the ten soil layers in each experiment. Figure 6.12 shows the temporal variation in the top six soil layers for the dry ensemble runs. The mean soil moisture anomaly in the ten soil layers during the period of April to October for the dry ensemble runs is approximately -0.1 mm^3/mm^3. As can be seen from Figure 6.12, it usually takes from a couple of days to a few months for soil moisture variations in each layer to level off. Here the persistence time is calculated as a point of inflection using the second derivative. This is expected since the top layer soil moisture has greater variations and is easier to change than the deep layer soil moisture (Wu and Dickinson 2004). Therefore, it takes longer time for deep soil layers to change when an initial soil moisture anomaly is applied (Figure 6.12 and Table 6.1). The response times reported here are consistent with other studies (Oglesby et al. 2002; Pielke et al. 1999). For instance, both Pieke et al. (1999) and Oglesby et al. (2002) found that it took a year or longer for the deep soil layers to recover from large initial soil moisture anomalies in both the Regional Atmospheric Modeling System (RAMS) regional model and CAM3.0.

The similar pattern of soil moisture change is also shown in W01_May runs. Compared with D01_May, W01_May has smaller mean value (0.4 mm^3/mm^3) and the persistence time for each soil layer (to the point of inflection using the second derivative) is much less (Figure 6.13 and Table 6.1).

Due to the different response time between the top and bottom soil layers, it is hypothesized that the top layer soil moisture (roughly from 10 to 50 cm depth) can persist long enough (a couple of months) to affect summer precipitation at monthly to seasonal scales and the bottom layer soil moisture can persist even longer (more than a year) to influence interannual to decadal summer precipitation. This can be inferred from the response time and variations in soil moisture in different soil layers. The results are consistent with several other studies (Forman et al. 2001; Kim and Wang 2007; Oglesby et al. 2002; Woodhouse and Overpeck 1998).

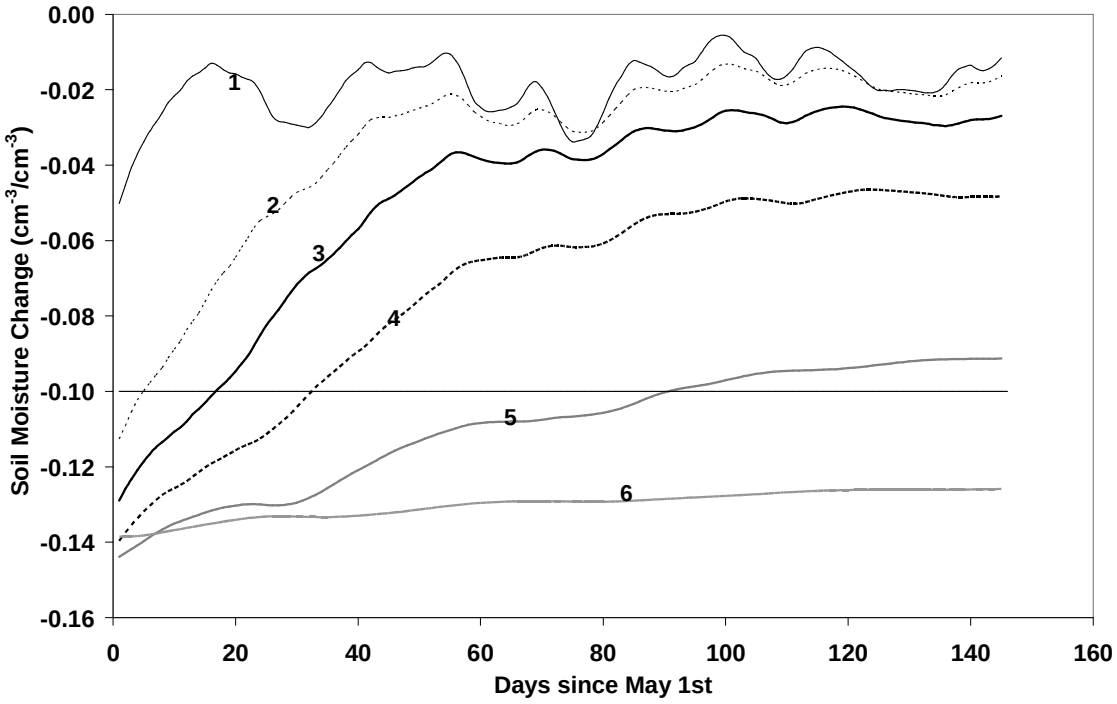

Figure 6.12 Ten-day running average of soil moisture anomalies for the entire GP in the top 6 soil layers in D01_May experiment as compared to the control experiment. The mean soil moisture anomaly in the 10 soil layers are approximately -0.1 mm^3/mm^3.

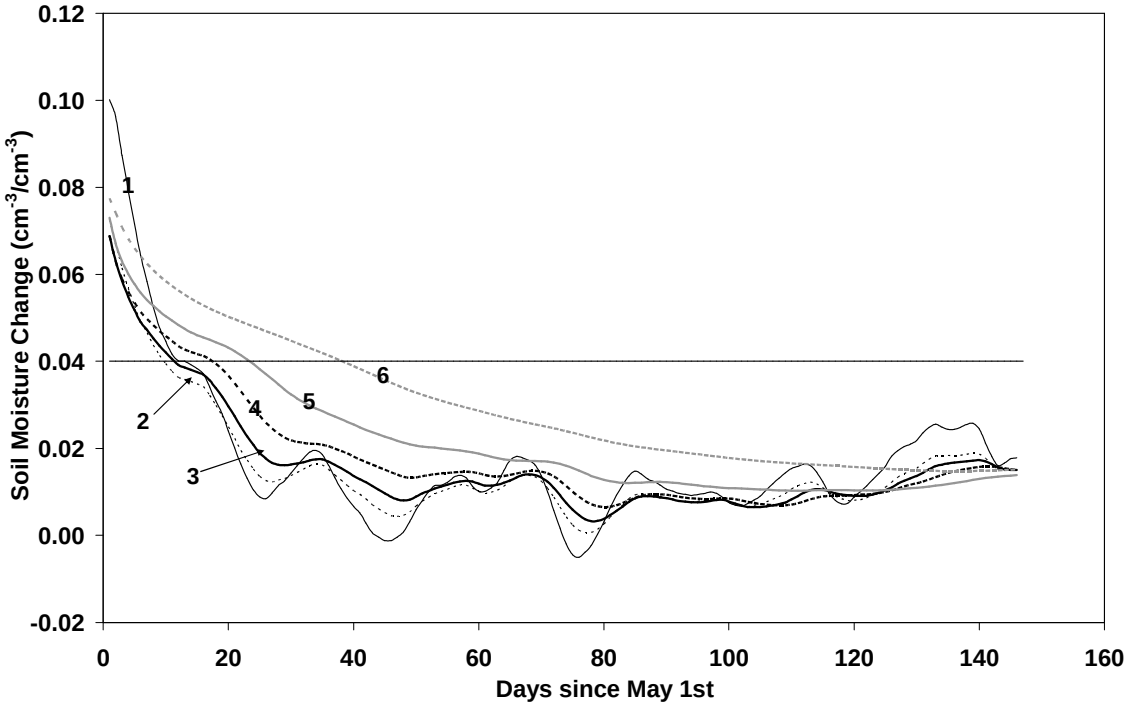

Figure 6.13 Same as in Figure 6.12, but for the W01_May experiment. The mean soil moisture anomaly in the 10 soil layers is ~0.04 mm^3/mm^3.

6.6 Influence of the timing of soil moisture anomalies on summer precipitation

The strength of land-atmosphere interaction depends on several factors, including the magnitude of anomalies, depth of the soil moisture anomalies, and timing of the soil moisture anomalies. There is strong agreement on how the magnitude and depth of soil moisture anomalies influences subsequent precipitation (DeLiberty and Legates 2008; Wu and Dickinson 2004), but there is little agreement about how the timing of soil moisture anomalies influences precipitation (Findell and Eltahir 1997; Huang et al. 1996; Oglesby et al. 2002; Pal and Eltahir 2001). Several studies have examined the effect of timing of soil moisture anomalies on precipitation and they have reached different conclusions. Oglesby et al. (2002) used the Community Climate Model version

3 Land Surface Model (CCM3/LSM) to investigate the nature of soil moisture-atmosphere interaction. They imposed normal atmospheric conditions (such as SST) and the soil moisture conditions during the driest and wettest March and June during the period 1958-1999 in the CCM3/LSM model and found that March runs have a slightly higher degree of predictability than June runs. However, overall they concluded that seasonality of soil moisture anomalies is not a major factor in land-atmosphere interaction. Findel and Eltahir (1997) examined the feedback between soil moisture and future precipitation using observed soil moisture data in Illinois and found a significantly temporal variation in the relationship between soil moisture and subsequent precipitation. They documented that significant soil moisture-precipitation correlations are only present in the summer (early June to mid-August) and not in other seasons. Pal and Eltahir (2001) investigated impact of the timing of soil moisture anomalies on the strength of soil moisture-atmosphere interaction over the U.S. Midwest using the NCAR regional climate model (RegCM) and found no significant correlations between them. In this study, soil moisture anomalies were imposed on the first day of April and the first day of May to investigate how the timing of soil moisture anomalies affects subsequent precipitation. In simulations starting on April 1st, the greatest decrease in precipitation occurred in June in D01_Apr while the most significant increase in precipitation is present in July in W01_Apr (Figure 6.14). Both D01_Apr and D01_May simulations suggest that effect of dry soil moisture anomalies on precipitation is most significant in June and July, respectively (i.e., the soil moisture memory is approximately 2 months). Bootstrap tests confirm that the precipitation response to April soil moisture anomalies is

significant and greatest in June in D01_Apr runs (results not shown). The time-lag effect is possibly due to the dominance of convective precipitation in summer seasons (Kim and Wang 2007). However, there are significant differences in precipitation response to wet soil moisture anomalies. Even though W01_May runs did not produce substantial precipitation increases in July and August, W01_Apr runs generated a significant increase in these months as evidenced in Figure 6.14. The regions of increased precipitation are consistent with that of decreased surface temperature. Therefore, our results reveal that dry soil moisture memories are usually persistent for approximately two months independent of when the soil moisture anomaly occurs, while wet soil moisture anomalies in April appear to influence precipitation for a longer period of time than those imposed in May. This finding is consistent with Oglesby et al. (2002) who found that soil moisture anomalies in March have a larger impact on summer precipitation than those in June. The difference in the precipitation response in W01_Apr and W01_May runs might be attributable to the seasonal sensitivity of atmospheric circulations to some external forcings such as snow cover, SST, and soil moisture (Palmer and Anderson 1994). Further studies are necessary to investigate the temporal sensitivity of atmospheric circulations on these external forcings.

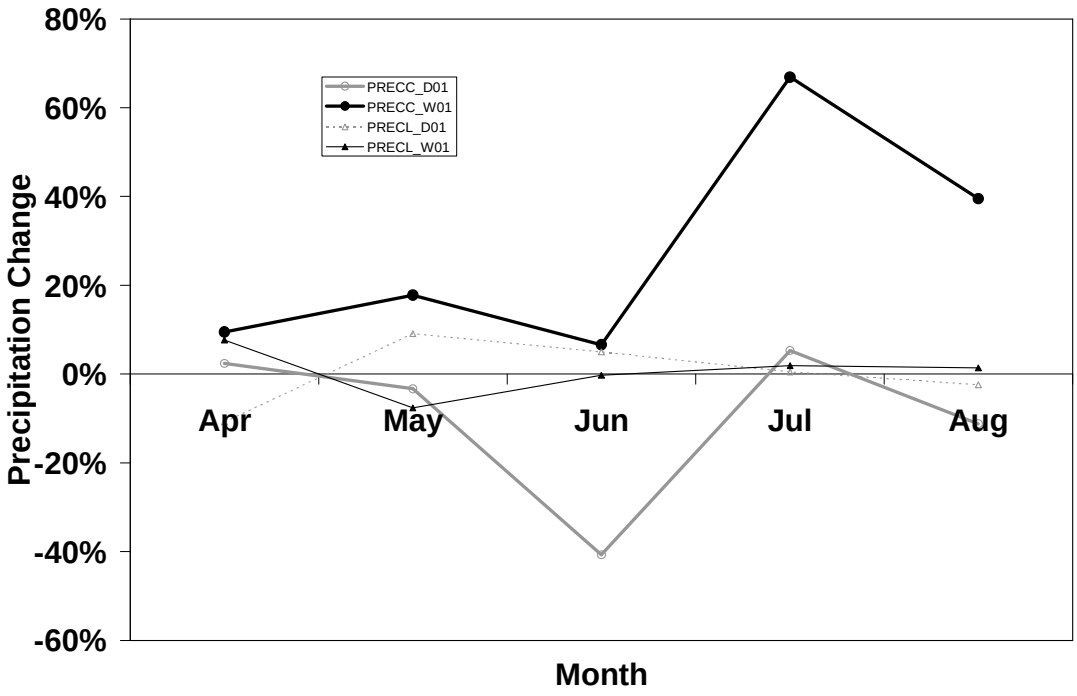

Figure 6.14 Averaged precipitation anomalies over the U.S. Great Plains in April through August in the D01_April and W01_April experiments. PRECC indicates convective precipitation rate and PRECL represents large-scale precipitation rate.

6.7 Conclusions

This study uses CAM3.0 to investigate the impact of spring soil moisture anomalies on summer precipitation in the GP. Results suggest that the sign, persistence, and timing of soil moisture anomalies can cause significant differences in summer precipitation response in the GP. In general, the influence of negative (dry) soil moisture anomalies can last approximately 2 months in the GP, regardless of whether the soil moisture anomalies are applied on either April 1st or May 1st. However, the magnitude of precipitation anomaly is approximately two times larger for the simulations initialized on May 1st as compared to April 1st. In addition, the simulations of persistent (1-month) dry

soil moisture anomalies resulted in larger decreases in summer precipitation that the short-lived (1-day) soil moisture anomalies. This implies that summer droughts are more severe when negative soil moisture anomalies persist for an extended period of time in spring.

The precipitation response to wet spring soil moisture anomalies is significantly different than the response to dry soil moisture anomalies and it depends on the timing of wet soil moisture anomalies. For W01_May runs, the impact on precipitation is immediate and greatest in May and it gradually weakens thereafter. In W01_Apr experiment, the precipitation anomalies in April, May, and June are decreasing in magnitude, similar to those in simulations initialized on May 1st, but the precipitation anomalies are largest in July and August indicating a time-lag effect of April soil moisture anomalies. This time-lag effect does not exist in the simulations starting on May 1st. Therefore, it appears that soil moisture anomalies on April 1st may have a longer memory and greater influence on summer precipitation than those on May 1st. This might be related to the seasonal sensitivity of atmospheric circulation to the initial soil moisture conditions. Comparing the results in W01_May and W30_May runs indicates that the precipitation response is approximately 3-4 times larger to the persistent soil moisture anomalies.

Even though wet soil moisture anomalies tend to produce larger precipitation anomalies than dry soil moisture anomalies during the first month, our results suggest that dry soil moisture anomalies tend to have longer lasting impact on summer precipitation than wet soil moisture anomalies. This is probably because once dry soil

moisture anomalies are present in the upper soil layers (~5-50 cm) it usually takes much longer (~5 days to more than 100 days) for these anomalies to dissipate as compared to wet soil moisture anomalies.

An important caveat of this study is that the results are based solely on CAM3.0 and therefore might be model-dependent due to the existence of significant variations between models (Koster et al. 2004). For instance, Ruiz-Barradas and Nigam (2005) argued that precipitation recycling might be too efficient in CAM3.0 which may lead to stronger land-atmosphere interactions in the GP. Therefore, further investigation of the land-atmosphere interaction using different models is necessary to verify these results.

7. SUMMARY AND CONCLUSIONS

7.1 Summary

Drought is a natural hazard that has caused significant loses to the society and the environment and is often represented as a deficit of rainfall during growth seasons for agriculture. These rainfall deficits are often linked to anomalies in large-scale atmospheric circulations and local land surface conditions. This dissertation attempted to improve the understanding of interacting effects of these factors on summer precipitation variation by focusing on two important factors (Niño SSTs and local soil moisture conditions) and their relative importance in causing summer precipitation variations. Specially, the goals of this research were to document the relationship of antecedent soil moisture and SSTs with summer precipitation in the GP and to investigate the physical mechanisms through which spring soil moisture anomalies affect summer precipitation. Due to the shortage of long-term observational soil moisture data, VIC-simulated soil moisture was selected after carefully evaluating three model-simulated soil moisture data against observations. Standardized Precipitation Index (SPI), calculated from PRISM monthly precipitation, was used to represent summer precipitation since the SPI is designed to be spatially invariable. Sea surface temperatures (SSTs) over the Niño regions were extracted from the extended reconstructed sea surface temperature data (ERSST) v.3. The temporal and spatial variations in soil moisture-precipitation relationship were documented using statistical analysis and sliding correlation. The contribution of Niño SST anomalies to summer precipitation variations was investigated to compare their relative contributions to those from local moisture recycling.

Persistence of soil moisture anomalies and SST anomalies was calculated to explain the strength of soil moisture-precipitation and SST-precipitation interactions. In addition, CAM3.0 was used to investigate the impacts of initial soil moisture anomalies and persistent soil moisture anomalies on summer precipitation in the GP. A number of sensitivity analyses were conducted to test the soil moisture-precipitation relationship in CAM3.0.

7.2 Conclusions

This study used both observational analysis and model simulations to investigate the soil moisture-precipitation relationship. The analysis revealed that soil moisture anomalies are significant in modifying summer precipitation only during the years when Niño SST persistence is low. When Niño SST persistence is strong, significant correlation exists between Niño SST and summer precipitation while the soil moisture-precipitation correlation is weak. Results also indicate that the impact of soil moisture anomalies and SST on summer precipitation varies greatly in space and time. Positive soil moisture-precipitation correlations are generally associated with high soil moisture persistence and negative soil moisture-precipitation correlations are linked to low soil moisture persistence. In addition, high SST persistence tends to favor (inhibit) negative (positive) soil moisture-precipitation correlations. Overall, this study suggests that both local soil moisture and remote SST anomalies influence summer precipitation in the U.S. Great Plains. The soil moisture anomalies are of greatest importance during years when Niño SST persistence is low.

Model results demonstrate that there are significant differences in precipitation response to soil moisture anomalies depending on their sign, timings and persistence. Dry soil moisture anomalies can last longer in affecting subsequent precipitation than wet soil moisture anomalies when initialized on May 1st. Dry soils can have significant influence on summer precipitation in the subsequent 2-3 months. The precipitation response to wet soil moisture anomalies is quicker and greater in magnitude than the response to dry soil moisture anomalies. Persistent soil moisture anomalies that are sustained for an entire month produced larger precipitation anomalies than soil moisture anomalies only applied on the first day of the month. Our results also suggest that the length of soil moisture memory also depends on when soil moisture anomalies occur. When initialized on April 1, wet soil moisture anomalies can have an impact on summer precipitation for a longer period of time than corresponding dry soil moisture anomalies initialized on the same date. The results from this study may be model-dependent due to the existence of inter-model variations in model performance. This may restrict the potential for making further general conclusions.

The major research findings of this dissertation are:

- By comparing three soil moisture models of different level of complexity, I found that Variable Infiltration Capacity (VIC) model is the most suitable model to estimate soil moisture variations in the U.S. Great Plains due to its stability in all climate regions and good model performance.
- Using statistical analysis methods, I demonstrated that both SSTs and soil moisture anomalies can have significant an influence on summer precipitation in

the U.S. Great Plains. However, their influences are spatially and temporally variable.

- By calculating persistence, I observed that strong SST-precipitation correlations are often associated with high persistence of SST anomalies and strong soil moisture-precipitation correlations are generally linked to high persistence of soil moisture anomalies.
- Using CAM3-CLM3 model, I found that summer precipitation responses to initial soil moisture conditions are different depending on the sign (dry/wet), timings and persistence of soil moisture anomalies.

Overall, this study makes a contribution to understanding the causes of summer precipitation variability in the U.S. Great Plains through the use of observational analyses and model simulations. This research contributes to the ongoing debate about the importance of land-atmosphere interactions in the climate system. There is still no consensus on whether soil moisture plays an important role in modifying summer precipitation. Previous conclusions of existence of strong soil moisture-precipitation interaction were mainly drawn from modeling studies. For instance, Schubert *et al*. (2004) found that approximately two thirds of the total low-frequency rainfall variance can be explained by land–atmosphere interactions (e.g. SM) using ensembles of long-term GCM forced with observed SSTs and only a small part of the remaining variance can be attributed to SST anomalies. This conclusion contrasts with Ruiz-Barradas and Nigam (2006) who analysed the interannual variability of GP precipitation using both observed precipitation and data from climate models. They found that model simulated

evaporation is up to four times larger than the highest observations, indicating that precipitation recycling is not realistically simulated by these models. In fact, the high precipitation recycling in General Circulation Models is the basis for claiming strong soil moisture-precipitation interaction. This study contributed to the debate by providing both spatial and temporal variations in soil moisture-precipitation interaction and conducting model simulations. The results of this study suggest that both soil moisture anomalies and SST anomalies can have significant influences on summer precipitation variations. Their influences are mainly controlled by their persistence. SST anomalies are the primary causes to precipitation change when SST anomaly persistence is high. Soil moisture can significantly affect summer precipitation only when its persistence is high and SST anomaly persistence is low. The highest correlations between spring SM and summer SPI are approximately 0.6-0.8 in the GP indicating that approximately 36%~64% of summer SPI variations can be attributed to antecedent SM conditions during high SM persistence years. These numbers are consistent with the peak correlations (r^2 >0.4) between spring SM and summer precipitation calculated by Findell and Eltahir (1997) using observational data in Illinois. This information can have potential to be used by the state government and environmental managers to predict drought and flood. Specifically, this study can be used to determine which factor plays a dominant role in affecting summer precipitation variation. During low SST persistence years, local soil moisture conditions may be a dominant factor in influencing summer precipitation. During high SST persistence years, SSTs are dominant and the role of

local soil moisture conditions is trivial (or secondary) in the summer precipitation variations. This research also provides a basis for rational planning.

7.3 Future research

This research focuses on soil moisture-precipitation interaction which is one of the land-atmosphere interactions. Vegetation and snow cover are also important land surface indicators and their interactions with summer precipitation are still not fully understood. I would like to examine the vegetation-precipitation interactions in order to improve the predictability of drought. This research will use remotely sensed data to provide vegetation information, such as Normalized Difference Vegetation Index.

The soil moisture comparison study suggests that model performance might vary by climate region. This issue has not been addressed in previous research. I will use Oklahoma Mesonet observations to investigate the impact of climate divisions on soil moisture model performance and to identify why climate conditions are important to influence soil moisture model performance.

REFERENCES

Abdulla, F. A., D. P. Lettenmaier, E. F. Wood, and J. A. Smith, 1996: Application of a macroscale hydrologic model to estimate the water balance of the Akansas-Red river basin. *J. Geophys. Res.,* **101,** 7449–7459.

Albertson, F. W., G. W. Tomanek, and A. Riegel, 1957: Ecology of drought cycles and grazing intensity on grasslands of central Great Plains. *Ecological Monographs*, **27,** 27-44.

American Meteorology Society,1997: Meteorological drought. *Bull. Amer. Meteor. Soc.,* **78,** 847-849.

Andreadis, K. M., E. A. Clark, A. W. Wood, A. F. Hamlet, and D. P. Lettenmaier, 2005: Twentieth-century drought in the conterminous United States. *J. Hydrometeor.,* **6,** 985-1001.

Arora, V. K. and G. J. Boer, 2006: The temporal variability of soil moisture and surface hydrological quantities in a climate model. *J. Clim*, **19,** 5875-5888.

Barros, A. P., 1996: An evaluation of model parameterizations of sediment pathways: A case study for the Tejo estuary. *Continental Shelf Research,* **16,** 1725-1749.

Bonan, G. B. and Coauthors, 2002: The land surface climatology of the community land model coupled to the NCAR community climate model. *J. Clim.*, **15,** 3123-3149.

Bosch, D. D., 2004: Comparison of capacitance-based soil water probes in coastal plain soils. *Vadose Zone Journal,* **3,** 1380-1389.

Box, G. E. P., W. G. Hunter, and J. S. Hunter, 1978: *Statistics for Experimenters: An Introduction to Design, Data Analysis and Model Building*. Wiley and Sons, 653 pp.

Brubaker, K. L., D. Entekhabi, and P. S. Eagleson, 1993: Estimation of continental precipitation recycling. *J. Clim.,* **6,** 1077-1089.

Chao, Y., M. Ghil, and J. C. McWilliams, 2000: Pacific interdecadal variability in this century's sea surface temperatures. *Geophys. Res. Lett.,* **27,** 2261-2264.

Chow, K. C., Johnny C. L. Chan, X. L. Shi, Y. M. Liu, and Y. H. Ding, 2008: Time-lagged effects of spring Tibetan Plateau soil moisture on the monsoon over China in early summer. *Int. J. Climatol.,* **28,** 55-67.

Collins, W. D. and Coauthors, 2006: The formulation and atmospheric simulation of the Community Atmosphere Model version 3 (CAM3). *J. Clim.,* **19,** 2144-2161.

Collins, W. D. and Coauthors, 2004: Description of the NCAR Community Atmosphere Model (CAM3). National Center for Atmospheric Research, 226 pp.

Conil, S., H. Douville, and S. Tyteca, 2007: The relative influence of soil moisture and SST in climate predictability explored within ensembles of AMIP type experiments. *Clim. Dynam.,* **28,** 125-145.

Dai, Y. J. and Coauthors, 2003: The Common Land Model. *Bull. Amer. Meteor. Soc.,* **84,** 1013-1023.

Daly, C., R. P. Neilson, and D. L. Phillips, 1994: A statistical-topographic model for mapping climatological precipitation over mountainous terrain. *J. Appl. Meteorol.,* **33,** 140-158.

DeLiberty, T. L. and D. R. Legates, 2008: Spatial variability and persistence of soil moisture in Oklahoma. *Physical Geography,* **29,** 121-139.

Dickson, R. R., 1984: Eurasian snow cover versus Indian monsoon rainfall - an extension of the Hahn-Shukla results. *J. Clim. Appl. Meteorol.,* **23,** 171-173.

Dirmeyer, P. A., Z. C. Guo, and X. Gao, 2004: Comparison, validation, and transferability of eight multiyear global soil wetness products. *J. Hydrometeor.,* **5,** 1011-1033.

Dong, J. R., W. Ni-Meister, and P. R. Houser, 2007: Impacts of vegetation and cold season processes on soil moisture and climate relationships over Eurasia. *J. Geophys. Res,* **112,** D09106, doi:10.1029/2006JD007774.

Douville, H., F. Chauvin, and H. Broqua, 2001: Influence of soil moisture on the Asian and African monsoons. Part I: Mean monsoon and daily precipitation. *J. Clim.*, **14,** 2381-2403.

Efron, B. and R. J. Tibshirani, 1993: *An Introduction to the Bootstrap*. *Monographs on Statistics and Applied Probabilty*, Chapman & Hall, 456 pp.

Ek, M. B. and A. A. M. Holtslag, 2004: Influence of soil moisture on boundary layer cloud development. *J. Hydrometeor.*, **5,** 86-99.

Ellis, A. W. and T. W. Hawkins, 2001: An apparent atmospheric teleconnection between snow cover and the North American monsoon. *Geophys. Res. Lett.,* **28,** 2653-2656.

Eltahir, E. A. B., 1998: A soil moisture rainfall feedback mechanism 1. Theory and observations. *Water Resources Research*, **34,** 765-776.

Entin, J. K. and Coauthors, 2000: Temporal and spatial scales of observed soil moisture variations in the extratropics. *J. Geophys. Res.*, **105,** 11865-11877.

Fasullo, J., 2004: A stratified diagnosis of the Indian monsoon-Eurasian snow cover relationship. *J. Clim.*, **17,** 1110-1122.

Findell, K. L. and E. A. B. Eltahir, 1997: An analysis of the soil moisture-rainfall feedback, based on direct observations from Illinois. *Water Resour. Res.*, **33,** 725-735.

Franchini, M. and M. Pacciani, 1991: Comparative-analysis of several conceptual rainfall runoff models. *Journal of Hydrology*, **122,** 161-219.

Gebremichael, M. and A. P. Barros, 2006: Evaluation of MODIS gross primary productivity (GPP) in tropical monsoon regions. *Romote Sensing of Environment*, **100,** 150-166.

Georgescu, M., C. P. Weaver, R. Avissar, R. L. Walko, and G. Miguez-Macho, 2003: Sensitivity of model-simulated summertime precipitation over the Mississippi River basin to the spatial distribution of initial soil moisture. *J. Geophys. Res.*, **108,** 8855, doi:10.1029/2002JD003107.

Guan, H., E. R. Vivoni, and J. L. Wilson, 2005: Effects of atmospheric teleconnections on seasonal precipitation in mountainous regions of the southwestern US: A case study in northern New Mexico. *Geophys. Res. Lett.* , **32,** L23701, doi:10.1029/2005GL023759.

Guo, Z. C. and P. A. Dirmeyer, 2006: Evaluation of the Second Global Soil Wetness Project soil moisture simulations: 1. Intermodel comparison. *J. Geophys. Res.*, **111,** D22S02, doi:10.1029/2006JD007233.

Guo, Z. C. and Coauthors, 2006: GLACE: The global land-atmosphere coupling experiment. Part II: Analysis. *J. Hydrometeor.*, **7,** 611-625.

Hahn, D. G. and J. Shukla, 1976: Apparent relationship between Eurasian snow cover and Indian monsoon rainfall. *J. Atmos. Sci.*, **33,** 2461-2462.

Hansen, M. C., R. S. Defries, J. R. G. Townshend, and R. Sohlberg, 2000: Global land cover classification at 1km spatial resolution using a classification tree approach. *Int. J. Remote Sens.*, **21,** 1331-1364.

Hu, Q. and S. Feng, 2001a: Variations of teleconnection of ENSO and interannual variation in summer rainfall in the central United States. *J. Clim.*, **14,** 2469-2480.

Hu, Q. and S. Feng, 2001b: Climatic role of the southerly flow from the Gulf of Mexico in interannual variations in summer rainfall in the central United States. *J. Clim.*, **14,** 3156-3170.

Hu, Q. and S. Feng, 2004: Why has the land memory changed? *J. Clim.*, **17,** 3236-3243.

Huang, J., H. M. van den Dool, and K. P. Georgakakos, 1996: Analysis of model-calculated soil moisture over the United States (1931-1993) and applications to long-range temperature forecasts. *J. Clim*, **9,** 1350-1362.

Illston, B. G. and Coauthors, 2008: Mesoscale monitoring of soil moisture across a statewide network. *Journal of Atmospheric and Oceanic Technology*, **25,** 167-182.

Jones, J. W. and Coauthors, 2003: The DSSAT cropping system model. *European Journal of Agronomy*, **18,** 235-265.

Kim, Y. and G. L. Wang, 2007: Impact of initial soil moisture anomalies on subsequent precipitation over North America in the coupled land-atmosphere model CAM3-CLM3. *J. Hydrometeor.*, **8,** 513-533.

Kimball, J. S., S. W. Running, and R. Nemani, 1997: An improved method for estimating surface humidity from daily minimum temperature. *Agr. Forest Meteorol.*, **85,** 87-98.

Koster, R. D. and M. J. Suarez, 2001: Soil moisture memory in climate models. *J. Hydrometeor.*, **2,** 558-570.

Koster, R. D., M. J. Suarez, R. W. Higgins, and H. M. Van den Dool, 2003: Observational evidence that soil moisture variations affect precipitation. *Geophys. Res. Lett.*, **30,** 1241, doi:10.1029/2002GL016571.

Koster, R. D. and Coauthors, 2004: Regions of strong coupling between soil moisture and precipitation. *Science*, **305,** 1138-1140.

Koster, R. D. and Coauthors, 2006: GLACE: The global land-atmosphere coupling experiment. Part I: Overview. *J. Hydrometeor.*, **7,** 590-610.

Kripalani, R. H., B. J. Kim, J. H. Oh, and S. E. Moon, 2002: Relationship between Soviet snow and Korean rainfall. *Int. J. Climatol.*, **22,** 1313-1325.

Kurtzman, D. and B. R. Scanlon, 2007: El Nino-Southern Oscillation and Pacific Decadal Oscillation impacts on precipitation in the southern and central United States: Evaluation of spatial distribution and predictions. *Water Resour. Res.*, **43,** W10427, doi:10.1029/2007WR005863.

Laird, K. R., S. C. Fritz, K. A. Maasch, and B. F. Cumming, 1996: Greater drought intensity and frequency before AD 1200 in the Northern Great Plains, USA. *Nature*, **384,** 552-554.

Larkin, T. J. and G. W. Bomar, 1983: *Climatic Atlas of Texas*. Texas Department of Water Resources, 151 pp.

Legates, D. R. and G. J. McCabe, 1999: Evaluating the use of "goodness-of-fit" measures in hydrologic and hydroclimatic model validation. *Water Resour. Res.,* **35,** 233-241.

Liang, X., D. P. Lettenmaier, and E. F. Wood, 1996a: One-dimensional statistical dynamic representation of subgrid spatial variability of precipitation in the two-layer variable infiltration capacity model. *J. Geophys. Res.*, **101(D16),** 21403-21422.

Liang, X., E. F. Wood, and D. P. Lettenmaier, 1996b: Surface soil moisture parameterization of the VIC-2L model: Evaluation and modification. *Global Planet. Change*, **13,** 195-206.

Liang, X., D. P. Lettenmaier, E. F. Wood, and S. J. Burges, 1994: A simple hydrologically based model of land-surface water and energy fluxes for general-circulation models. *J. Geophys. Res.*, **99,** 14415-14428.

Lin, S. J., 2004: A "vertically Lagrangian" finite-volume dynamical core for global models. *Mon. Wea. Rev.*, **132,** 2293-2307.

Liong, S. Y., J. Shreeram, and Y. Ibrahim, 1995: Catchment calibration using fractional-factorial and central-composite-designs-based response-surface. *Journal of Hydraulic Engineering-ASAE,* **121,** 507-510.

Liu, Y. Q. and R. Avissar, 1999: A study of persistence in the land-atmosphere system using a general circulation model and observations. *J. Clim.*, **12,** 2139-2153.

Mather, J.R., 1978: *The Climatic Water Budget in Environmental Analysis*. Lexington Books, 239 pp.

Maurer, E. P., G. M. O'Donnell, D. P. Lettenmaier, and J. O. Roads, 2001: Evaluation of the land surface water budget in NCEP/NCAR and NCEP/DOE reanalyses using an off-line hydrologic model. *J. Geophys. Res.*, **106 (D16),** 17841-17862.

Maurer, E. P., A. W. Wood, J. C. Adam, D. P. Lettenmaier, and B. Nijssen, 2002: A long-term hydrologically based dataset of land surface fluxes and states for the conterminous United States. *J. Climate*, **15,** 3237-3251.

McKee, T. B., N. J. Doesken, and J. Kleist, 1993: The relationship of drought frequency and duration to time scales. *In: Proceedings of the 8th Conference on Applied Climatology,* AMS, Boston, MA, 179-184.

McKee, T. B., N. J. Doesken, and J. Kleist, 1995: Drought monitoring with multiple time scales. *In: Proceedings of the 9th Conference on Applied Climatology*, AMS, Boston, MA, 233-236.

Meehl, G. A., 1994: Influence of the land-surface in the Asian summer monsoon - external conditions versus internal feedbacks. *J. Clim.*, **7,** 1033-1049.

Meng, L. and S. M. Quiring, 2008: A comparison of soil moisture models using Soil Climate Analysis Network observations. *J. Hydrometeor.*, **9,** 641-659.

Meng, L. and S. M. Quiring, 2009a: Observation relationship of sea surface temperatures and precedent soil moisture with summer precipitation in the U.S. Great Plains. *Int. J. Climatol.***,** Accepted.

Meng, L. and S. M. Quiring, 2009b: Examining the influence of spring soil moisture anomalies on summer precipitation in the U.S. Great Plains using the Community Atmosphere Model version 3 (CAM3). *J. Geophys. Res***,** Submitted.

Miller, D.A. and R.A. White, 1998: A conterminous United States multi-layer soil characteristics data set for regional climate and hydrology modeling. *Earth Interactions*, **2,** 1-26.

Miller, P. R. and Coauthors, 2002: Pulse crop adaptation in the northern Great Plains. *Agronomy Journal*, **94,** 261-272.

Mo, K. C. and M. Ghil, 1987: Statistics and dynamics of persistent anomalies. *J. Atmos. Sci.*, **44,** 877-901.

Namias, J., 1991: Spring and summer 1988 drought over the contiguous United-States - causes and prediction. *J. Clim.*, **4,** 54-65.

Namias, J., X. J. Yuan, and D. R. Cayan, 1988: Persistence of North Pacific sea surface temperature and atmospheric flow patterns. *J. Clim.*, **1,** 682-703.

National Assessment Synthesis Team, 2000: Climate change impacts on the United States: The potential consequences of climate variability and change. Available online at http://www.usgcrp.gov/usgcrp/Library/nationalassessment/overviewwater.htm.

Nijssen, B., R. Schnur, and D. P. Lettenmaier, 2001: Global retrospective estimation of soil moisture using the variable infiltration capacity land surface model, 1980-93. *J. Clim.*, **14,** 1790-1808.

Nuttonson, M. Y., 1965: Global agronomic analogues for the Great Plains region of the United States and an outline of its physiography, climate, and farm crops. *Am. Inst. of Crop Ecol***.,** Washington, DC.

Oglesby, R. J. and D. J. Erickson, 1989: Soil-moisture and the persistence of North-American drought. *J. Clim*, **2,** 1362-1380.

Oglesby, R. J., S. Marshall, D. J. Erickson, J. O. Roads, and F. R. Robertson, 2002: Thresholds in atmosphere-soil moisture interactions: Results from climate model studies. *J. Geophys. Res.*, **107 (D14),** 4224, doi:10.1029/2001JD001045.

Ojima, D. and Coauthors, 1999: Potential climate change impacts on water resources in the Great Plains. *Journal of the American Water Resources Association*, **35,** 1443-1454.

Oleson, K. W. and Coauthors, 2004: Technical description of the Community Land Model (CLM), National Center for Atmospheric Research, 174 pp.

Padbury, G. and Coauthors, 2002: Agroecosystems and land resources of the northern Great Plains. *Agronomy Journal*, **94,** 251-261.

Paegle, J., K. C. Mo, and J. NoguesPaegle, 1996: Dependence of simulated precipitation on surface evaporation during the 1993 United States summer floods. *Mon. Wea. Rev.*, **124,** 345-361.

Pal, J. S. and E. A. B. Eltahir, 2001: Pathways relating soil moisture conditions to future summer rainfall within a model of the land-atmosphere system. *J. Clim.*, **14,** 1227-1242.

Pal, J. S. and E. A. B. Eltahir, 2002: Teleconnections of soil moisture and rainfall during the 1993 midwest summer flood. *Geophys. Res. Lett.*, **29,** 1865, doi: 10.1029/2002GL014815.

Palmer, T. N. and D. L. T. Anderson, 1994: The prospects for seasonal forecasting - a review paper. *Quarterly Journal of the Royal Meteorological Society*, **120,** 755-793.

Pan, Z. T., E. Takle, M. Segal, and R. Turner, 1996: Influences of model parameterization schemes on the response of rainfall to soil moisture in the central United States. *Monthly Weather Review*, **124,** 1786-1802.

Pielke, R. A., G. E. Liston, J. L. Eastman, L. X. Lu, and M. Coughenour, 1999: Seasonal weather prediction as an initial value problem. *J. Geophys. Res.*, **104,** 19463-19479.

Priestley, C.H.B. and R.J. Taylor, 1972: On the assessment of surface heat flux and evaporation using large scale parameters. *Mon. Wea. Rev.*, **100,** 81-92.

Qian, B. D. and M. A. Saunders, 2003: Summer UK temperature and its links to preceding Eurasian snow cover, North Atlantic SSTs, and the NAO. *J. Clim.*, **16,** 4108-4120.

Qian, Y. F., Y. Q. Zheng, Y. Zhang, and M. Q. Miao, 2003: Responses of China's summer monsoon climate to snow anomaly over the Tibetan Plateau. *Int. J. Climatol.*, **23,** 593-613.

Quiring, S. M., 2004: Developing a real-time agricultural drought monitoring system for Delaware. *Publications in Climatology*, **LVII,** 104 pp.

Quiring, S. M. and T. N. Papakyriakou, 2005: Characterizing the spatial and temporal variability of June-July moisture conditions in the Canadian prairies. *Int. J. Climatol.*, **25,** 117-138.

Ritchie, J. T., 1998: Soil water balance and plant stress. *Understanding Options for Agricultural Production*, G. Y. T. Tsuji Y., Gerrit Hoogenboom, Philip K. Thornton, Eds., Kluwer Academic Publishers, 45-58.

Ritchie, J. T. and S Otter, 1985: Description and performance of CERES-Wheat: A user-oriented wheat yield model. *Agricultural and Forest Meteorology*, US Department of Agriculture, ARS, 38, 159-175.

Ritchie, J.T., 1972: Model for predicting evaporation from a row crop with incomplete cover. *Water Resour. Res.*, **8,** 1204-1213.

Robock, A. and Coauthors, 2003: Evaluation of the North American Land Data Assimilation System over the southern Great Plains during the warm season. *J. Geophys. Res.* , **108,** 8846.

Ruiz-Barradas, A. and S. Nigam, 2005: Warm season rainfall variability over the US great plains in observations, NCEP and ERA-40 reanalyses, and NCAR and NASA atmospheric model simulations. *J. Clim.*, **18,** 1808-1830.

Ruiz-Barradas, A. and S. Nigam, 2006: Great plains hydroclimate variability: The view from North American regional reanalysis. *J. Clim.*, **19,** 3004-3010.

Sau, F., K. J. Boote, W. M. Bostick, J. W. Jones, and M. I. Minguez, 2004: Testing and improving evapotranspiration and soil water balance of the DSSAT crop models. *Agron. J.*, **96,** 1243-1257.

Schar, C., D. Luthi, U. Beyerle, and E. Heise, 1999: The soil-precipitation feedback: A process study with a regional climate model. *J. Clim.*, **12,** 722-741.

Schneider, J. M., D. K. Fisher, R. L. Elliott, G. O. Brown, and C. P. Bahrmann, 2003: Spatiotemporal variations in soil water: First results from the ARM SGP CART network. *J. Hydrometeor.*, **4,** 106-120.

Schubert, S. D., M. J. Suarez, P. J. Pegion, R. D. Koster, and J. T. Bacmeister, 2004: Causes of long-term drought in the US Great Plains. *J. Clim.*, **17,** 485-503.

Seyfried, M. S. and M. D. Murdock, 2004: Measurement of soil water content with a 50-MHz soil dielectric sensor. *Soil Sci. Soc. Am. J.*, **68,** 394-403.

Seyfried, M. S., L. E. Grant, E. Du, and K. Humes, 2005: Dielectric loss and calibration of the hydra probe soil water sensor. *Vadose Zone Journal*, **4,** 1070-1079.

Shafer, M. A., C. A. Fiebrich, D. S. Arndt, S. E. Fredrickson, and T. W. Hughes, 2000: Quality assurance procedures in the Oklahoma Mesonetwork. *Journal of Atmospheric and Oceanic Technology*, **17,** 474-494.

Sheffield, J. and Coauthors, 2003: Snow process modeling in the North American Land Data Assimilation System (NLDAS): 1. Evaluation of model-simulated snow cover extent. *J. Geophys. Res.*, **108,** 8849, doi:10.1029/2002JD003274.

Shukla, J. and Y. Mintz, 1982: Influence of land-surface vvapo-transpiration on the Earths climate. *Science*, **215,** 1498-1501.

Sklut, M., 2005: Investigating SST influence of the North Atlantic Oscillation using the NCAR Community Atmospheric Model, Department of Geography, University of Delaware, 122 pp.

Smith, T. M., R. W. Reynolds, T. C. Peterson, and J. Lawrimore, 2008: Improvements to NOAA's historical merged land-ocean surface temperature analysis (1880-2006). *J. Clim.*, **21,** 2283-2296.

Thornthwaite, C.W., 1948: An approach towards rational classification of climate. *The Geographical Review*, **38**.

Thornthwaite, C.W. and J.R. Mather, 1955: The water balance. *Publications in Climatoloty, Laboratory of Climatoloty*, **8,** 104 pp.

Thornton, P. E. and S. W. Running, 1999: An improved algorithm for estimating incident daily solar radiation from measurements of temperature, humidity, and precipitation. *Agr. Forest Meteorol.*, **93,** 211-228.

Ting, M. F. and H. Wang, 1997: Summertime US precipitation variability and its relation to Pacific sea surface temperature. *J. Clim.*, **10,** 1853-1873.

Vinnikov, K. Y., A. Robock, N. A. Speranskaya, and A. Schlosser, 1996: Scales of temporal and spatial variability of midlatitude soil moisture. *J. Geophys. Res.*, **101,** 7163-7174.

Weaver, F. E. and F. W. Albertson, 1938: Major changes in grassland as a result of continued drought. *Botanical Gazette*, **100,** 576-591.

Weaver, J. E. and F. W. Albertson, 1936: Effects of the great drought on the prairies of Iowa, Nebraska, and Kansas. *Ecology*, **17,** 567-639.

Western, A. W., R. B. Grayson, and G. Bloschl, 2002: Scaling of soil moisture: A hydrologic perspective. *Annual Review of Earth and Planetary Sciences*, **30,** 149-180.

Wilhite, D.A., 2000: Drought as a natural hazard: Concepts and definitions. *Drought: A Global Assessment*, D.A. Wilhite, Ed., Routledge Publishers, 3-18.

Williams, J. R., C. A. Jones, and P. T. Dyke, 1984: A modeling approach to determining the relationship between erosion and soil productivity. *Transactions of the Asae*, **27,** 129-144.

Willmott, C. J. and K. Matsuura, 2005: Advantages of the mean absolute error (MAE) over the root mean square error (RMSE) in assessing average model performance. *Climate Research*, **30,** 79-82.

Wood, E. F., D. Lettenmaier, X. Liang, B. Nijssen, and S. W. Wetzel, 1997: Hydrological modeling of continental-scale basins. *Annual Review of Earth and Planetary Sciences*, **25,** 279-300.

Wood, E.F., D.P. Lettenmaier, and V.G. Zartarian, 1992: A land-surface hydrology parameterization with subgrid variability for general circulation mdels. *J. Geophys. Res.*, **97(D3),** 2717-2728.

Woodhouse, C. A. and J. T. Overpeck, 1998: 2000 years of drought variability in the central United States. *Bull. Amer. Meteor. Soc.*, **79,** 2693-2714.

Wu, T. W. and Z. A. Qian, 2003: The relation between the Tibetan winter snow and the Asian summer monsoon and rainfall: An observational investigation. *J. Clim.*, **16,** 2038-2051.

Wu, W. R. and R. E. Dickinson, 2004: Time scales of layered soil moisture memory in the context of land-atmosphere interaction. *J. Clim.*, **17,** 2752-2764.

Xue, Y., T. M. Smith, and R. W. Reynolds, 2003: Interdecadal changes of 30-yr SST normals during 1871-2000. *J. Clim.*, **16,** 1601-1612.

Xue, Y. K., 1996: The impact of desertification in the Mongolian and the Inner Mongolian grassland on the regional climate. *J. Clim*, **9,** 2173-2189.

Xue, Y. K., F. J. Zeng, and C. A. Schlosser, 1996: SSiB and its sensitivity to soil properties - A case study using HAPEX-Mobilhy data. *Global Planet. Change*, **13,** 183-194.

Xue, Y. K., P.J. Sellers, F. J. Zeng, and C. A. Schlosser, 1997: Comments on "Use of midlatitude soil moisture and meteorological observations to validate soil moisture simulations with biosphere and bucket models." *J. Clim.*, **10,** 374-376.

Yildiz, O. and A. P. Barros, 2007: Elucidating vegetation controls on the hydroclimatology of a mid-latitude basin. *Journal of Hydrology*, **333,** 431-448.

Zhang, H. and C. S. Frederiksen, 2003: Local and nonlocal impacts of soil moisture initialization on AGCM seasonal forecasts: A model sensitivity study. *J. Clim.*, **16,** 2117-2137.

Zhang, J. Y., W. C. Wang, and J. F. Wei, 2008: Assessing land-atmosphere coupling using soil moisture from the Global Land Data Assimilation System and observational precipitation. *J. Geophys. Res*, **113,** D17119, doi:10.1029/2008JD009807.

Zheng, X. Y. and E. A. B. Eltahir, 1998: A soil moisture rainfall feedback mechanism 2. Numerical experiments. *Water Resour. Res.*, **34,** 777-785.

Zhu, C. M., D. P. Lettenmaier, and T. Cavazos, 2005: Role of antecedent land surface conditions on North American monsoon rainfall variability. *J. Clim.*, **18,** 3104-3121.

VITA

Name: Lei Meng

Address: Department of Geography,
College of Geosciences
Texas A&M University
College Station, TX 77843-3147

Email Address: leimeng@tamu.edu

Education: B.S., Geology, Nanjing University, Nanjing, China, 2000
M.S., Soil Science, China Agricultural University, Beijing, China, 2003
M.S., Geology, University of Illinois, Urbana, IL, USA, 2005
Ph.D., Geography, Texas A&M University, College Station, TX, USA, 2009